

THE STEERING RELATIONSHIP BETWEEN THE FIRST AND SECOND AXLES OF A 6X6 OFF-ROAD MILITARY VEHICLE

CARL-JOHANN VAN EEDEN

Submitted in partial fulfilment of the requirements for
the degree

M Eng (Mechanical Engineering)

in the

Faculty of Engineering, Built Environment and
Information Technology

University of Pretoria

2007

THE STEERING RELATIONSHIP BETWEEN THE FIRST AND SECOND AXLES OF A 6X6 OFF-ROAD MILITARY VEHICLE

By

Carl-Johann van Eeden

Study leader: Mr P.S. Els

Department of Mechanical and Aeronautical Engineering

University of Pretoria

Summary

The steering arrangement of a 6x6 off-road military vehicle was investigated, with the aim to determine if a variable steering ratio between the first and second steering axle of the vehicle will make an improvement in the steady and transient state handling of the vehicle.

Low speed manoeuvring was evaluated, comparing the vehicle steering geometry with Ackerman geometry. For steady state handling, a bicycle model was developed, and constant radius simulations at various track radii, vehicle speeds and steering ratios (ratio between the first and second steering axle) was performed. For transient dynamic simulations, a mathematical model was developed that included a simple driver model to steer the vehicle through a single lane change, again at various speeds and steering ratios.

The vehicle was instrumented, and actual constant radii tests, as well as single lane change tests were performed. The measurements enabled the comparison of simulated and measured results. Although basic mathematical models were used, acceptable correlation was obtained for both steady state and transient dynamic behaviour.

The results indicated that for this specific vehicle geometry, where the centre of mass is above the second axle, no marked improvement would be obtained by implementing a variable ratio steering system.

The mathematical model was changed to simulate a vehicle with longer wheelbase and different centre of mass. With the new geometry, theoretical slip angles (and therefore tire wear) reductions were more noticeable.

It was concluded that a variable ratio system between the front and second axle would not be an economically viable improvement for this vehicle, since the improvement achieved will not warrant the additional cost and complexity added to the vehicle.

Keywords: Variable steering ratio, steady state handling, transient handling, multi axle vehicle, off-road, bicycle model, three axle model, four axle model, GPS measurements, slip angle.

DIE STUURVERHOUDING TUSSEN DIE EERSTE EN TWEDE AS VAN 'N 6X6 MILITÊRE VELD-RY VOERTUIG

Deur

Carl-Johann van Eeden

Studie leier: Mnr P.S. Els

Departement Meganiese en Lugvaartkundige Ingenieurswese

Universiteit van Pretoria

Opsomming

Die stuurverhouding van 'n 6x6 militêre veld-ry voertuig is ondersoek, met die doel om te bepaal of 'n variëerbare stuurverhouding tussen die eerste en tweede stuur as van die voertuig 'n verbetering in die gestadigde en ongestadigde hantering van die voertuig sal gee.

Lae spoed manueverbaarheid is bepaal en vergelyk met die Ackerman stuur geometrie. Vir gestadigde hantering, is 'n fietsmodel ontwikkel, en 'n konstante radius simulاسie vir verskeie radiuse, voertuigspoede en stuurverhoudings (verhouding tussen die eerste en tweede stuur as) is gedoen. Vir ongestadigde hantering simulاسies, is 'n wiskundige model saamgestel wat 'n eenvoudige bestuurdermodel implementeer, om die voertuig deur 'n enkelbaan-verandering te stuur, weer by verskeie voertuigspoede en stuurverhoudings.

Die voertuig is geïstrumenteer, en konstante radius toetse, sowel as enkelbaan verandering toetse is uitgevoer. Die metings is vergelyk met simulاسie resultate. Alhoewel basiese wiskundige modelle gebruik is, is aanvaarbare ooreenstemming verkry vir beide gestadigde en ongestadigde dinamiese gedrag.

Die resultate toon aan dat vir die spesifieke voertuig geometrie, waar die massamiddelpunt van die voertuig bo-op die tweede as geplaas is, geen merkbare verbetering verkry word met 'n variëerbare stuurverhouding nie.

Die model is verander om 'n voertuig te simuleer met 'n langer wielbasis en 'n nuwe massa middelpunt posisie. Met hierdie geometrie kon die teoretiese glijhoeke (en daarom bandslytasie) verminder word.

Daar is gevind dat 'n variëerbare stuurverhouding tussen die eerste en tweede as van die spesifieke voertuig nie ekonomies lewensvatbaar sal wees nie, aangesien daar nie 'n merkbare verbetering verkry word wat die addisionele koste en kompleksiteit sal regverdig nie.

Sleutel woorde: Variëerbare stuur verhoudig, gestadigde toestand hantering, oorgangs hantering, multi as voertuig, veld-ry, fiets model, drie-as model, vier-as model, GPS metings, glij hoek.

Acknowledgements

Dr Schalk Els

Dr Stefan Nell

Renette van Eeden

Karla van Eeden

Table of Contents

Paragraph	Description	Page number
1	Background	15
2	Problem statement	17
3	Aim of the study	17
4	Literature study	18
4.1	Multi-wheel steering	18
5	Test vehicle information	23
6	Mechanical integration of steering ratio changes	25
7	Steady state handling	26
7.1	Introduction	26
7.2	Low speed turning	26
7.3	High speed cornering	28
7.4	Introduction to the tire model	28
7.5	Tire cornering forces	30
7.6	Cornering equations	31
7.7	Understeer gradient	33
8	Tire wear	35
9	Test vehicle low speed turning requirements	37
10	Constant radius: expanding the cornering equations to a four axle configuration	38
11	Constant radius bicycle model	44
11.1	Developing the three axle bicycle model	44
12	Constant radius: simulation results, simplified bicycle model	47
13	Transient state handling	57
13.1	Equations of motion, two degree of freedom model, two axles	57
13.2	Equations of motion, two degree of freedom model, four axles	60
14	Test track dimensions	64
15	Driver/steering model	65

16	Simulink model	67
17	Simulink model simulation results	69
18	Vehicle measurements	75
18.1	Introduction	75
18.2	GPS measurements	75
18.3	Test equipment	75
18.4	Test vehicle and measurement positions	76
18.5	Test procedure	80
18.6	Steering calibration measurements	81
18.7	GPS measurements	85
18.8	Test results, constant radius test	86
19	Test results, single lane change	89
20	Simulated vs. measured results	91
20.1	Introduction	91
20.2	Constant radius test	91
20.3	Single lane change	92
21	Vehicle specific characteristics	96
21.1	Vehicle geometry	96
21.2	Tire and driver model	99
21.3	Speed ranges	99
21.4	Tire wear	99
22	Conclusion	100
23	Recommendations	101
24	References	102

Appendix A: Matlab routine to convert linear measured displacement to angular displacements	104
Appendix B: Measured CCW plot data manipulation	107
Appendix C: Constant radius test – Matlab M file	110
Appendix D: Lane change – Matlab M file	122
Appendix E: Lane change data manipulation – Matlab M file	126

Alphabetical Symbols

a	Distance between the first and second axle
A_{11}	Matrix coefficient row 1 column 1
A_{12}	Matrix coefficient row 1 column 2
A_{21}	Matrix coefficient row 2 column 1
A_{22}	Matrix coefficient row 2 column 2
aa	Distance between the first axle and centre of mass
A_r	Ackerman ratio
a_y	Lateral acceleration
b	Distance between the second axle and centre of mass
B_1	Matrix coefficient row 1 column 1
B_2	Matrix coefficient row 2 column 1
bb	Distance between the centre of mass and the second axle
c	Distance between the centre of mass and third axle
cc	Distance between the second axle and third axle
CC_α	Cornering coefficient
C_F	Force centre
$C_{F\alpha}$	Cornering force stiffness
CG	Centre of gravity
C_T	Turn centre
C_{yf1}	Cornering stiffness of the first axle tire
C_{yf2}	Cornering stiffness of the second axle tire
C_{yr}	Cornering stiffness of the rear tire
$C_{\alpha f}$	Cornering stiffness of the front tire
$C_{\alpha r}$	Cornering stiffness of the rear tire
d	Distance between the third axle and fourth axle
di	Inner wheel steering angle
do	Outer wheel steering angle
e	Distance between first axle and third axle

f	Distance between second and third axle
F_y	Lateral force
F_{yf}	Lateral (cornering) force at the front axle
F_{yf1}	Lateral (cornering) force at the first axle
F_{yf2}	Lateral (cornering) force at the second axle
F_{yr}	Lateral (cornering) force at the rear axle
F_{yr1}	Lateral (cornering) force at the third axle
F_{yr2}	Lateral (cornering) force at the fourth axle
g	Gravitational acceleration constant
G	Centre of mass
I	Second moment of inertia
K	Understeer gradient (deg/g)
L	Wheelbase
M	Mass of the vehicle
M_c	Moment due to combined rear axle forces
R	Radius of the turn
S_r	Steering ratio
t	Track width
u	Velocity component y direction
V	Forward velocity
V_{ay}	Velocity component y direction
V_{ax}	Velocity component x direction
V_{char}	Characteristic speed
V_{crit}	Critical speed
W_f	Load on the front axle
W_r	Load on the rear axle
X_t	X position at time t
Y_t	Y position at time t

Greek Symbols

δ_0	Outside wheel angle
δ_i	Inside wheel angle
δ	Ackerman angle
α_{re}	Equivalent slip angle rear axle
α_{f1}	Slip angle first axle
α_{f2}	Slip angle second axle
α_{r1}	Slip angle third axle
α_{r2}	Slip angle fourth axle
Δ	Off-tracking distance
δ_1	Average steering angle first axle
δ_2	Average steering angle second axle
α_r	Slip angle third axle
α	General slip angle
ψ	Heading angle
ν	Path angle from the X – axis
τ	Time constant [s]
β	Attitude angle
ψ	Heading angle
ψ_t	Heading angle at time t

Abbreviations

ADAMS	Automatic Dynamic Analysis of Mechanical Systems
AFV	Armoured Fighting Vehicle
AMV	Armoured Modular Vehicle
ARMSCOR	Armourments Corporation of South Africa
BPW	Bergische Patentachsenfabrik GmbH
CVED	Combat Vehicle Electric Drive
DADS	Dynamic Analysis and Design System
EMAS	Electronic Multi Axle Steering
ETD	Electrical Technology Demonstrator
GPS	Global Positioning System
GVM	Gross Vehicle Mass
LWB	Long Wheel Base
OEM	Original Equipment Manufacturer
PCF	Positive Centre Feel
RMS	Root Mean Square
SAE	Society of Automotive Engineers
SANDF	South African National Defence Force
SUV	Sports Utility Vehicle

List of Figures

Figure 1 : Rooikat AFV	15
Figure 2 : Rooikat steering system	15
Figure 3 : Rooikat hydraulic steering system	16
Figure 4 : 1915 Jeffery quad four-wheel-steer truck [1]	18
Figure 5 : 1940 Nash quad all-wheel-drive and steer [1]	18
Figure 6 : EMAS automatic hydraulic steering [2]	19
Figure 7 : Addax multi-wheel steer	19
Figure 8 : Patria AMV	20
Figure 9 : Multi-steer trailer and truck	20
Figure 10 : Steerable trailer axles from BPW [6]	21
Figure 11 : Multidrive truck-trailer combination [7]	21
Figure 12 : EMAS automatic hydraulic steering [2]	22
Figure 13 : Bison dimensions	23
Figure 14 : Test vehicle: Bison	24
Figure 15 : Steering linkages	25
Figure 16 : Ackerman steering angle	26
Figure 17 : Ackerman steering, eight wheel vehicle steering with first and second axles	27
Figure 18 : Measuring tire data	29
Figure 19 : Measured tire data	30
Figure 20 : Tire cornering force properties [9]	30
Figure 21 : Cornering of a bicycle model [9]	31
Figure 22 : Change of steer angle with speed [9]	34
Figure 23 : Tire life for different tire pressures [23]	35
Figure 24 : Ackerman steering Bison	37
Figure 25 : Slip angle diagram	38
Figure 26 : Detail slip angle diagram	39
Figure 27 : Scale drawing of an 8x8 geometry	42
Figure 28 : Bison three axle bicycle model	44
Figure 29 : RMS slip angles, constant radius test	48

Figure 30 : RMS steering angles	49
Figure 31 : RMS slip angles and steering angles	50
Figure 32 : Slip and steer angles - 20 meter radius	51
Figure 33 : Slip and steer angles - 40 meter radius	52
Figure 34 : Slip and steer angles - 60 meter radius	52
Figure 35 : Slip angle vs. vehicle speed	53
Figure 36 : Steering angle vs. vehicle speed – 20 meter radius	54
Figure 37 : Steering angle vs. vehicle speed – 40 meter radius	54
Figure 38 : Steering angle vs. vehicle speed – 60 meter radius	55
Figure 39 : Steering angle vs. lateral acceleration – 20 meter radius	55
Figure 40 : Steering angle vs. lateral acceleration – 40 meter radius	56
Figure 41 : Steering angle vs. lateral acceleration – 60 meter radius	56
Figure 42 : Angles and velocity components [10]	57
Figure 43 : Velocity components at path points [10]	58
Figure 44 : Free body diagram [10]	59
Figure 45 : Single lane change track dimensions	64
Figure 46 : Driver model	65
Figure 47 : Simulink driver model	66
Figure 48 : Simulink diagram	67
Figure 49 : Time to complete the maneuver	69
Figure 50 : Maximum slip angle	70
Figure 51 : Slip angles – 30 km/h	71
Figure 52 : Slip angles – 60 km/h	71
Figure 53 : RMS slip angles	72
Figure 54 : Simulated trajectory	73
Figure 55 : Simulated yaw angle - 30 km/h	74
Figure 56 : Instrumented vehicle on the test track	76
Figure 57 : Rear GPS	77
Figure 58 : Rear GPS antenna position	77
Figure 59 : First axle displacement meter position	78

Figure 60 : Second axle displacement meter position	78
Figure 61 : Vehicle speed measurement	79
Figure 62 : Front GPS antenna position	79
Figure 63 : Lane change track dimensions	80
Figure 64 : Measuring steering angles. The position of the plumb line are shown	81
Figure 65 : Steering angle calibration, measured data	82
Figure 66 : Measured steering angles for steering wheel positions	82
Figure 67 : Calibrated steering angle	83
Figure 68 : First and second axle calibrated steering angles	84
Figure 69 : Steering ratio, 0.7	84
Figure 70 : Front and rear GPS data	85
Figure 71 : GPS lane change data, front and rear GPS, 4 vehicle speeds	86
Figure 72 : Lateral acceleration, constant radius test	87
Figure 73 : Yaw rate, constant radius test	87
Figure 74 : Roll, constant radius test	87
Figure 75 : Steering angle comparison, constant radius test	88
Figure 76 : Steering single and speed comparison, constant radius test	88
Figure 77 : Measured first axle wheel speed and lateral acceleration - 28 km/h	89
Figure 78 : Steering angles on first and second axles measured data - 28 km/h	90
Figure 79 : Roll and yaw measured data - 28 km/h	90
Figure 80 : (Result of Figure 34 and Figure 76)	91
Figure 81 : (Result of Figure 34 and Figure 76)	92
Figure 82 : Single lane change measured vs. simulated trajectories	93
Figure 83 : Measured steering angle single lane change - 43 km/h	94
Figure 84 : Simulated steering angle single lane change - 50 km/h	95
Figure 85 : LWB vehicle	96
Figure 86 : LWB slip angles	97
Figure 87 : Bison slip angles	98
Figure 88 : LWB vehicle, maximum slip angles	98
Figure 89 : 8x8 MAN	99

1. Background

Continuous improvement in driveline technology, led the SANDF and ARMSCOR to investigate the integration of a Diesel-Electric transmission system in a combat vehicle. Project CVED (Combat Vehicle Electric Drive) was initiated. The aim of the project was to increase internal volume, reduce vehicle mass, and increase overall vehicle performance.

As part of the project, an investigation was conducted on the feasibility of changing the existing Rooikat steering system to a lighter compact unit, since the mechanical steering linkages in the current Rooikat weighs in excess of 1.5 tonnes. The investigation found that that the Rooikat can be converted to use a complete hydraulic steering system that will increase the available internal volume. The Rooikat is shown in Figure 1.



Figure 1 : Rooikat AFV

The Rooikat Armour Fighting Vehicle (AFV) original steering system is shown in Figure 2.

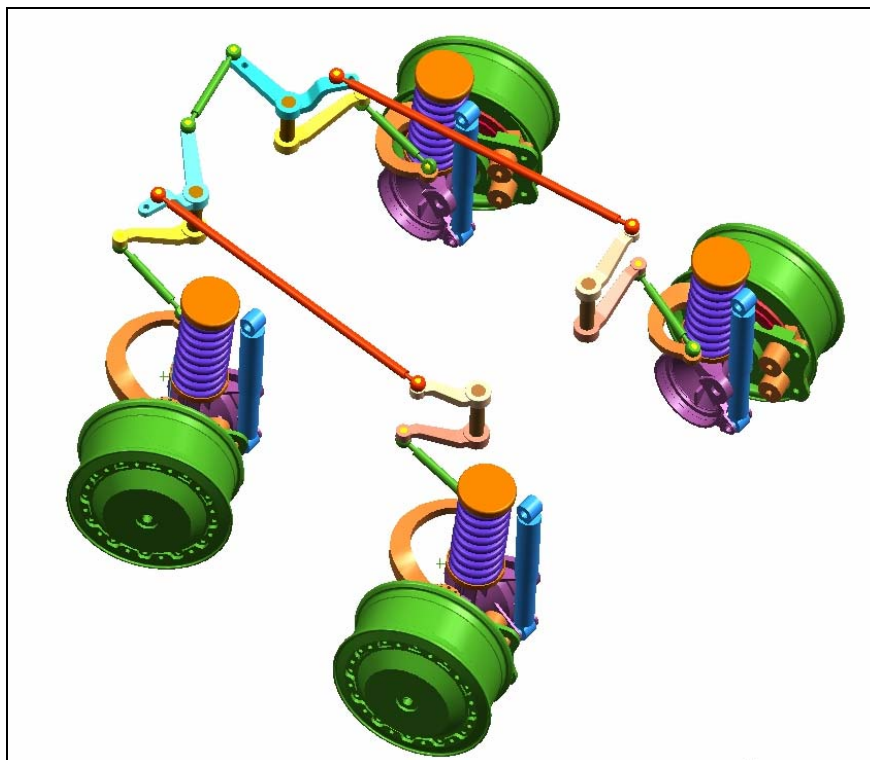


Figure 2 : Rooikat steering system

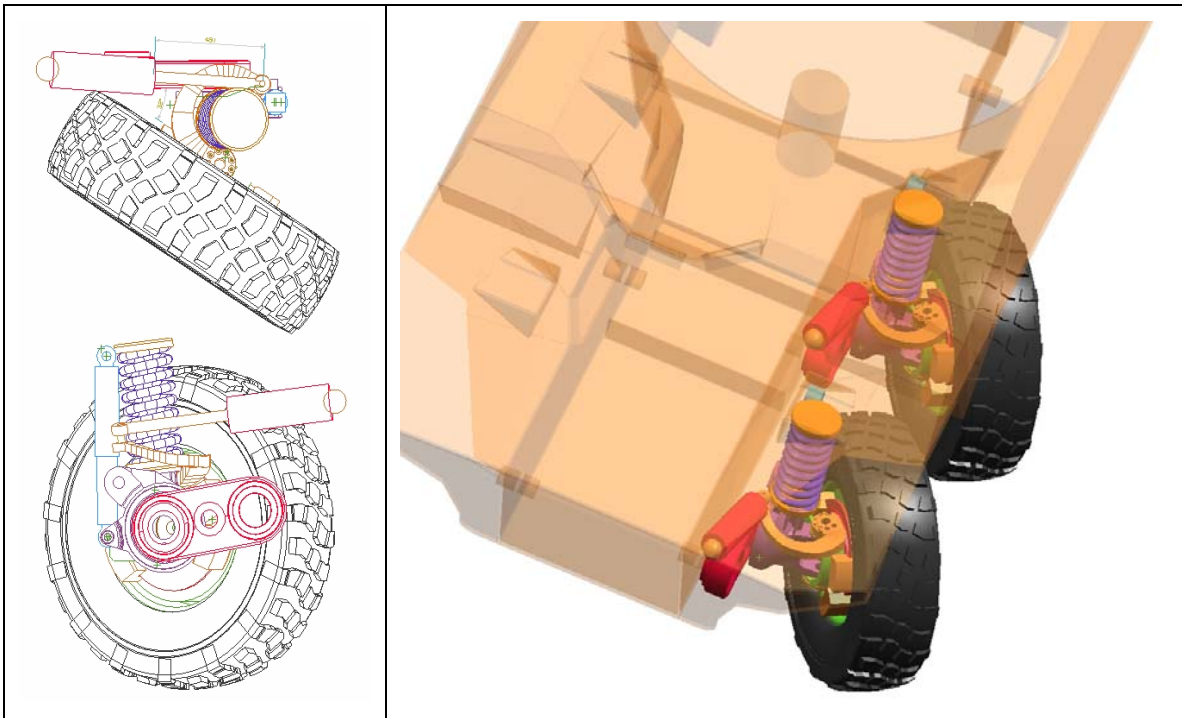


Figure 3 : Rooikat hydraulic steering system

Because of the large steering forces generated and required, the system chosen and shown in Figure 3 is a hydraulic system. Hydraulic cylinders, with built-in linear transducers to determine the exact position of individual wheels is shown, mounted onto the existing trailing arm steering components. The need for a large mechanical steering reduction box is eliminated using the above concept.

The legal implications of the above conversion were excluded from this investigation. The cost of the conversion was prohibitive, and it was decided that the existing system would be retained.

The Rooikat steering investigation suggested that the steering wheel angles can be controlled individually, and the question was raised if the individual control of steering wheel angles would improve manoeuvrability and improve vehicle handling. It was decided to conduct an investigation on individual steering angles on a multi-steer off-road vehicle.

As a first attempt, the possibility to vary the steering ratio between the first and second axles was investigated. The simplification to look at axles instead of individual wheels makes it possible to use a bicycle model in the theoretical analysis. The mathematical complexity to vary the ratios between axles only is reduced compared to individual wheel control. If the modification proved worthwhile, the concept may be expanded to full individual steering.

As a first choice, an 8x8 vehicle as test vehicle would have been ideal, since the 8x8 configuration is the norm in armoured fighting vehicles in the 20 tonne to 30 tonne class, due to mobility and wheel load advantages. However, as will be discussed in following paragraphs, only a 6x6 vehicle was available for tests, and was therefore used. Where applicable, mathematical relationships for an 8x8 vehicle was derived, and then simplified to make it applicable to a 6x6 twin steer vehicle.

2. Problem statement

Investigate the control of individual steering axle ratio of a 6x6 off-road vehicle, to determine the steering ratios that will lead to improved steady and transient vehicle handling at low and high speed.

3. Aim of the study

The aim of this study is to continue with the initial steering investigation, as done on the CVED programme, by analysing and designing a new steering system, where the steering ratio between the first and second axles can be controlled to improve manoeuvrability and handling at low and high vehicle speeds.

The study will investigate and identify optimum steering ratio's for a given vehicle speed, in order to improve vehicle handling and reduce tire wear. The study will start with low speed manoeuvrability, where the Ackerman principle is required. At increased vehicle speeds, the appropriate steering wheel angles for steady state manoeuvres will be investigated. The constant radius test was chosen for the steady state evaluation. For transient state conditions, a steering wheel step input will be investigated, as being generated during a single lane change manoeuvre.

The result of the study will be a recommendation regarding a steering axle relationship, dependant on vehicle speed, enabling a hydraulic or other steering system, with appropriate control system, to adjust steering axle ratios to improve vehicle handling. As a first attempt, the steering ratio between the first and second axle is investigated. Should the study indicate a marked improvement in handling or other benefit, the concept may be further expanded to look at individual wheel angles as well.

4. Literature study

4.1. Multi-wheel steering

The concept of multi-wheel steering is not new. Some of the more notable four-wheel-steer 4x4's are shown in Figure 4 and Figure 5. Examples include the 1900-1902 Cotta Cottamobile, the 1904-1907 Four-wheel-drive truck, the 1906-1912 American trucks, the 1913-1928 Jefferey (Nash from 1916-1928) Quad 3-ton truck, the 1914 Golden West truck and the 1915-1917 Beech Creek truck [1].

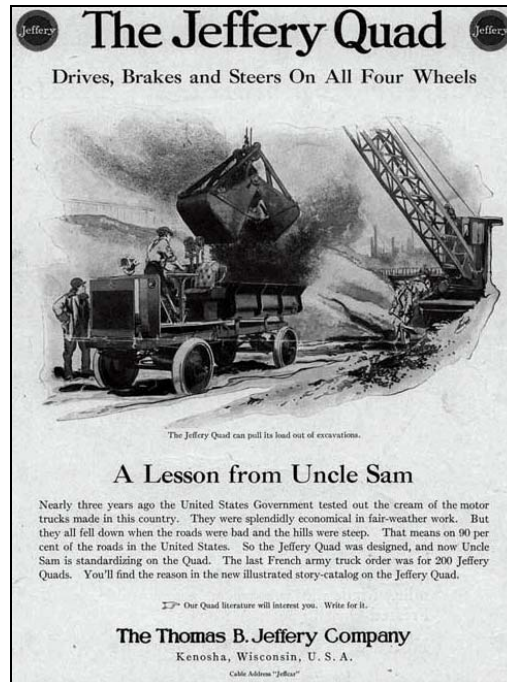


Figure 4 : 1915 Jeffery quad four-wheel-steer truck [1]



Figure 5 : 1940 Nash quad all-wheel-drive and steer [1]

Four-wheel steering has found itself into commercial and production vehicles. An example of the EMAS [2] Automatic Hydraulic Steering fitted to a Ford Pickup and SUV is shown in Figure 6. The improved low speed manoeuvrability can clearly be seen.



Figure 6 : EMAS automatic hydraulic steering [2]

Various multi-axle steering vehicles have been developed to investigate and demonstrate the advantages of multi-wheel steering on light and heavy vehicles.

In South Africa, the University of Pretoria developed a four-wheel steer vehicle based on Volkswagen Golf driveline components to investigate four-wheel steering algorithms [3]. On the heavy vehicle side, the best example of a 6x6 multi-wheel steer vehicle is the Addax [4], developed by ARMSCOR and Ermetek. The vehicle comprised of three axles that can be steered individually. The control of individual steering angles enables the evaluation of different steering control philosophies. The vehicle is shown in Figure 7 in crab steer mode (all wheels turned in the same direction) on the left hand side and opposite steer of the first and last axle (with the central axle locked in the dead ahead direction) on the right hand side.



Figure 7 : Addax multi-wheel steer [4]

The study indicated that rear axle steering improved handling, reduced tire wear and improved slow speed manoeuvring.



Figure 8 : Patria AMV

As a second example, the Patria AMV [5], shown in Figure 8, steers mechanically with the first two axles. When low speed manoeuvring is required at maximum steering lock, the last axle could be counter-steered electrically to reduce the turning radius. The practical implementation of all wheel steering on this type of vehicle is relatively simple, since the wheel-stations on the first, second, third and fourth axles are identical. The last axle is locked mechanically to eliminate steering in conventional steering mode. The Patria vehicle also has the ability to skid steer, using the brake system to clamp either the left or right hand side wheels. The skid steer system enables manoeuvring on surfaces where loose gravel is present. (On high friction surfaces, skid steering is not recommended due to the high forces transmitted to the driveline and suspension).

Multi-wheel steering is also used in truck-trailer combinations. Truck-tractors steer the second axles of the truck, as well as the trailer axles to reduce turning radii and tire wear.

A trailer with a steerable second axle is shown in Figure 9.



Figure 9 : Multi-steer trailer and truck

Commercial trailer manufactures and axle system suppliers such as BPW [6], offers a range of steerable trailer axles, as shown in Figure 10. A mechanical link, a hydraulic system or the fifth wheel may be used to actuate the rear axle set.

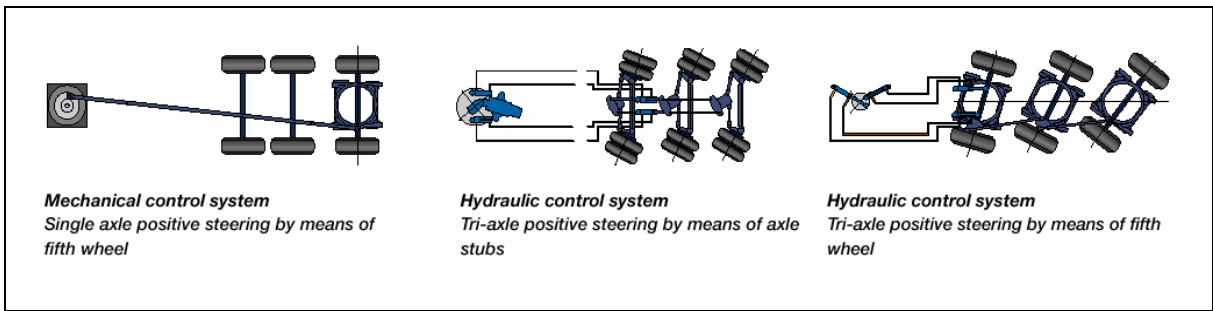


Figure 10 : Steerable trailer axes from BPW [6]

The multi-wheel drive/steering concept has been taken further by Multidrive [7]. The Multidrive truck-trailer combination drives with all four axles. The trailer axles are linked to the truck by a telescopic drive shaft. The trailer axles are also steered, by linking the trailer axles to the truck chassis using an a-frame. Superior off-road manoeuvrability and mobility is claimed. The concept is shown in Figure 11.

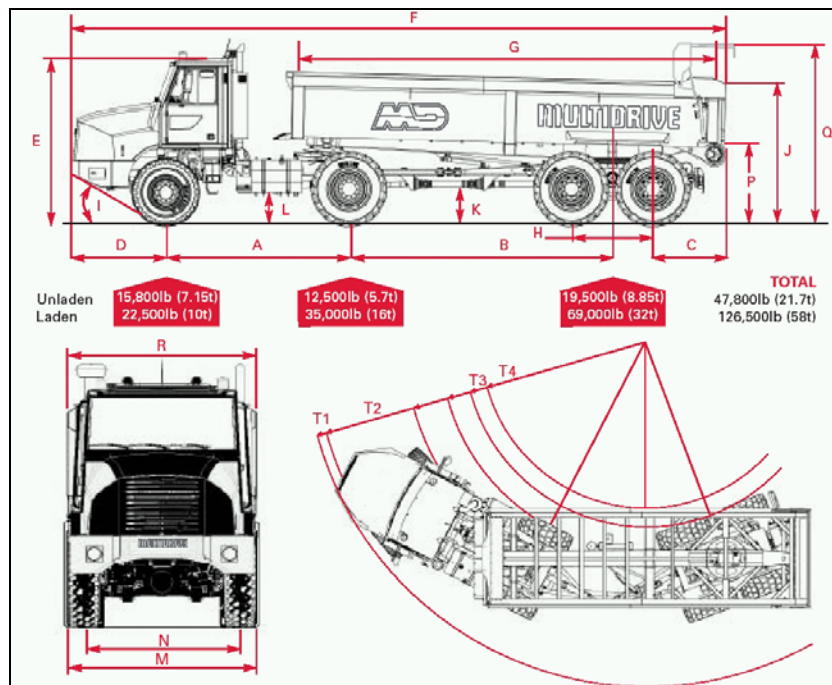


Figure 11 : Multidrive truck-trailer combination [7]

However, it should be noted that in all the examples above, the aim of a second steering axle was to achieve low speed manoeuvrability, and reduced tire scrub, and not necessarily improved handling at higher vehicle speeds.

Commercial off the shelf systems to control the individual axle angles have been developed, and an example is shown in Figure 12.

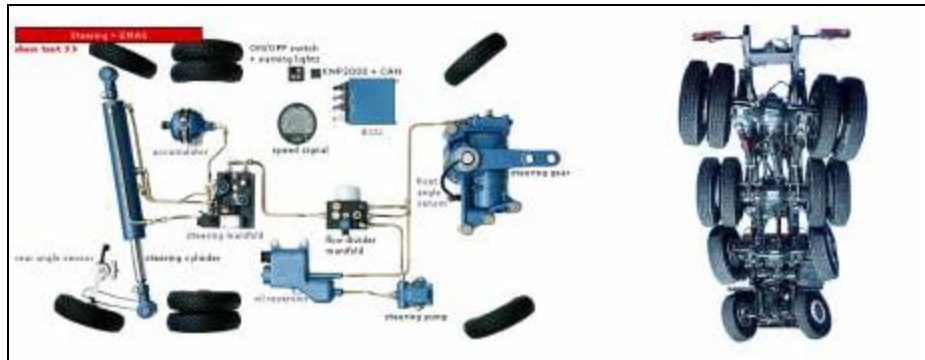


Figure 12 : EMAS automatic hydraulic steering [2]

These systems are primarily used to reduce tire wear and improve slow speed handling, where a reduced turning circle is of benefit.

5. Test vehicle information

As mentioned in paragraph 1, the ideal choice for a test vehicle would have been a twin axle steered 8x8 vehicle. However, due to availability, a 6x6 vehicle was used for the study.

The test vehicle used for the simulations and testing is the Bison weapon platform (BKW460M) [8]. Bison was developed for the SANDF as a concept demonstrator, and was never released for serial production. ARMSCOR uses the vehicle for tire testing and other technology development work. The vehicle is fitted with an ADE447T engine and six speed ZF WG200 automatic transmission.

The vehicle was evaluated in the unladen condition. Figure 13 indicates the main dimensions and position of the centre of mass of the test vehicle. Figure 14 shows the test vehicle on the test track. Table 1 indicates the measured wheel and axle mass, and Table 2 indicates the axle distances of the test vehicle. Table 3 indicates vehicle dimensions.

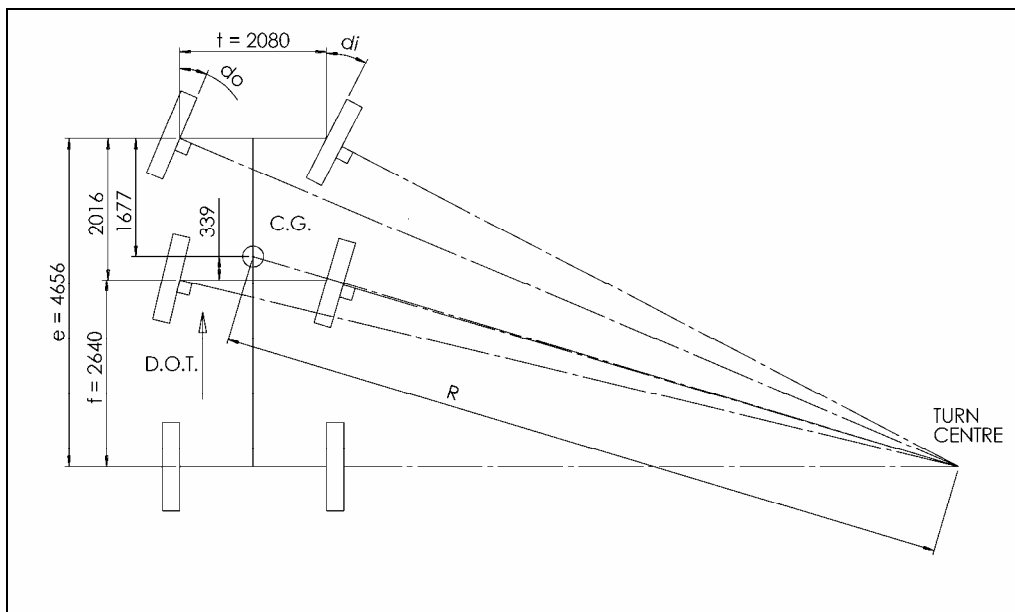


Figure 13 : Bison dimensions

Table 1 : Measured axle mass

Axle number	Left wheel [kg]	Right wheel [kg]	Axle total [kg]
1	2370	2490	5220
2	2760	2310	5070
3	2120	1800	3920
		Total	14210 kg

Table 2 : Axle distances

Axle number	Distance [mm]
1 to 2	2016
1 to 3	4656

Table 3 : Bison parameters

Description	Parameter
Vehicle track width	2080 mm
Height of centre of gravity	1515 mm
Width of vehicle	2325 mm
Height of cab	3030 mm
Tires	16.00 x 20 Michelin XL radial
Tire rolling radius	625 mm
Tire pressure	450 kPa



Figure 14 : Test vehicle: Bison

6. Mechanical integration of steering ratio changes

During the study planning phase, a high level investigation was done to determine the feasibility and practical arrangements on Bison, should the steering ratio be changed.

As a first step, for testing purposes only, the existing vehicle's steering system could be modified to accept stationary ratio changes, should it be required. Incidentally, the Bison vehicle is well suited to implement ratio changes. The steering system of the vehicle is mounted on the outside of the vehicle, and the first and second axle is connected with a series of mechanical links, as shown in Figure 15.

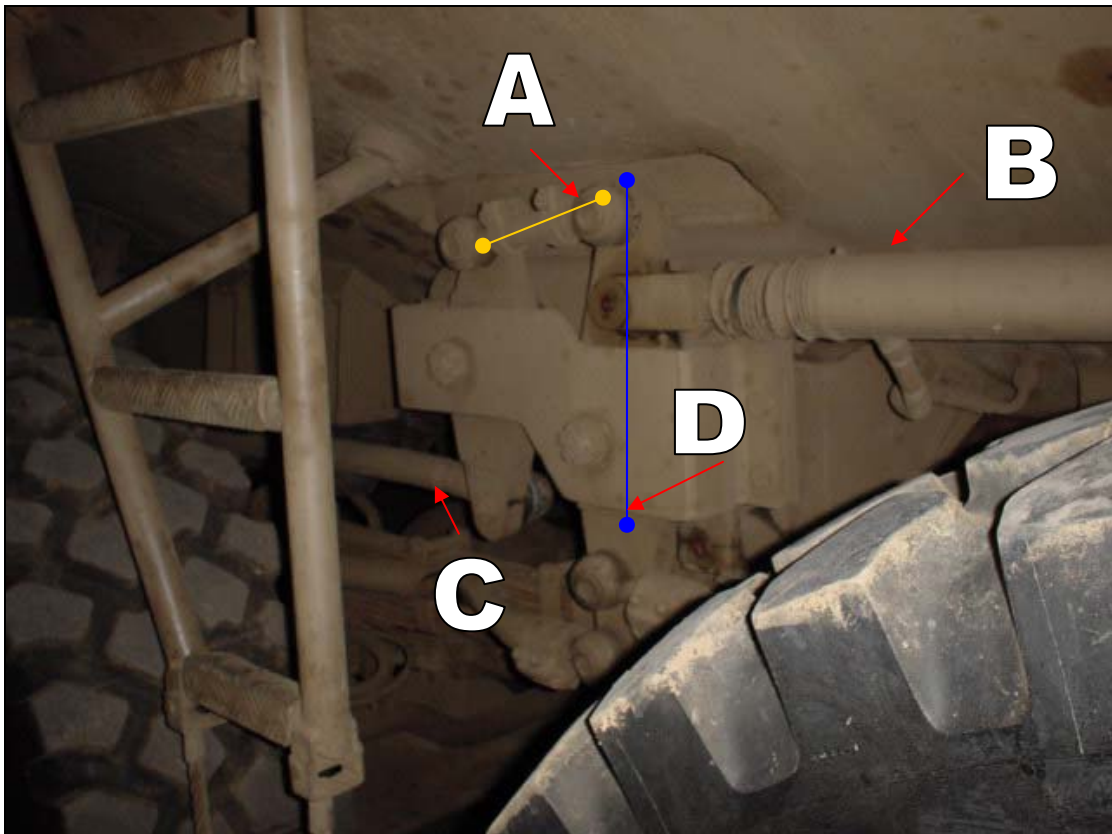


Figure 15 : Steering linkages

In Figure 15, *A* indicates the steering link between the first and second axle (yellow line), *B* indicates the hydraulic cylinder providing power assistance, *C* indicates the steering link to the front axle, and *D* (blue line), indicates the steering link to the second axle.

Ratio changes may be achieved by replacing link *A* with different lengths, or making an adjustable link using a thread system.

7. Steady state handling

7.1. Introduction

The cornering behaviour of a motor vehicle is an important performance mode often equated with handling. "Handling" is a loosely used term meant to imply the responsiveness of a vehicle to driver input, or the ease of control. As such, handling is an overall measure of the vehicle-driver combination. The driver and vehicle is a "closed-loop" system - meaning that the driver observes the vehicle direction or position, and corrects his/her input to achieve the desired motion. For purposes of characterizing only the vehicle, "open-loop" behaviour is used. Open-loop refers to vehicle response to specific steering inputs, and is more precisely defined as "directional response" behaviour [9,10].

The most commonly used measure of open-loop response is the understeer gradient. Understeer gradient is a measure of performance under steady-state conditions, although the measure can be used to infer performance properties under conditions that are not quite steady-state (quasi-steady-state conditions).

Open-loop cornering, or directional response behaviour, will be examined in this section. The approach is to first analyse turning behaviour at low speed, and then consider the differences that arise under high-speed conditions.

7.2. Low speed turning

At low speed, the tires of a vehicle does not need to develop lateral forces. The tires roll with no slip angle and the vehicle negotiates a turn, as described in Figure 16.

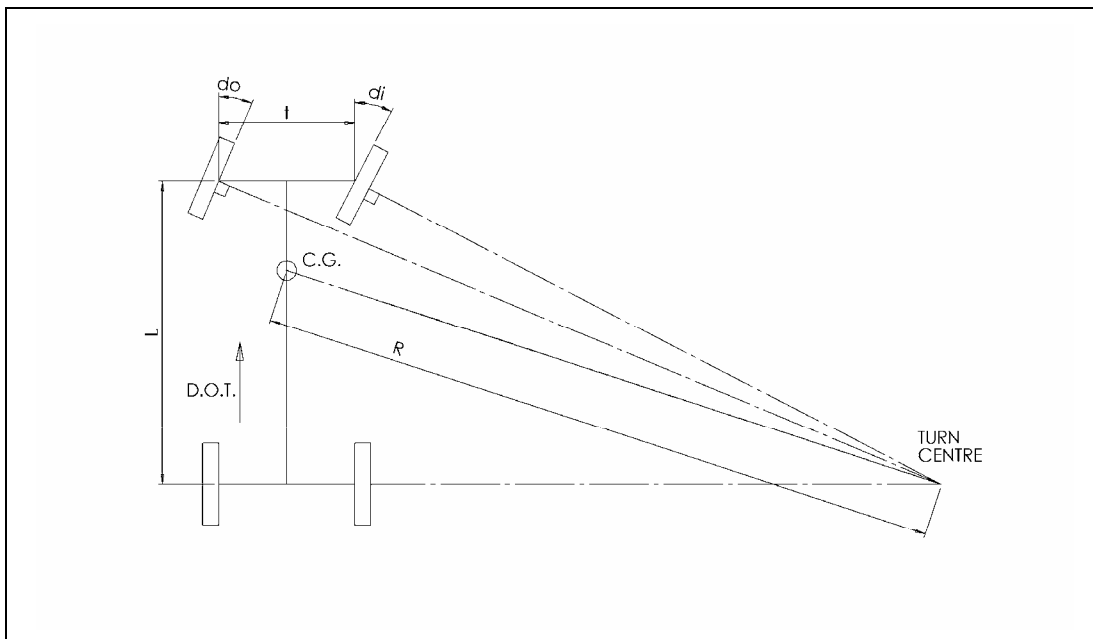


Figure 16 : Ackerman steering angle

If the rear wheels have no slip angle, the centre of the turn is situated on the projection line of the rear axle. Also, a perpendicular line from each of the front wheels should pass through the point of turn. If the line does not pass through the same point, the front tires will fight each other in the turn, with sideslip producing tire scrub. The ideal turning angles of the front wheels are determined by the geometry, as seen in Figure 16.

For proper geometry in the turn, assuming small steering angles, the steering angles (small angles) are given by:

$$\text{Outside wheel angle } \delta_o \cong \frac{L}{(R+t/2)} \quad (7.1)$$

$$\text{Inside wheel angle } \delta_i \cong \frac{L}{(R-t/2)} \quad (7.2)$$

The average angle of the front wheels (assuming small steering angles) is defined as the Ackerman angle:

$$\text{Ackerman angle } \delta = L/R \quad (7.3)$$

The term "Ackerman steering" or "Ackerman geometry" are often used to denote the exact geometry of the front wheels shown in Figure 16. The correct angles are dependent on the wheelbase of the vehicle and the angle of turn. Errors, or deviations, from the Ackerman geometry in the left-right steer angles can have a significant influence on front tire wear. Errors do not have a significant influence on directional response; however, they do affect the centreing torques in the steering system. With correct Ackerman geometry, the steering torques tend to increase consistently with steer angle, thus providing the driver with a natural feel in the feedback through the steering wheel. With the other extreme of parallel steer, the steering torques grows with angle initially, but may diminish beyond a certain point, and even become negative (tending to steer more deeply into the turn). This type of behaviour in the steering system is undesirable.

A four-axle vehicle, steering with the first and second axles, is shown in Figure 17.

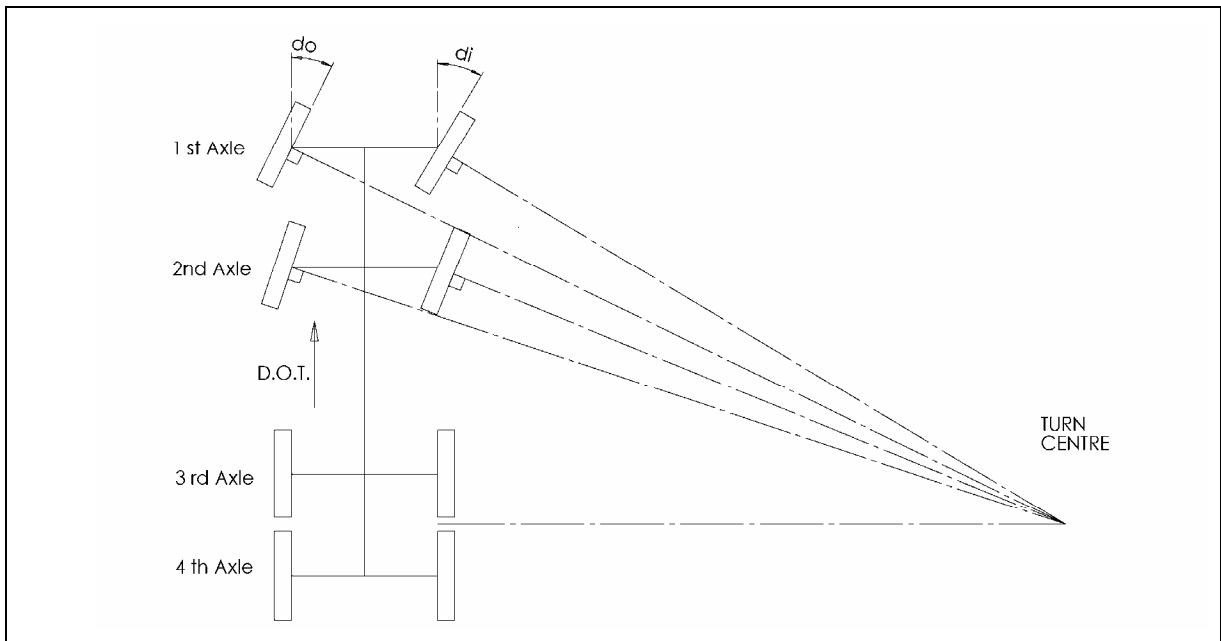


Figure 17 : Ackerman steering, eight wheel vehicle steering with first and second axles

The individual steering angles, for a specific turning radius, can be determined by halving the distance between the third and fourth axles, and connecting it perpendicular with the individual steering wheels, as shown in Figure 17, as per [11].

The other significant aspect of low-speed turning is the off-tracking that occurs at the rear wheels. The off-tracking distance, Δ , may be calculated from simple geometry relationships as:

$$\Delta = R[1 - \cos(L/R)] \quad (7.4)$$

Using the expression for a series expansion of the cosine, namely:

$$\cos z = 1 - \frac{z^2}{2!} + \frac{z^4}{4!} - \frac{z^6}{6!} \dots \quad (7.5)$$

Then:

$$\Delta \cong \frac{L^2}{2R} \quad (7.6)$$

For obvious reasons, off-tracking is primarily of concern with long-wheelbase vehicles such as trucks and buses. For articulated trucks, the geometric equations become more complicated and are known as "tractrix" equations.

7.3. High speed cornering

At high speed, the turning equations differ because lateral acceleration will be present. To counteract the lateral acceleration the tires must develop lateral forces, and slip angles will be present at each wheel.

7.4. Introduction to the tire model

The tire contact patch is the only contact between the wheeled vehicle and the road. It is therefore important to review tire models that may be used in the theoretical analysis. A brief background on tire models is given in the following paragraphs. Since actual measured tire data was available, measured data was used during the theoretical analysis.

7.4.1. Tire model literature review

Most notable among tire researchers and tire model developers is Pacejka [12-18], who developed the "*Magic Formula Tire Model*". This model developed by Pacejka is a semi-empirical one.

A variety of theoretical tire models are used in vehicle simulations. The models are often adapted for specific needs and use. Levels of accuracy and complexity may be and have been introduced in the various categories of utilization.

Many researchers in vehicle dynamics and four-wheeled-steer vehicles [19-21] have made use of the following tire model:

$$F_y = \alpha \cdot C_{F_\alpha} \quad (7.7)$$

Where the side force F_y is equal to the product of the cornering stiffness coefficient $C_{F\alpha}$ and the slip angle α . Recent studies on four-wheel-steer have made use of the simple model, even when more accurate models are available. The reason for this is that at low to moderate levels of lateral acceleration this model proves satisfactory. Secondly and more importantly, the model is easy to implement. The dynamic implementation of $C_{F\alpha}$ is further discussed in paragraph 7.5.

For the present study, measured tire data was available, as shown in paragraph 7.4.2.

Throughout the theoretical calculation, a second order polynomial has been fitted through the applicable measured data (tire load and tire pressure). Where required, the slope of the side force slip angle was determined, and used as $C_{F\alpha}$.

In this study, the linear tire model was deemed sufficient as a first order calculation; in order to determine first order tendencies for steady and transient state handling. If it was found that large benefit might be obtained from implementing individual steering angles, the models may be refined to include the non-linear side force slip angle relationship.

The handling manoeuvres that were performed, were not on the limit of the vehicle and the tires, since it was envisaged that any benefit that may be obtained by including variable steering axle ratios, should be implemented in normal driving situations, and not only in the instance where on-the-limit driving requires marginal improvement.

7.4.2. Measured tire data

Measured side force vs. slip angle data was available, and was used to calculate the cornering stiffness coefficient $C_{F\alpha}$. A typical tire data-measuring set-up is shown in Figure 18. A towing vehicle pulls a trailer equipped with an axle of which the wheel slip angles may be adjusted. The drawbar pull, as well as side force is measured, enabling the calculation of the tire side force generated. The actual heading angle of the trailer is also measured with a fifth wheel.



Figure 18 : Measuring tire data

The measured data is shown in Figure 19. As indicated, data for two axle loads (2370 kg and 4020 kg) and two tire pressures (400 kPa and 600 kPa) were available.

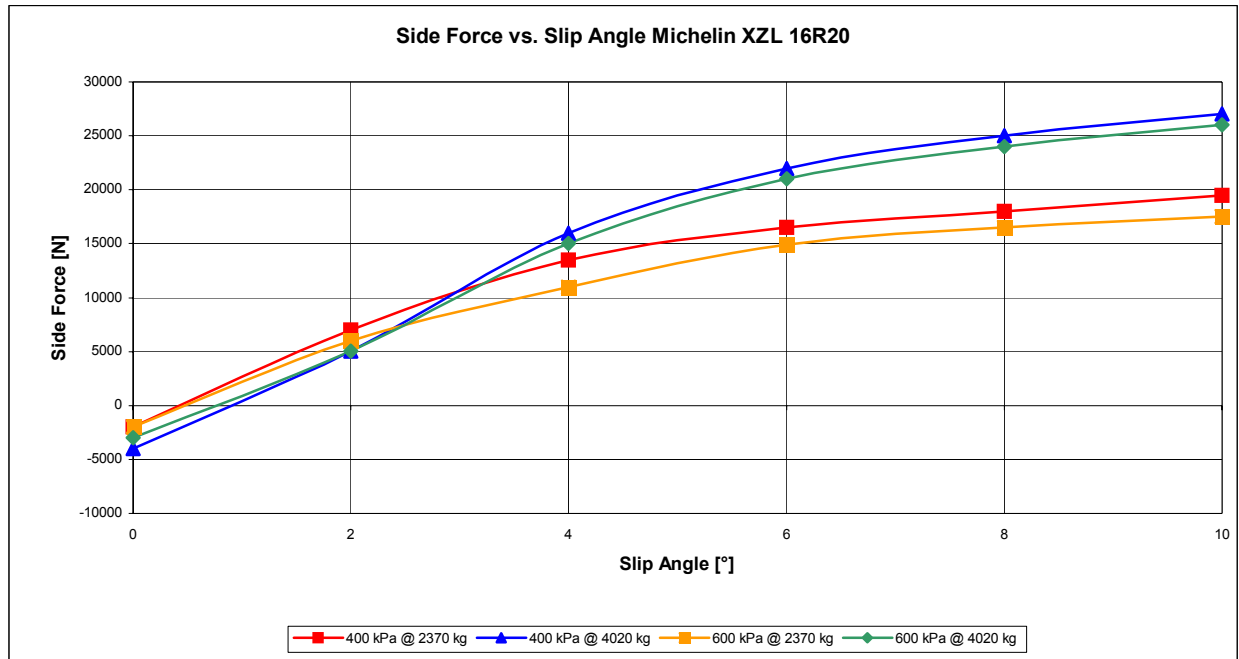


Figure 19 : Measured tire data

From Figure 19 it may be seen that the measured values have force offsets at a zero slip angle. Throughout the calculations in the investigation, the measured data was normalised by adjusting the curves with a positive offset, to obtain a zero force at zero slip angle.

Unless stated otherwise, the value for $C_{F\alpha}$:

$$C_{F\alpha} = 241780 \text{ N/rad (or } 4212 \frac{\text{N}}{\circ}) \tag{7.8}$$

7.5. Tire cornering forces

Under cornering conditions, in which the tire must develop a lateral force, the tire will also experience lateral slip as it rolls. The angle between its direction of heading and its direction of travel is known as slip angle, α . These are illustrated in Figure 20 [9].

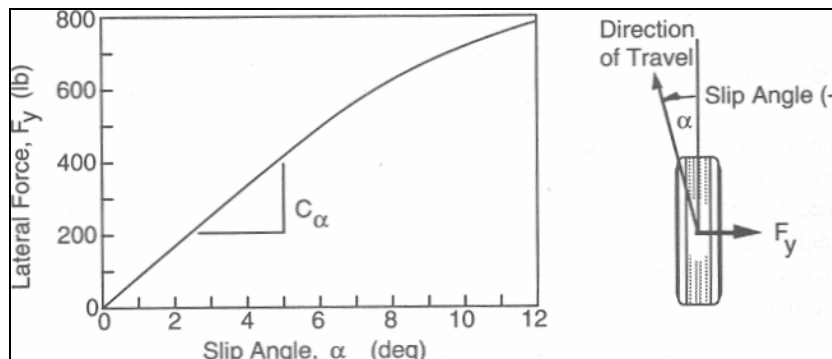


Figure 20 : Tire cornering force properties [9]

As discussed in paragraph 7.4.1, the lateral force, denoted by F_y , is called the "cornering force" when the camber angle is zero. At a given tire load, the cornering force grows with slip angle. At low slip angles (5 degrees or less) the relationship is linear.

A positive slip angle produces a negative force (to the left) on the tire, implying that $C_{F\alpha}$ must be negative; however, SAE defines cornering stiffness as the negative of the slope, such that $C_{F\alpha}$ takes on a positive value.

The cornering stiffness is dependent on many variables. Tire size and type (radial- vs. bias-ply construction), number of plies, cord angles, wheel width, and tread are significant variables. For a given tire, the load and inflation pressure are the main variables. Speed does not strongly influence the cornering forces produced by a tire.

Cornering coefficients are usually largest at light loads, diminishing continuously as the load reaches its rated value (Tire & Rim Association rated load [22]). At 100 % load, the cornering coefficient is typically in the range of 0.2 (kg cornering force per kg load per degree of slip angle).

7.6. Cornering equations

The steady-state cornering equations are derived from the application of Newton's Second Law along with the equation describing the geometry in turns (modified by the slip angle conditions necessary on the tires). For purposes of analysis, it is convenient to represent the vehicle by the bicycle model shown in Figure 21 [9].

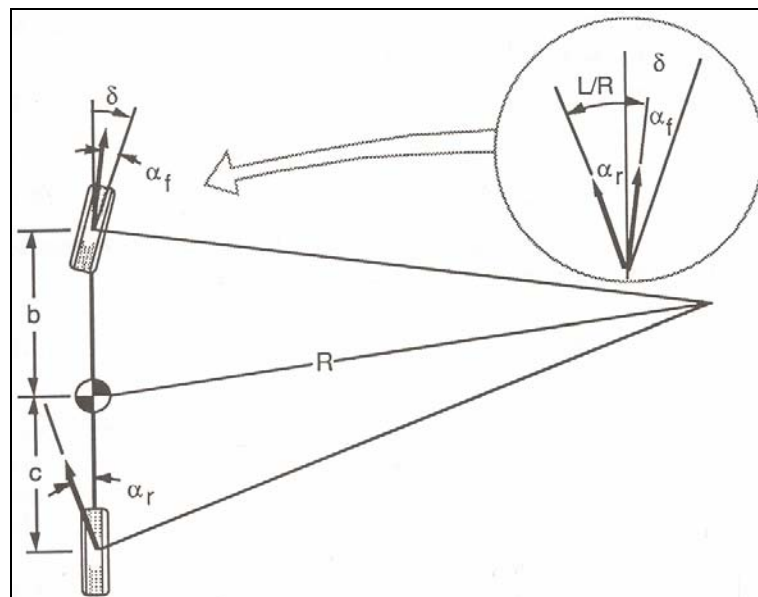


Figure 21 : Cornering of a bicycle model [9]

At high speeds the radius of turn is much larger than the wheelbase of the vehicle. Then small angles can be assumed, and the difference between steer angles on the outside and inside front wheels is negligible. Thus, for convenience, the two front wheels can be represented by one wheel at a steer angle, δ , with a cornering force equivalent to both wheels. The same assumption is made for the rear wheels.

For a vehicle travelling forward with a speed of V , the sum of the forces in the lateral direction from the tires must equal the mass times the centripetal acceleration [9].

$$\sum F_y = F_{yf} + F_{yr} = \frac{MV^2}{R} \quad (7.9)$$

where:

F_{yf} = Lateral (cornering) force at the front axle

F_{yr} = Lateral (cornering) force at the rear axle

M = Mass of the vehicle

V = Forward velocity

R = Radius of the turn

Also, for the vehicle to be in a moment equilibrium about the centre of gravity, the sum of the moments from the front and rear lateral forces must be zero [9]:

$$F_{yf}b - F_{yr}c = 0 \quad (7.10)$$

Thus:

$$F_{yf} = F_{yr}c/b \quad (7.11)$$

Substituting yields:

$$M V^2/R = F_{yr} (c/b+1) = F_{yr} (b+c)/b = F_{yr}L/b \quad (7.12)$$

$$F_{yr} = M b/L (V^2/R) \quad (7.13)$$

But $M b/L$ is simply the portion of the vehicle mass carried on the rear axle (i.e., W_r/g); thus the lateral force developed at the rear axle must be W_r/g times the lateral acceleration at that point. Solving for F_{yf} in the same fashion will indicate that the lateral force at the front axle must be W_f/g times the lateral acceleration.

With the required lateral forces known, the slip angles at the front and rear wheels are also established [9]. That is:

$$\alpha_f = W_f V^2 / (C_{af} g R) \quad \text{and} \quad (7.14)$$

$$\alpha_r = W_r V^2 / (C_{ar} g R) \quad (7.15)$$

Using the geometry of the vehicle in the turn, from Figure 21, it can be seen that [9]:

$$\delta = L/R + \alpha_f - \alpha_r \quad (7.16)$$

Now substituting for α_f and α_r gives:

$$\delta = \frac{L}{R} + \frac{W_f V^2}{C_{af} g R} - \frac{W_r V^2}{C_{ar} g R} \quad (7.17)$$

$$\delta = \frac{L}{R} + \left(\frac{W_f}{C_{af}} - \frac{W_r}{C_{ar}} \right) \frac{V^2}{gR} \quad (7.18)$$

where [9]:

δ	=	Steer angle at the front wheels (rad)
L	=	Wheelbase
R	=	Radius of turn
V	=	Forward speed
g	=	Gravitational acceleration constant
W_f	=	Load on the front axle
W_r	=	Load on the rear axle
C_{af}	=	Cornering stiffness of the front tires (n/rad)
C_{ar}	=	Cornering stiffness of the rear tires (n/rad)

7.7. Understeer gradient

The equation is often written in a shorthand form as follows [9]:

$$\delta = L/R + K a_y \quad (7.19)$$

where:

K	=	Understeer gradient (rad/g)
a_y	=	Lateral acceleration (g)

The above equation is very important to the turning response properties of a vehicle. It describes how the steer angle of the vehicle must be changed with the radius of turn, R, or the lateral acceleration, $V^2/(gR)$. The term $(W_f/C_{af} - W_r/C_{ar})$ determines the magnitude and direction of the steering inputs required. It consists of two terms, each of which is the ratio of the load on the axle (front or rear) to the cornering stiffness of the tires on the axle. It is called the "Understeer gradient", and will be denoted by the symbol, K, which has the units of degrees/g. Three possibilities exist [9]:

$$1) \quad \text{Neutral steer: } W_f / C_{af} = W_r / C_{ar} \rightarrow K = 0 \rightarrow \alpha_f = \alpha_r \quad (7.20)$$

On a constant-radius turn, no change in steer angle will be required as the speed is varied. Specifically, the steer angle required to make the turn will be equivalent to the Ackerman angle, L/R. Physically, the neutral steer case corresponds to a balance on the vehicle such that the "force" of the lateral acceleration at the CG causes an identical increase in slip angle at both the front and rear wheels [9]:

$$2) \quad \text{Understeer:} \quad W_f / C_{af} > W_r / C_{ar} \rightarrow K > 0 \rightarrow \alpha_f > \alpha_r \quad (7.21)$$

On a constant-radius turn, the steer angle will have to increase with speed in proportion to K (deg/g) times the lateral acceleration in g's. Thus it increases linearly with the lateral acceleration and with the square of the speed. In the understeer case, the lateral acceleration at the CG causes the front wheels to slip sideways to a greater extent than at the rear wheels. Thus to develop the lateral force at the front wheels necessary to maintain the radius of turn, the front wheels must be steered to a greater angle [9].

$$3) \quad \text{Oversteer:} \quad W_f / C_{af} < W_r / C_{ar} \rightarrow K < 0 \rightarrow \alpha_f < \alpha_r \quad (7.22)$$

On a constant-radius turn, the steer angle will have to decrease as the speed (and lateral acceleration) is increased. In this case, the lateral acceleration at the CG causes the slip angle on the rear wheels to increase more than at the front. The outward drift at the rear of the vehicle turns the front wheels inward, thus diminishing the radius of turn. The increase in lateral acceleration that follows causes the rear to drift out even further and the process continues unless the steer angle is reduced to maintain the radius of turn.

The way in which steer angle changes with speed on a constant-radius turn for each of these cases is illustrated in Figure 22. With a neutral steer vehicle, the steer angle to follow the curve at any speed is simply the Ackerman angle.

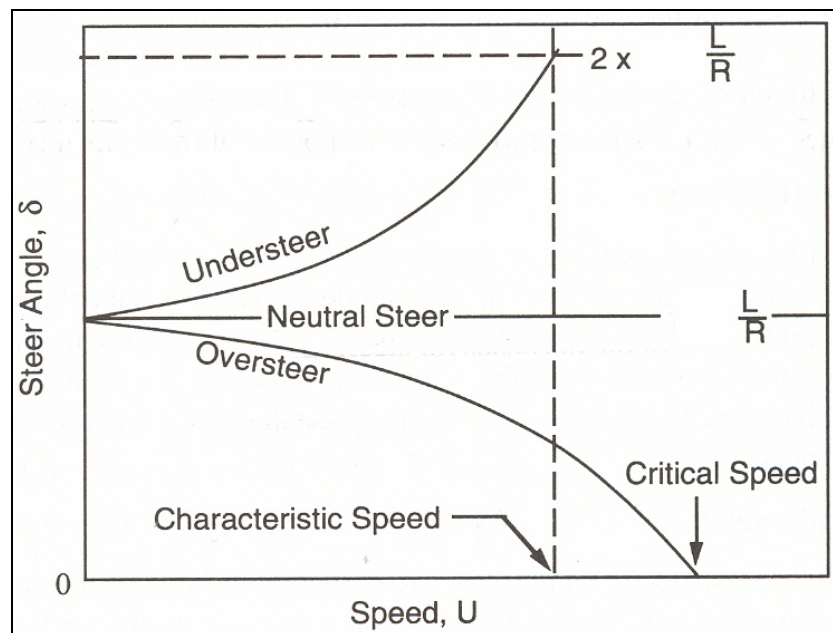


Figure 22 : Change of steer angle with speed [9]

With understeer the angle increases with the square of the speed, reaching twice the initial angle at the characteristic speed. In the oversteer case, the steer angle decreases with the square of the speed and becomes zero at the critical speed value.

8. Tire wear

In the present study, tire wear may be one of the greatest advantages of variable ratio steering systems. Information from tire manufactures on the reasons for tire wear is therefore given in the following paragraph.

According to Michelin [23] the greatest impact on tire life is tire pressure, as illustrated in the figure published on their web site, and shown in Figure 23. The figure indicates that if the tire pressure drops below 60% or is increased above 120% of the recommended pressure per axle load, the incorrect pressure will result in loss of service of more than 50%.

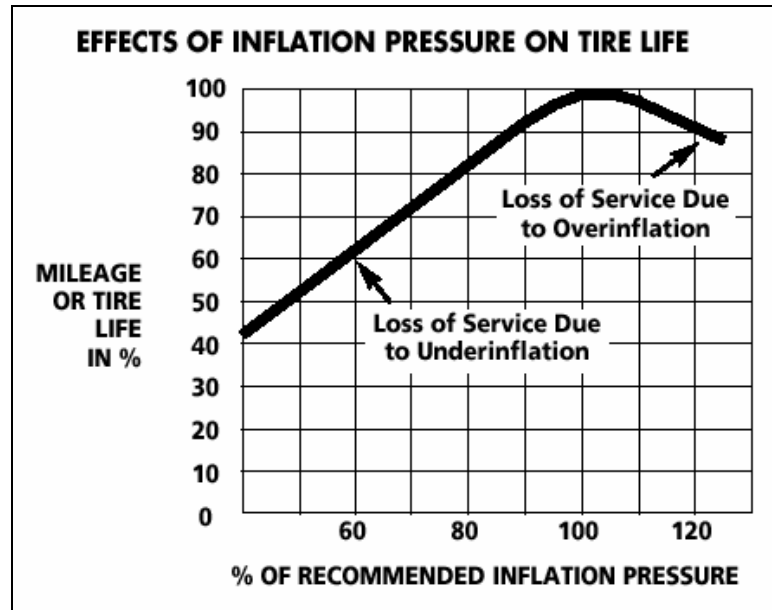


Figure 23 : Tire life for different tire pressures [23]

According to tire manufacturers and tire specialists (Supaquick [24], Yokohama [25], Dunlop [26] and Continental [27]), tire wear is also influenced by:

- Seasonal and climatic conditions
- The road or track it is used on, including the surface characteristics, the path that is followed (straight line compared to curves)
- Incorrect inflation pressures
- Incorrect tire fitment
- Poor maintenance
- Driving style
- The load on the tire and the load rating of the tire
- The rotational speed of the tire
- The number of stop/start cycles, and the severity of the manoeuvres

- Correct tire fitment, balancing and rim size

A study on tire wear on a 6x6 all wheel steer vehicle was performed, as described in [4]. The rear axle of the vehicle was used to evaluate tire wear, by driving through an obstacle course, using different steering control strategies. An improvement of between 11% and 52% in tire wear was achieved, where the steering geometry follows the Ackerman steering principle closely, i.e. roll without slip.

As described in paragraph 4.1, trailer system manufactures have developed various steering methods to reduce tire wear.

9. Test vehicle low speed turning requirements

The Ackerman angle is defined as the steering angle that is required to enable the wheels on the steering axle to roll without slip. For a three-axle vehicle, steering with the first and second axle, the tuning point is defined as the intersection of the line parallel to the rear axle, intersecting with lines perpendicular with the steering wheels.

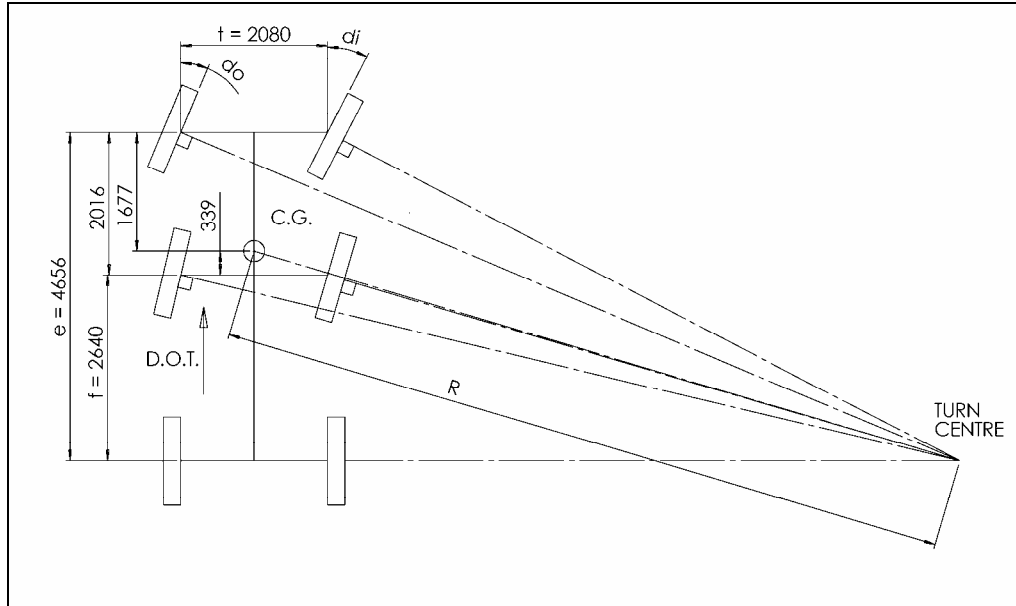


Figure 24 : Ackerman steering Bison

The average Ackerman angle for the first axle is therefore the wheelbase (distance between first and last axle) divided by the radius of turn, R .

The average Ackerman angle for the second axle is the distance between second and third axle divided by the radius of turn. The Ackerman ratio between the second and first axle is therefore:

e = distance between first and last axle

f = distance between second and last axle

Ar = Ackerman ratio

$$Ar = \frac{f/R}{e/R} = \frac{f}{e} = \frac{2640}{4656} = 0.57 \quad \text{or} \quad (\text{steering angle of 2}^{\text{nd}} \text{ axle}) = 0.57 \times (\text{steering angle 1}^{\text{st}} \text{ axle}) \quad (9.1)$$

The above definition is therefore independent of the track width and the turning circle.

In the following paragraphs, two different steering ratios are used and mentioned. One is the Ackerman steering ratio and the other the actual steering ratio. The Ackerman ratio is the theoretical steering ratio based on the vehicle geometry, in this case approximately 0.57. An actual steering ratio of the vehicle is also measured and referred to. This ratio was determined by physical measurement, and is described in 18.6. (It was found that the measured ratio, in the region of zero steering angle, is closer to 0.7).

10. Constant radius: expanding the cornering equations to a four axle configuration

As mentioned in the paragraphs above, it was originally intended to use an 8x8 vehicle. The bicycle model can be expanded to a four-axle vehicle. The model is then simplified to a three-axle vehicle, as described in the following paragraphs.

A simple bicycle model can be constructed to calculate the steering and slip angles of a four-axle vehicle, steering with the first and second axles. Because of the constant angular speed, the slip angles must give no moment about the centre of mass G . Rolling resistance and aerodynamic forces are neglected. The vehicle is rotating around C_T , the turn centre. The tire forces are perpendicular to the wheels, and intersect at the force centre C_F . The line of action of the resultant force on the vehicle is through the CG towards the point C_F . This force has the desired centripetal component towards C_T .

The steer angles for the vehicle can be defined as the angles between the perpendicular tire forces from the front and rear axles.

Figure 25 shows a scaled layout of a vehicle negotiating a 20 meter radius turn. A positive under steer angle (i.e. $\alpha_f > \alpha_r$) is assumed. An enlarged view is shown in Figure 26.

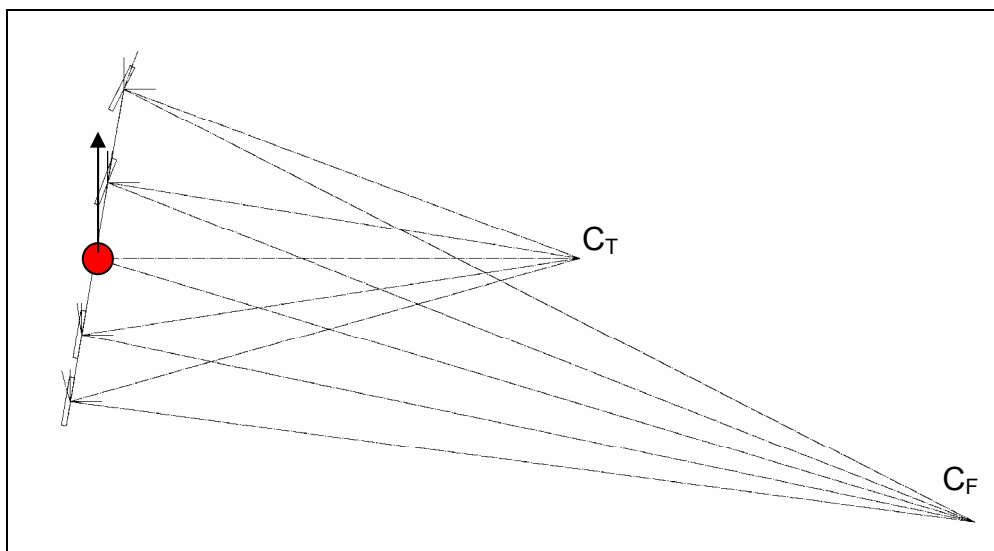


Figure 25 : Slip angle diagram

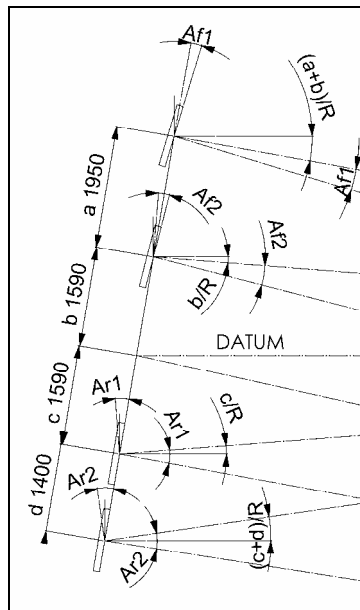


Figure 26 : Detail slip angle diagram

The steer angles for the vehicle can be defined as the angles between the perpendicular tire forces from the front and rear axles.

The geometry of the vehicle is defined as:

- R = Radius of the turn
- a = Distance between the first and second axles
- b = Distance between the second axle and centre of mass
- c = Distance between the centre of mass and third axle
- d = Distance between the third and fourth axle
- t = Track width

The Ackerman angle (all angles in radians, unless noted otherwise and small angles assumed) for the first axle is therefore:

$$\text{First axle Ackerman} : (a + b + c + d / 2) / (R)$$

$$\text{Second axle Ackerman} : (b + c + d / 2) / (R)$$

The steer angle of the third and fourth axles, relative to a datum line, can be shown to be:

$$\text{Wheels_angle_to_datum_rear} = \alpha_{r1} - \frac{c}{R} - (\alpha_{r2} - \frac{(c+d)}{R}) \tag{10.1}$$

The first axle angle relative to the datum can be shown to be:

$$\text{First_axle_angle_to_datum} = \alpha_{f1} + \frac{(a+b)}{R} \tag{10.2}$$

The second axle angle relative to the datum can be shown to be:

$$\text{Second_axle_angle_to_datum} = \alpha_{f2} + \frac{(b)}{R} \quad (10.3)$$

The steering angle of the first axle is therefore the difference of the first axle and the reference axle (third and fourth axle):

$$\begin{aligned} \text{Steering_angle_first_axle} : \delta_1 &= \alpha_{f1} + \frac{(a+b)}{R} - \left[\alpha_{r1} - \frac{c}{R} - \left(\alpha_{r2} - \frac{(c+d)}{R} \right) \right] \\ \delta_1 &= \alpha_{f1} - \alpha_{r1} + \alpha_{r2} + \frac{(a+b)}{R} + \frac{c}{R} - \frac{(c+d)}{R} \\ \delta_1 &= \alpha_{f1} - \alpha_{r1} + \alpha_{r2} + \frac{(a+b-d)}{R} \end{aligned} \quad (10.4)$$

The steering angle of the second axle is therefore the difference of the second axle and the reference axle (third and fourth axle):

$$\begin{aligned} \text{Steering_angle_2nd_axle} : \delta_2 &= \alpha_{f2} + \frac{(b)}{R} - \left[\alpha_{r1} - \frac{c}{R} - \left(\alpha_{r2} - \frac{(c+d)}{R} \right) \right] \\ \delta_2 &= \alpha_{f2} + \frac{(b)}{R} - \alpha_{r1} + \frac{c}{R} + \alpha_{r2} - \frac{(c+d)}{R} \\ \delta_2 &= \alpha_{f2} - \alpha_{r1} + \alpha_{r2} + \frac{(b-d)}{R} \end{aligned} \quad (10.5)$$

For a vehicle travelling forward with a speed of V, the sum of the forces in the lateral direction from the tires must equal the mass times the centripetal acceleration:

$$\sum F_y = F_{yf1} + F_{yf2} + F_{yr1} + F_{yr2} = M V^2/R \quad (10.6)$$

where:

- F_{yf1} = Lateral (cornering) force at the first axle
- F_{yf2} = Lateral (cornering) force at the second axle
- F_{yr1} = Lateral (cornering) force at the third axle
- F_{yr2} = Lateral (cornering) force at the fourth axle
- M = Mass of the vehicle
- V = Forward velocity
- R = Radius of the turn

Also, for the vehicle to be in a moment equilibrium about the centre of gravity, the sum of the moments from the front and rear lateral forces must be zero.

$$F_{yf1}(a+b) + F_{yf2}(b) - F_{yr1}(c) - F_{yr2}(c+d) = 0 \quad (10.7)$$

The lateral tire forces can be expressed as a function of the cornering stiffness and the slip angle required to develop the cornering force:

$$\alpha_{f1}C_{yf1}(a+b) + \alpha_{f2}C_{yf2}(b) - \alpha_{r1}C_{yr1}(c) - \alpha_{r2}C_{yr2}(c+d) = 0 \quad (10.8)$$

$$\alpha_{f1}C_{yf1} + \alpha_{f2}C_{yf2} + \alpha_{r1}C_{yr1} + \alpha_{r2}C_{yr2} = M V^2/R \quad (10.9)$$

A steering relationship between the first and second axle is chosen to follow the Ackerman principle. Define the steering ratio between the first and second axle as Sr . The relationship is a mechanical relationship between the first and second axle that is controlled by the steering geometry.

$$\delta_2 = Sr \times \delta_1 \quad (10.10)$$

The equations can therefore be summarised below:

$$\delta_1 = \alpha_{f1} - \alpha_{r1} + \alpha_{r2} + \frac{(a+b-d)}{R} \quad (10.11)$$

$$\delta_2 = \alpha_{f2} - \alpha_{r1} + \alpha_{r2} + \frac{(b-d)}{R} \quad (10.12)$$

$$\delta_2 = Sr \times \delta_1 \quad (10.13)$$

$$\alpha_{f1}C_{yf1}(a+b) + \alpha_{f2}C_{yf2}(b) - \alpha_{r1}C_{yr1}(c) - \alpha_{r2}C_{yr2}(c+d) = 0 \quad (10.14)$$

$$\alpha_{f1}C_{yf1} + \alpha_{f2}C_{yf2} + \alpha_{r1}C_{yr1} + \alpha_{r2}C_{yr2} = M V^2/R \quad (10.15)$$

The above relations are shown on a scale drawing of a typical 8x8 vehicle geometry in Figure 27.

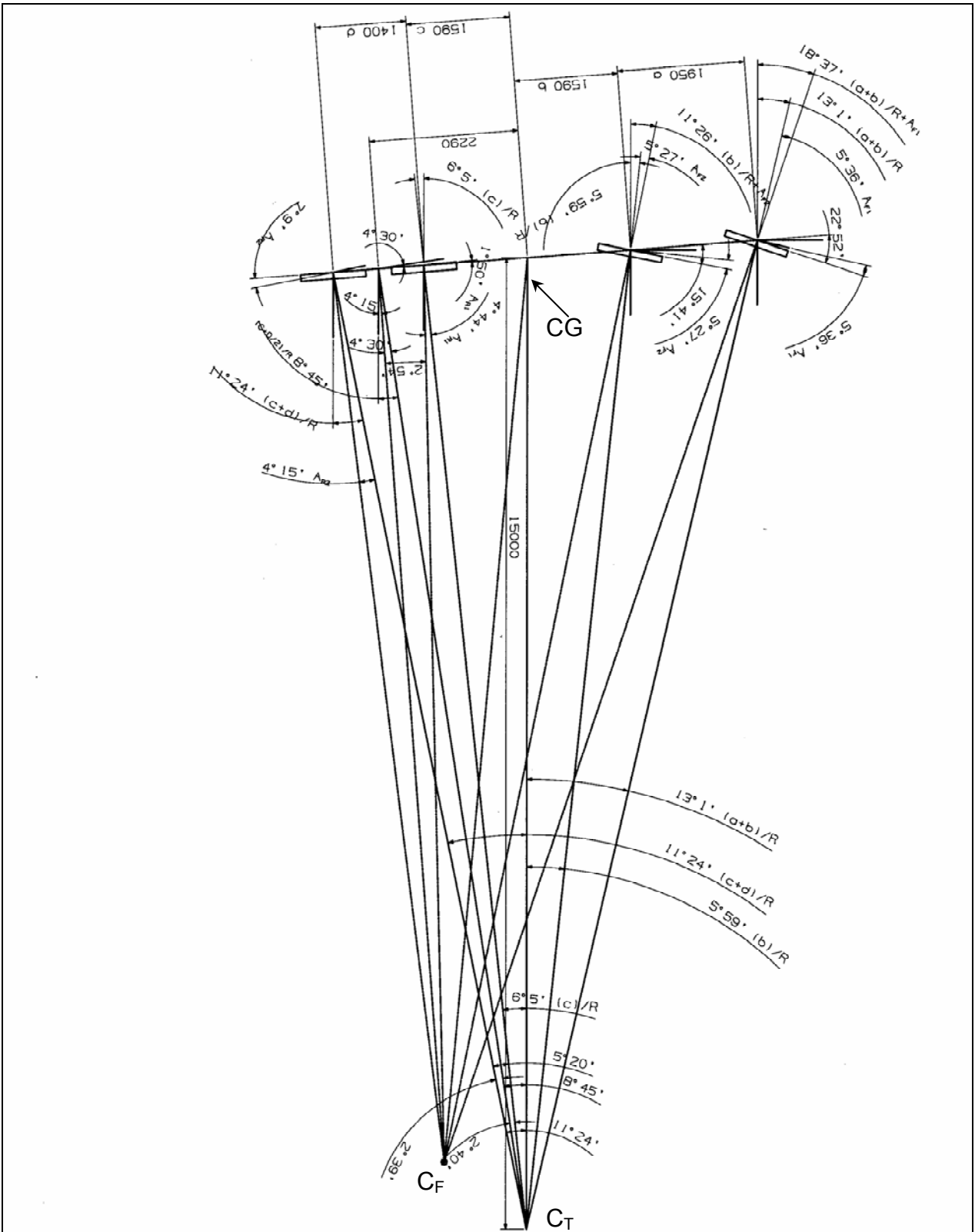


Figure 27 : Scale drawing of an 8x8 geometry

The following six parameters are unknown:

$$\alpha_{f1}, \alpha_{f2}, \alpha_{r1}, \alpha_{r2}, \delta_1, \delta_2, Sr$$

The equations can be rearranged in matrix format:

$$\begin{bmatrix} 1 & 0 & -1 & 0 & 1 & -1 \\ 0 & 1 & 0 & -1 & 1 & -1 \\ -Sr & 1 & 0 & 0 & 0 & 0 \\ 0 & 0 & (a+b)C_{yf1} & (b)C_{yf2} & -(c)C_{yr1} & -(c+d)C_{yr2} \\ 0 & 0 & C_{yf1} & C_{yf2} & C_{yr1} & C_{yr2} \\ 1 & 0 & 0 & 0 & 0 & 0 \end{bmatrix} \cdot \begin{bmatrix} \delta_1 \\ \delta_2 \\ \alpha_{f1} \\ \alpha_{f2} \\ \alpha_{r1} \\ \alpha_{r1} \end{bmatrix} = \begin{bmatrix} (a+b-d)/R \\ (b-d)/R \\ 0 \\ 0 \\ Mv^2/R \\ iterate \end{bmatrix}$$

To solve for the six unknown parameters using five equations, the steering angle for the first axle may be chosen, and the slip angles calculated, by varying the steering angle, all the possible solutions can be compared, and the steering angle suited for a specific radius and vehicle speed or other requirement.

The unknowns may be solved using Gauss elimination, by writing the matrix in the form $[A]\{x\}=\{b\}$, ensuring that x is non-singular and calculating $\{x\} = [A]^{-1}\{b\}$.

The lack of a test vehicle necessitates that the above equations be simplified and tailored for a 6x6 vehicle. The process is described in paragraph 11. The method of solving the equations using Matlab is also discussed.

11. Constant radius bicycle model

11.1. Developing the three axle bicycle model

Figure 28 assumes a positive under steer angle, i.e. $\alpha_f > \alpha_r$

The steer angles of the first axle and the second axle are determined first.

The steer angles for the vehicle can be defined as the angles between the perpendicular tire forces from the front and rear axles.

The model may be simplified to suit the 6x6 geometry, as shown in Figure 28.

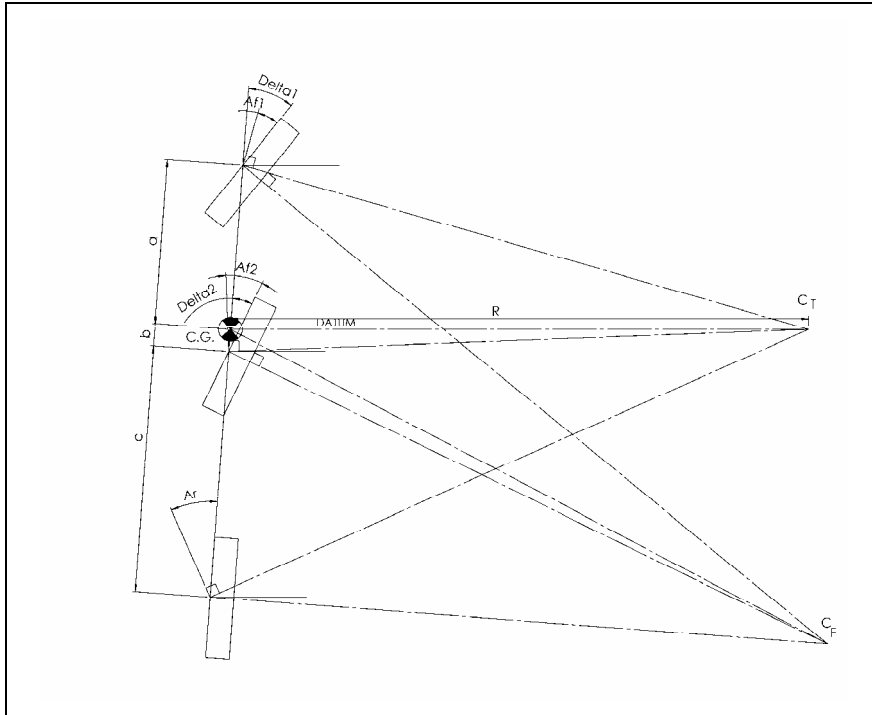


Figure 28 : Bison three axle bicycle model

The rear axle angle relative to the datum can be shown to be:

$$\text{Rear_axle_angle_to_datum_rear} = \left(\alpha_r - \frac{(b+c)}{R} \right) \quad (11.1)$$

The first axle angle relative to the datum can be shown to be:

$$\text{First_axle_angle_to_datum} = \alpha_{f1} + \frac{(a)}{R} \quad (11.2)$$

The second axle angle relative to the datum can be shown to be:

$$\text{Second_axle_angle_to_datum} = \alpha_{f2} - \frac{(b)}{R} \quad (11.3)$$

The steering angle of the first axle is therefore the difference of the first axle and the reference axle (third axle):

$$\text{Steering_angle_first_axle} : \delta_1 = \alpha_{f1} - \alpha_r + \frac{(a+b+c)}{R} \quad (11.4)$$

The steering angle of the second axle is therefore the difference of the second axle and the reference axle (third axle):

$$\text{Steering_angle_second_axle} : \delta_2 = \alpha_{f2} - \alpha_r + \frac{(c)}{R} \quad (11.5)$$

For a vehicle travelling forward with a speed of V , the sum of the forces in the lateral direction from the tires must equal the mass times the centripetal acceleration.

$$\sum F_y = F_{yf1} + F_{yf2} + F_{yr} = M V^2/R \quad (11.6)$$

Therefore where:

- F_{yf1} = Lateral (cornering) force at the first axle
- F_{yf2} = Lateral (cornering) force at the second axle
- F_{yr} = Lateral (cornering) force at the third axle
- M = Mass of the vehicle
- V = Forward velocity
- R = Radius of the turn

Also, for the vehicle to be in a moment equilibrium about the centre of gravity, the sum of the moments from the front and rear lateral forces must be zero:

$$F_{yf1}(a) - F_{yf2}(b) - F_{yr}(b+c) = 0 \quad (11.7)$$

The lateral tire forces can be expressed as a function of the cornering stiffness and the slip angle required to develop the cornering force:

$$\alpha_{f1}C_{yf1}(a) - \alpha_{f2}C_{yf2}(b) - \alpha_r C_{yr}(b+c) = 0 \quad (11.8)$$

and substituting into equation 11.6:

$$\alpha_{f1}C_{yf1} + \alpha_{f2}C_{yf2} + \alpha_r C_{yr} = M V^2/R \quad (11.9)$$

A steering relationship (Sr) between the first and second axle is chosen to follow the Ackerman principle. The relationship is a mechanical relationship between the first and second axle that is controlled by the steering geometry:

$$\delta_2 = Sr \times \delta_1 \quad (11.10)$$

The equations can therefore be summarised below:

$$\delta_1 = \alpha_{f1} - \alpha_r + \frac{(a+b+c)}{R} \quad (11.11)$$

$$\delta_2 = \alpha_{f2} - \alpha_r + \frac{(c)}{R} \quad (11.12)$$

$$\delta_2 = Sr \times \delta_1 \quad (11.13)$$

$$\alpha_{f1}C_{yf1}(a) - \alpha_{f2}C_{yf2}(b) - \alpha_r C_{yr}(b+c) = 0 \quad (11.14)$$

$$\alpha_{f1}C_{yf1} + \alpha_{f2}C_{yf2} + \alpha_r C_{yr} = M V^2/R \quad (11.15)$$

The following five parameters are unknown:

$$\alpha_{f1}, \alpha_{f2}, \alpha_r, \delta_1, \delta_2, Sr$$

To solve for the five unknown parameters a matrix is compiled:

$$\begin{bmatrix} 1 & 0 & -1 & 0 & +1 \\ 0 & 1 & 0 & -1 & +1 \\ 0 & 0 & C_{yf1} & C_{yf2} & C_{yr} \\ 0 & 0 & (a)C_{yf1} & -(b)C_{yf2} & -(b+c)C_{yr1} \\ -Sr & 1 & 0 & 0 & 0 \end{bmatrix} \cdot \begin{bmatrix} \delta_1 \\ \delta_2 \\ \alpha_{f1} \\ \alpha_{f2} \\ \alpha_r \end{bmatrix} = \begin{bmatrix} (a+b+c)/R \\ (c)/R \\ Mv^2/R \\ 0 \\ 0 \end{bmatrix}$$

A Matlab routine to solve the above equations is shown in Appendix C: Constant radius test – Matlab M file.

The unknowns may be solved using Gauss elimination, by writing the matrix in the form $[A]\{x\}=\{b\}$, ensuring that x is non-singular and calculating $\{x\} = [A]^{-1}\{b\}$.

The following philosophy was followed:

- i. Define a set of steering ratios from 0.3 to 1.2
- ii. Define a set of vehicle speeds, from 20 km/h to 80 km/h
- iii. Define a vehicle mass and geometry
- iv. Solve for the steering angles and slip angles

12. Constant radius: simulation results, simplified bicycle model

From paragraph 11, a matrix can be solved to determine the required steering angles for the vehicle to perform a constant radius test. The following parameters are used as input to calculate the steering angles and wheel slip angles:

- i. Vehicle speed : V
- ii. Radius of turn : R
- iii. Steering ratio between first and second axle : Sr (Indicated as “Ratio” in the graphs)
- iv. Tire characteristics:
Measured tire data was used as input for the calculation
- v. Vehicle mass:
Results were calculated for the vehicle in the unladen configuration
- vi. Vehicle centre of mass:
Were calculated using the measured axle mass in the empty configuration
- vii. Vehicle geometry

In an attempt to determine the effect of the steering ratio (ratio between the average angle of the first and second steering axle angle) on steering angles and slip angles, the model parameters were varied to determine the effect of vehicle speed, radius of the track and steering ratio (between the first and second axles).

The following assumptions were made, in order to simplify the calculations:

- i. No load transfer from left to right (and vice versa) was included
- ii. A linear tire model was used
- iii. Camber changes were neglected
- iv. Constant steering ratio between first and second axles was assumed
- v. Negative steering ratios were evaluated as well, even though it may not be a practical solution

The results are shown and discussed in the following paragraphs.

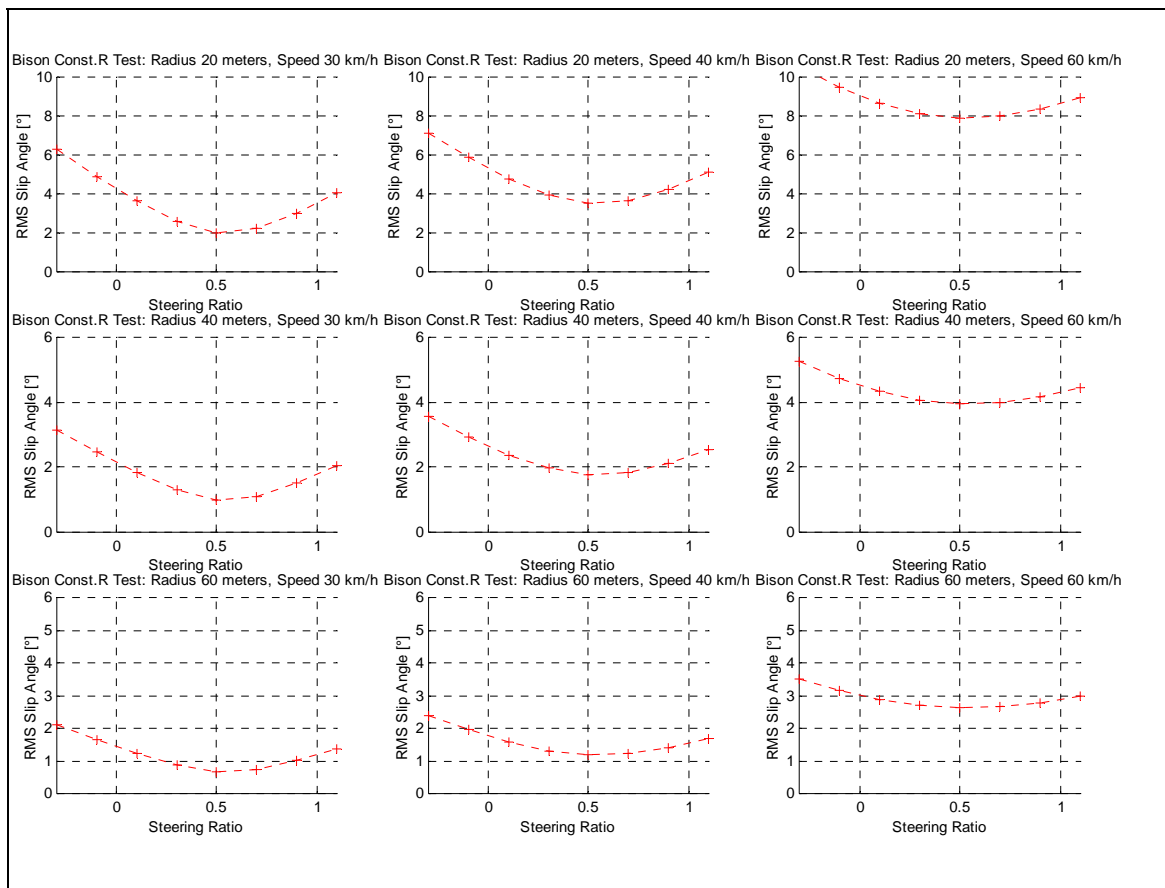


Figure 29 : RMS slip angles, constant radius test

Figure 29 shows a matrix of radius and speed combinations. In the matrix columns from left to right, speed values of 30 km/h, 40 km/h and 60 km/h are indicated. In the rows, results of radii 20 meters, 40 meters and 60 meters are shown. The RMS values of the slip angles of the three axles are calculated.

From the above, it is possible to determine the steering ratio where the slip angles are a minimum. The steering ratio required to minimize the slip angles for low and high speed, small and large radii are 0.5. As will be discussed, this may be used if for example it is necessary to minimize tire wear for a specific application.

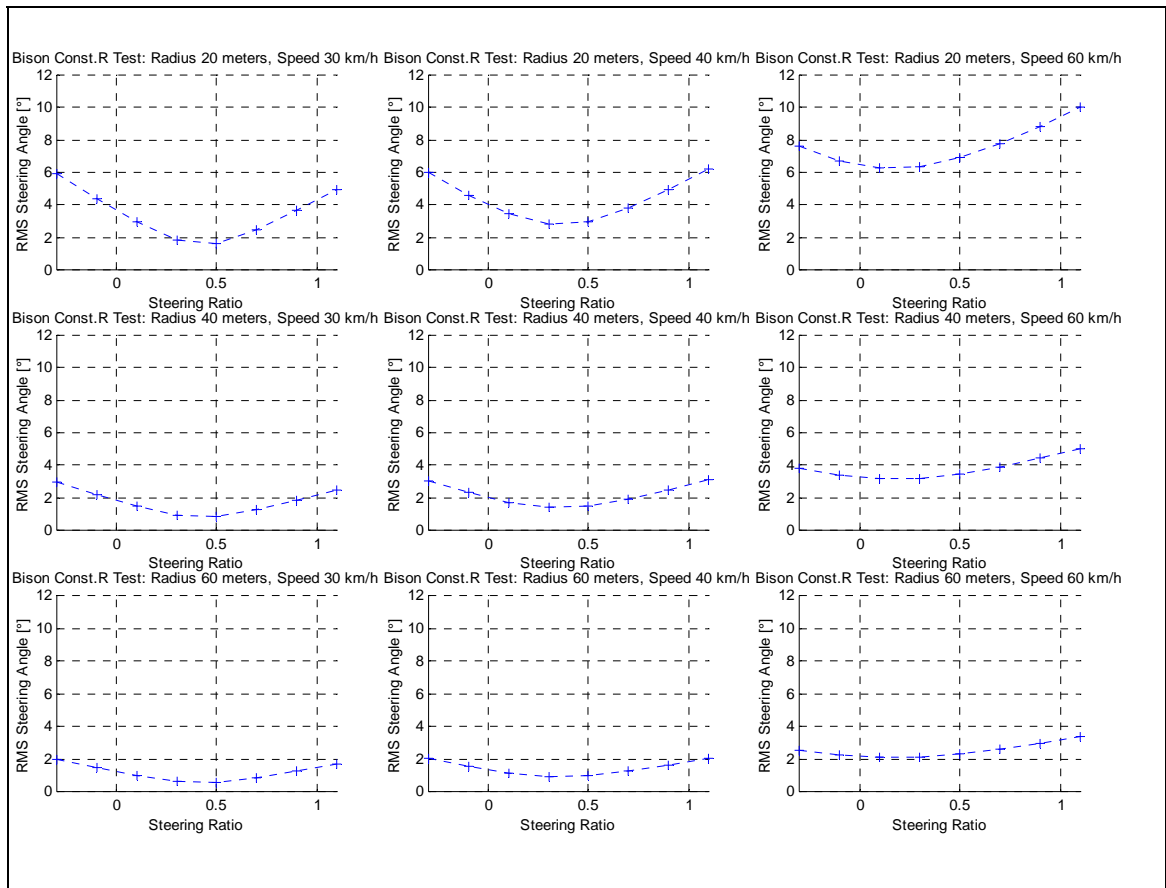


Figure 30 : RMS steering angles

Figure 30 indicates a similar matrix structure, but with the RMS angle of the steering axles (first two axles) plotted. If an attempt is made to minimize the steering angle required during steady state handling, regardless of tire wear and handling, Figure 30 indicates that for low speed the steering ratio should be approximately 0.4 to 0.5. For higher speeds, results indicate that the steering angle should be in the region of 0.3 for the given parameters.

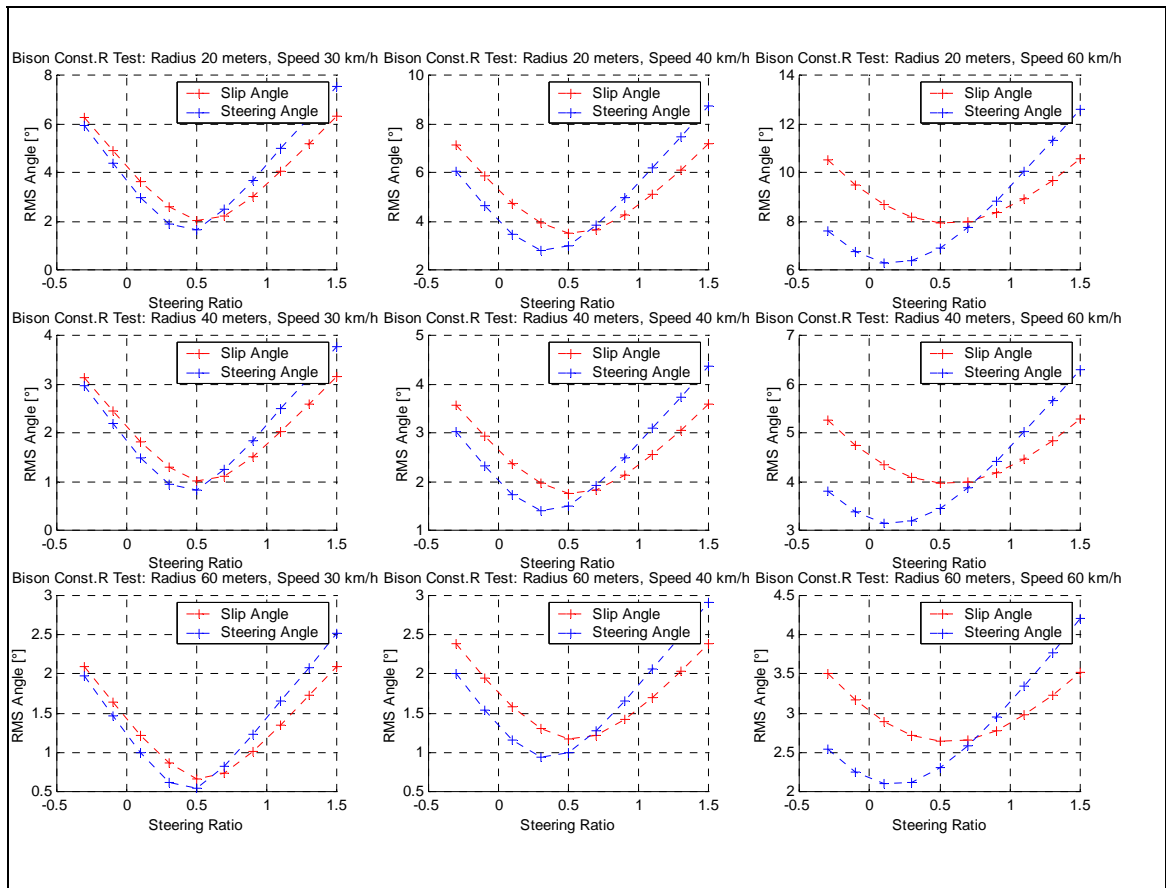


Figure 31 : RMS slip angles and steering angles

Figure 31 summarises the above by again showing the matrix structure, with both the RMS slip and steering angles plotted on the same axes. The results indicate that at slow speeds a minimum steering angle and slip angle occurs at roughly the same steering ratio. At high speed a different steering ratio is required to minimize either the slip angle or steering angle.

It was shown in equation 9.1 that the steering ratio of the Bison vehicle is approximately 0.57, which, according to the simulation results, is therefore appropriate for minimising the slip angles at low speed.

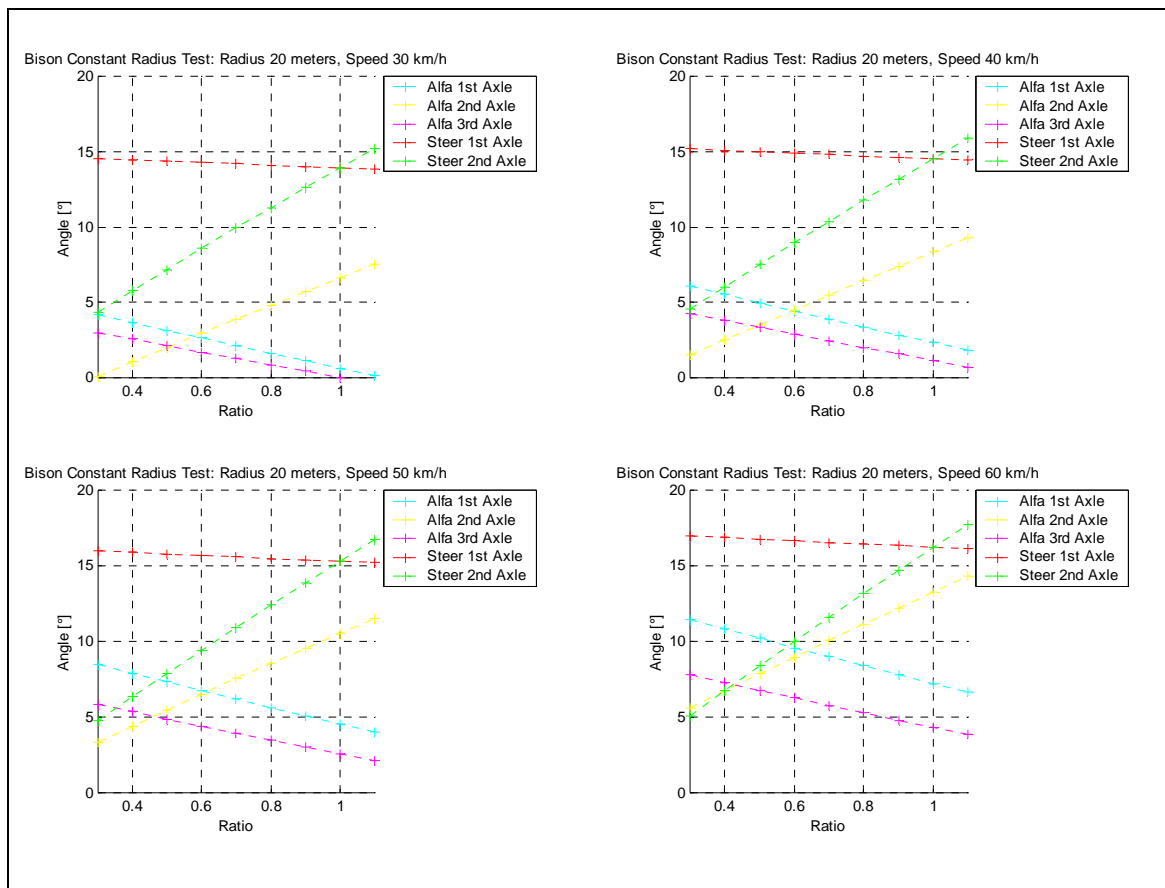


Figure 32 : Slip and steer angles - 20 meter radius

Figure 32 indicates a typical simulation result for a radius of 20 meters, and a speed increase from 30 km/h to 60 km/h. The slip angles of the three axles and steering angles of the first and second axles are plotted for the different steering ratios considered in Figure 32. At low speed, an intersection of the lines of at least two axles may be found at a steering ratio of 0.5, and at high speed (60 km/h) a ratio of 0.6 may be used to minimize the slip angles and therefore tire wear.

The results of the 40 meter and 60 meter radius are shown in Figure 33 and Figure 34.

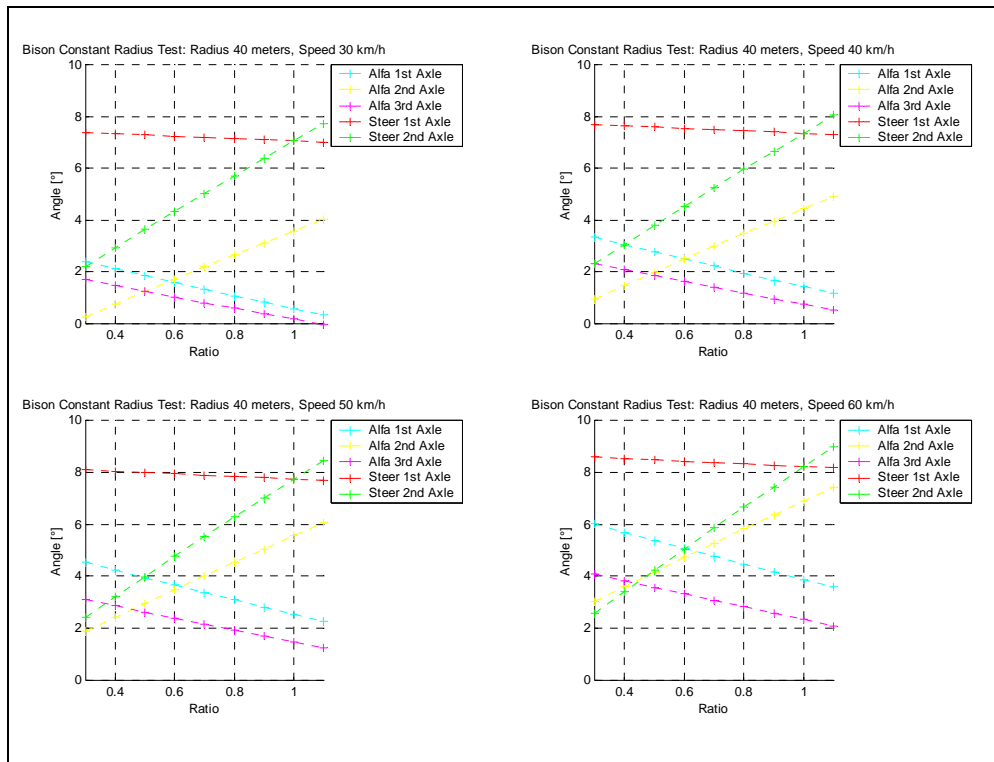


Figure 33 : Slip and steer angles - 40 meter radius

Figure 33 indicates that the slip angle of the second and third axles are equal at a steering ratio of 0.5 for a radius of 40 meters and 30 km/h, and at 60 km/h the ratio moves to 0.4 to equalise the slip angles on the axes. A similar result for the 60 meter radius is shown in Figure 34.

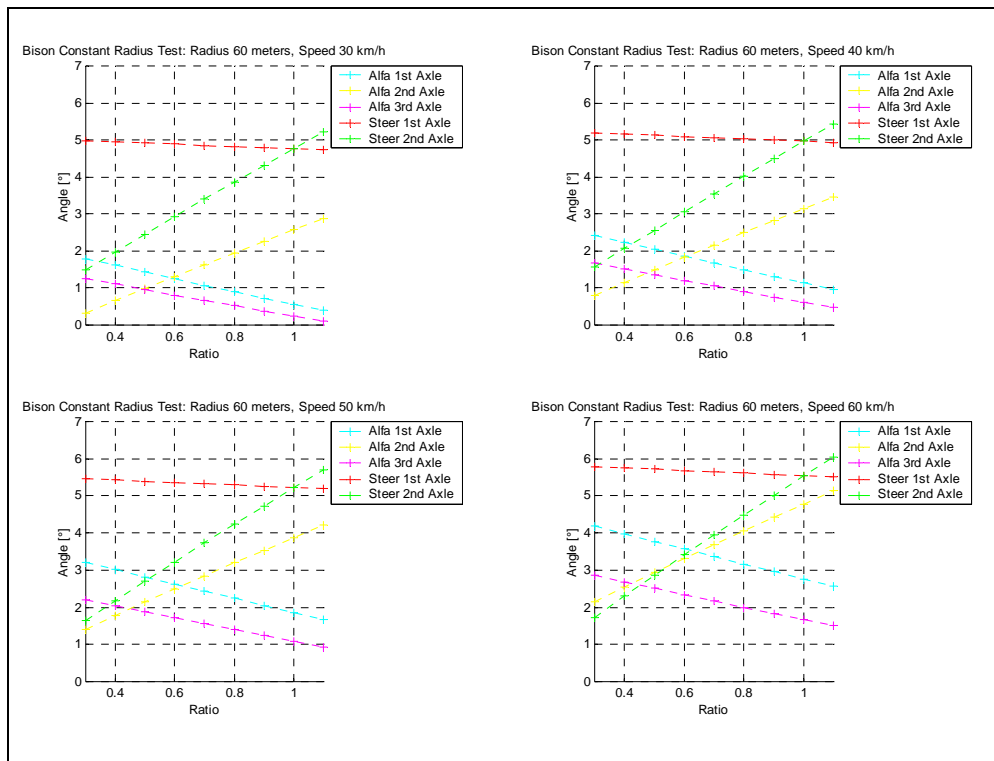


Figure 34 : Slip and steer angles - 60 meter radius

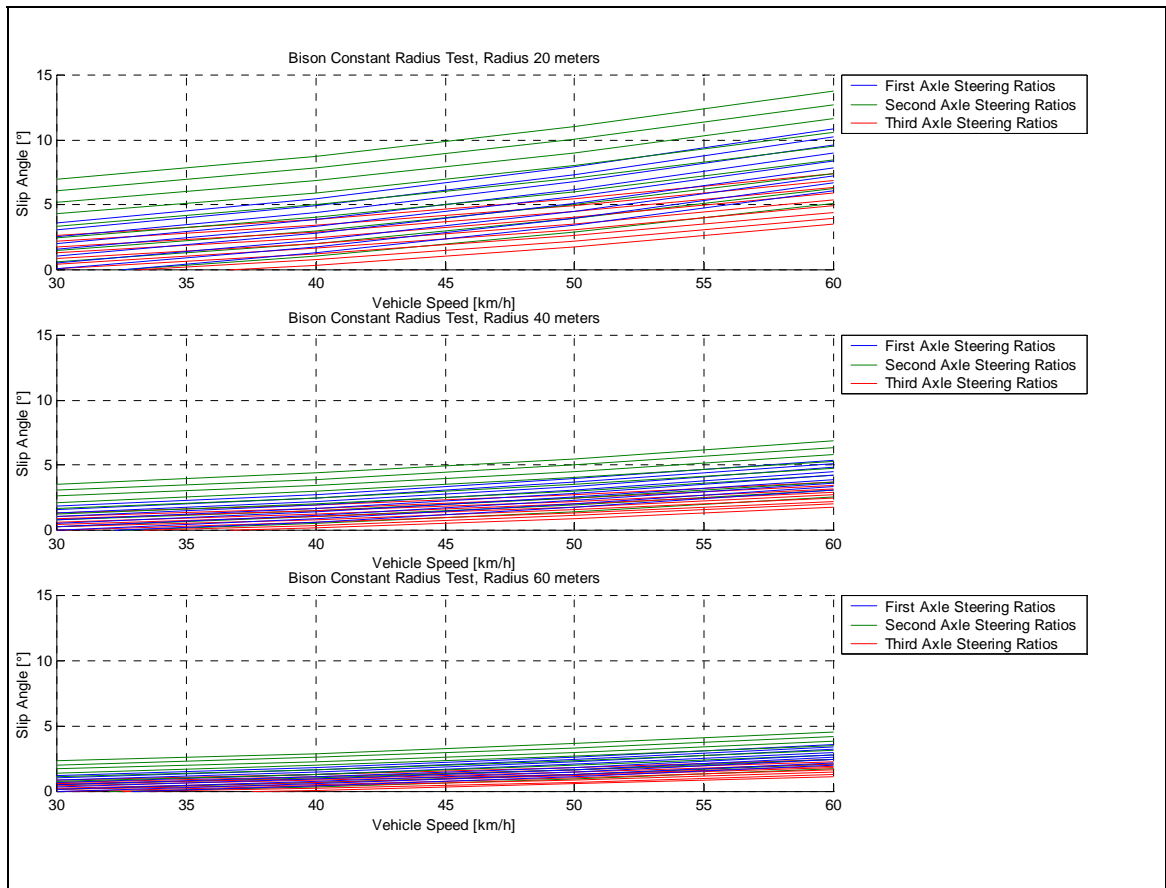


Figure 35 : Slip angle vs. vehicle speed

In Figure 35 the slip angles are plotted against the vehicle speed, for three different track radii and a range of different steering ratios (ratio's of 0.3 to 1.1). It summarises the effect of changing the steering ratio between the first and second axles, therefore changing the slip angles of the tires. The effect is more dramatic for small radii, since the centrifugal reaction forces are larger for the small radii.

The above results may be plotted as steering angle against vehicle speed, to determine over or understeer behaviour. Selected results are shown in the following figures. For clarity, steering ratios of 0.5, 0.7 and 1 were selected. The results for a radius of 20 meters, 40 meters and 60 meters are shown in Figure 36 to Figure 41. An increased steering angle for an increase in speed is required, characteristic of an understeer vehicle. The minimum steering angle is achieved with a steering ratio of 1, since it ensures the largest side-force to be generated by the tire contact patch.

As a further check, consider the wheelbase of Bison to be 4.656 meters, and a radius of 20 meters is attempted. The ratio L/R or Ackerman steering angle for the first axle is therefore 0.2328 rad or 13.3 degrees. This value corresponds to the 14 degrees indicated at 30 km/h in Figure 36.

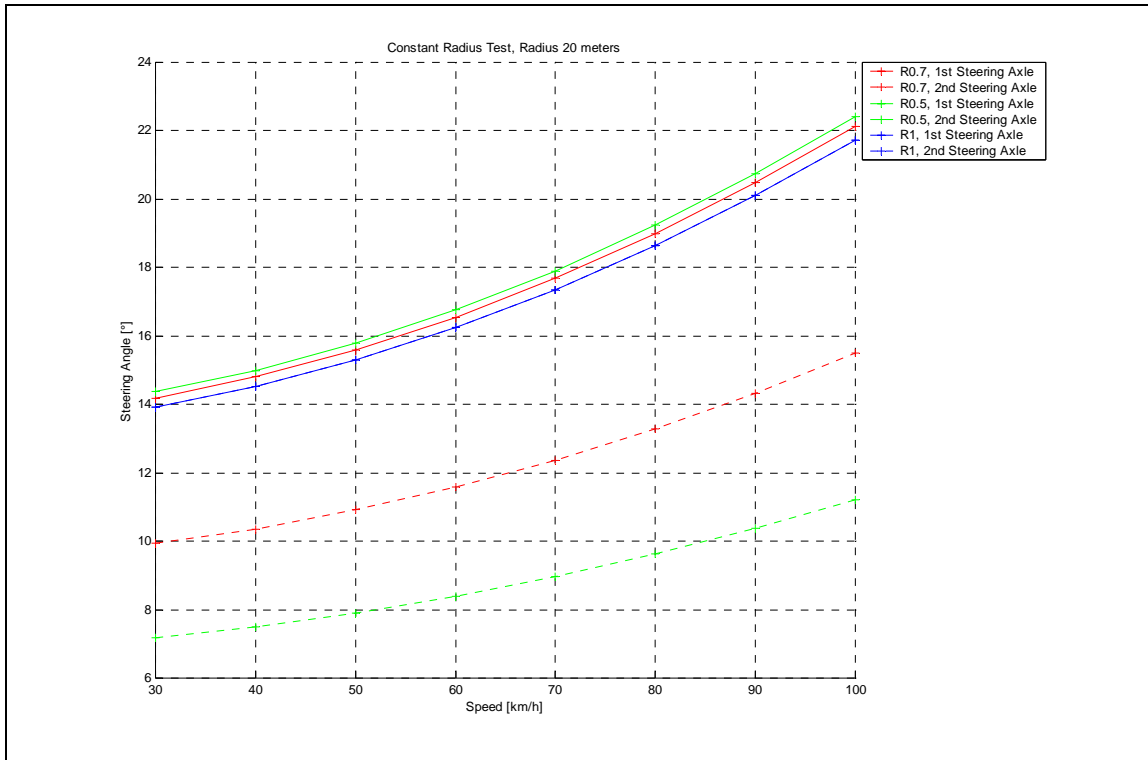


Figure 36 : Steering angle vs. vehicle speed – 20 meter radius

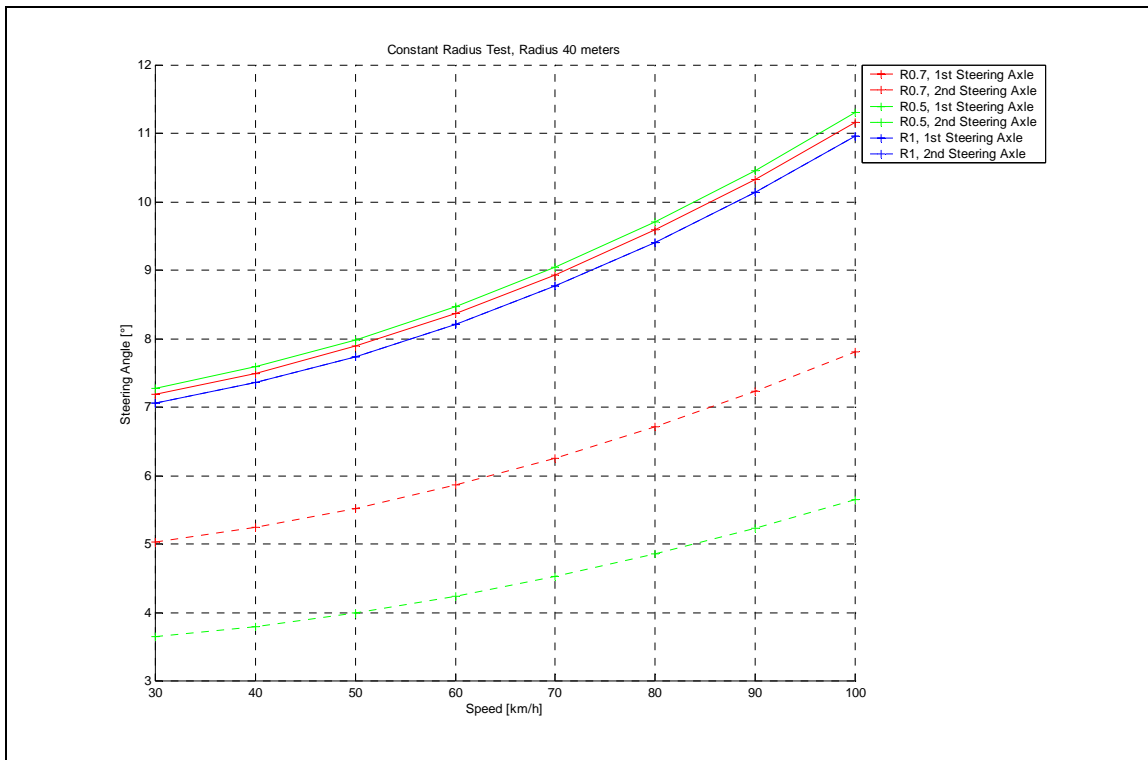


Figure 37 : Steering angle vs. vehicle speed – 40 meter radius

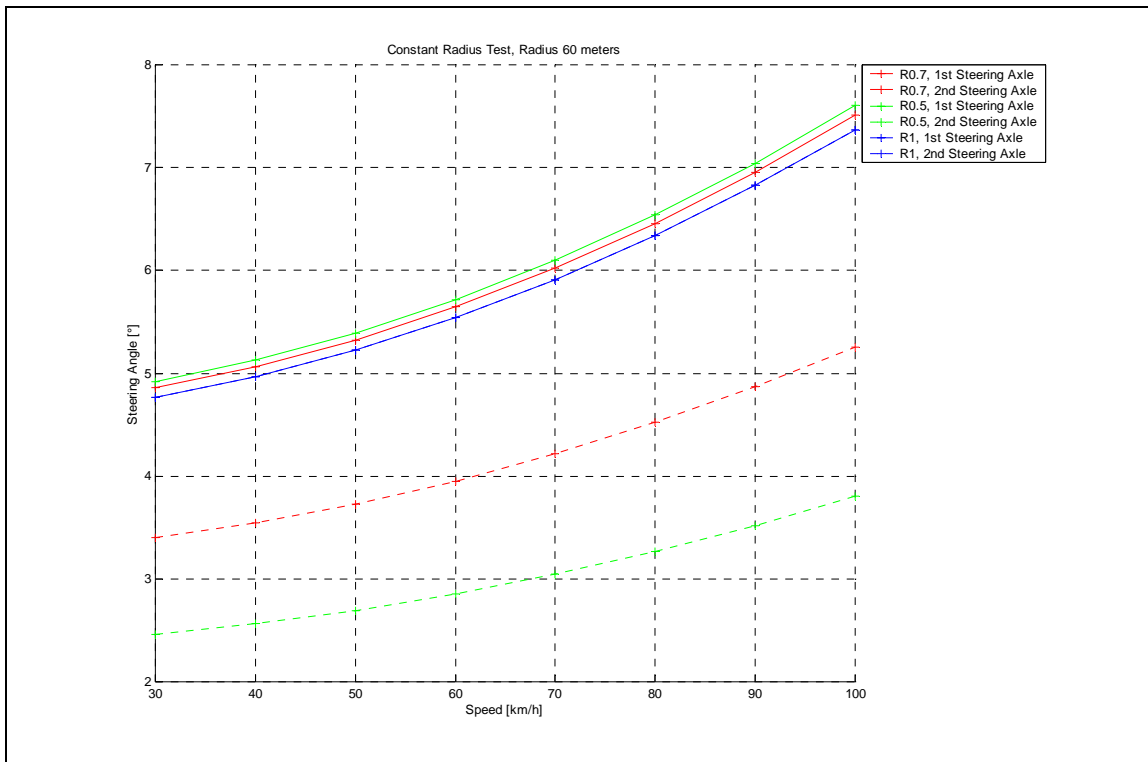


Figure 38 : Steering angle vs. vehicle speed – 60 meter radius

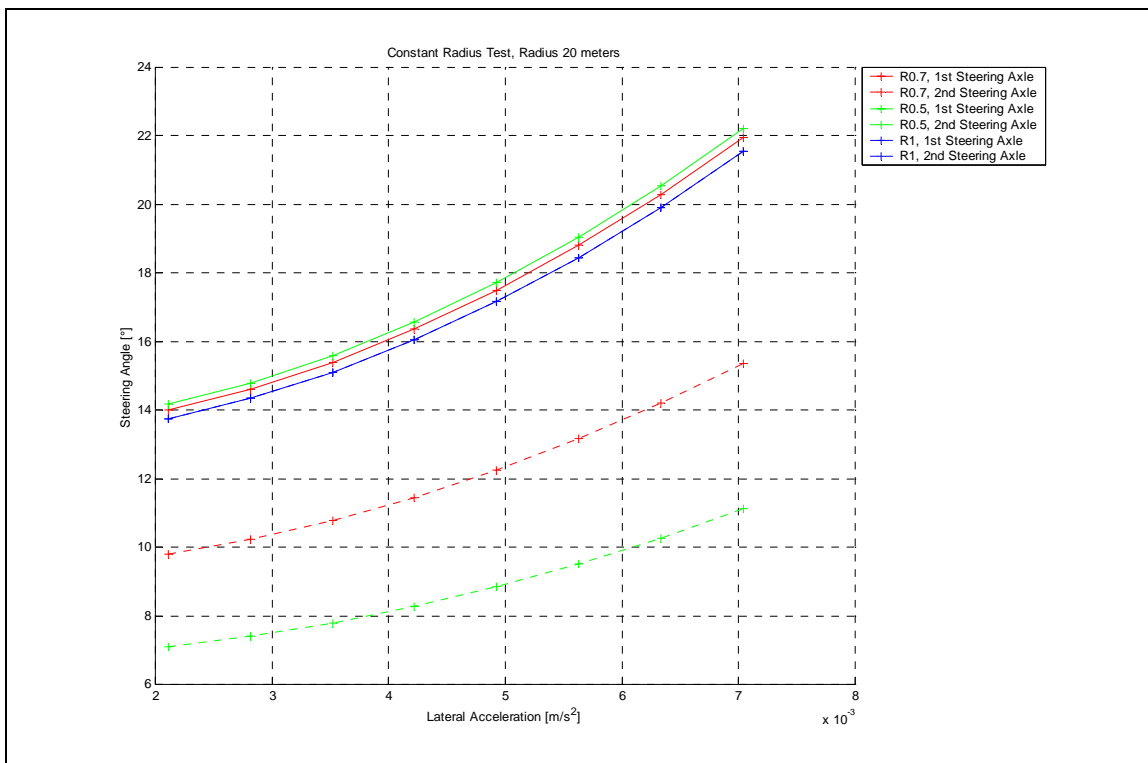


Figure 39 : Steering angle vs. lateral acceleration – 20 meter radius

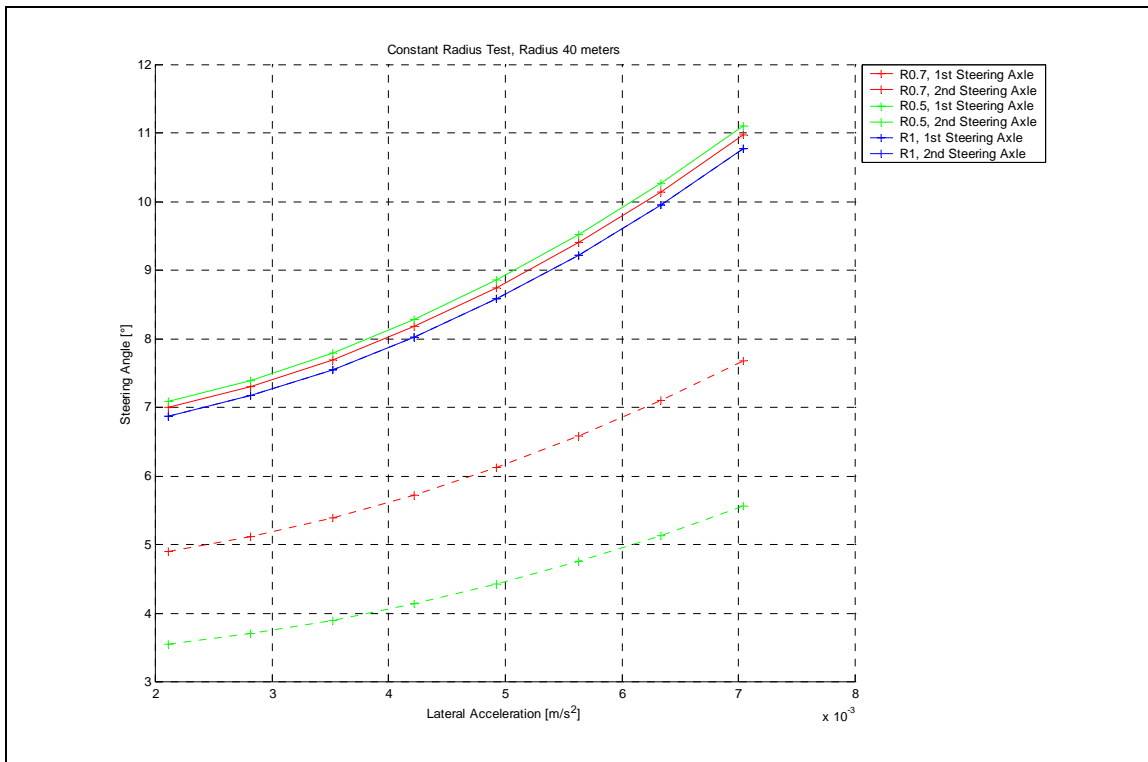


Figure 40 : Steering angle vs. lateral acceleration – 40 meter radius

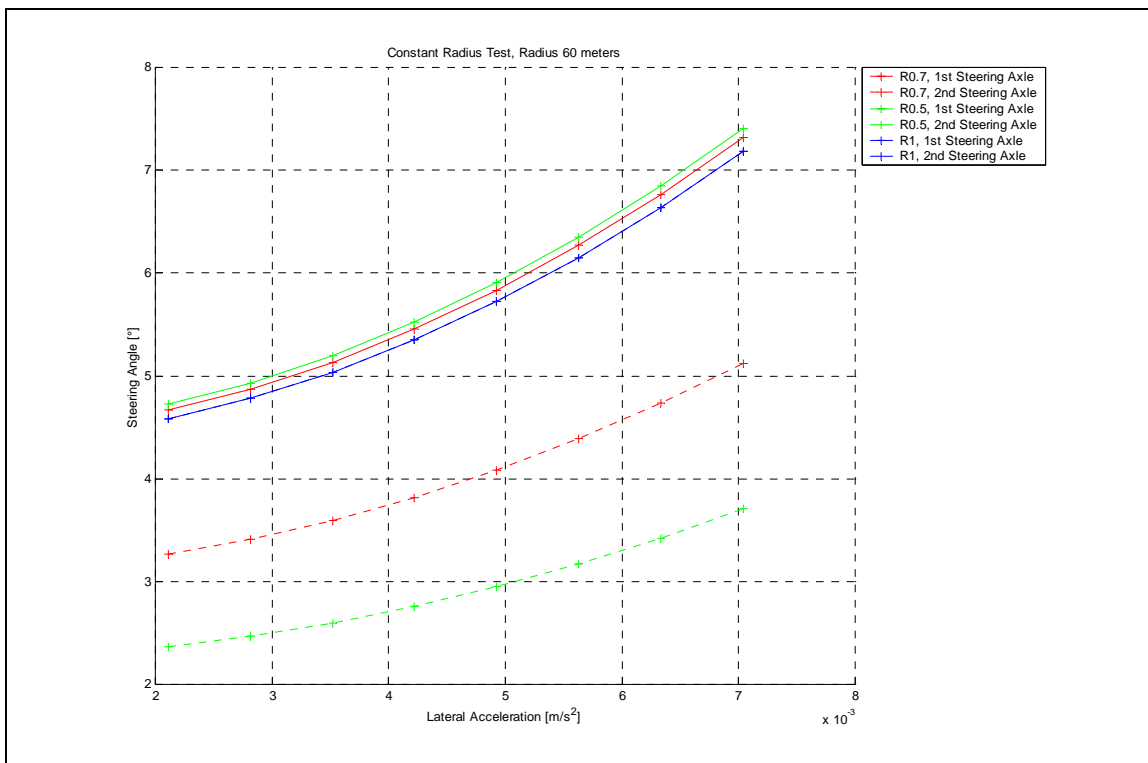


Figure 41 : Steering angle vs. lateral acceleration – 60 meter radius

13. Transient state handling

The bicycle model of a two-axle vehicle has been expanded to include four axles, and then reduced to three axles. The equations of motion are derived below. The equations have been solved using Matlab and Simulink routines, and the results of the simulation are discussed. It is also necessary to investigate transient response, as this situation is more likely to be encountered in actual vehicle use.

13.1. Equations of motion, two degree of freedom model, two axles

The lateral acceleration can be expressed in terms of the absolute motion. The vehicle is shown in Figure 42 in the XY plane, moving in the primary X-direction [10].

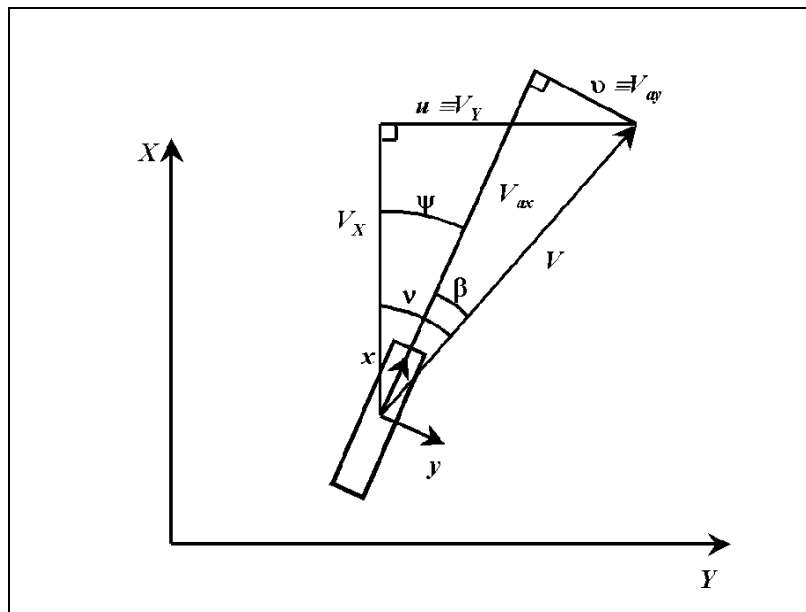


Figure 42 : Angles and velocity components [10]

The path angle from the X-axis is ν , the heading angle is ψ , and the attitude angle is β . The total speed V tangent to the path may be resolved into V_{ax} and V_{ay} [10].

$$V_{ax} = V \cos \beta \cong V \tag{13.1}$$

$$V_{ay} = v = V \sin \beta \cong V \beta \tag{13.2}$$

$$V_y \cong u \cong \nu V \tag{13.3}$$

The vehicle has yaw angular velocity $r = d\psi/dt$.

V_{ax} is the component, in the x direction, of the absolute velocity.

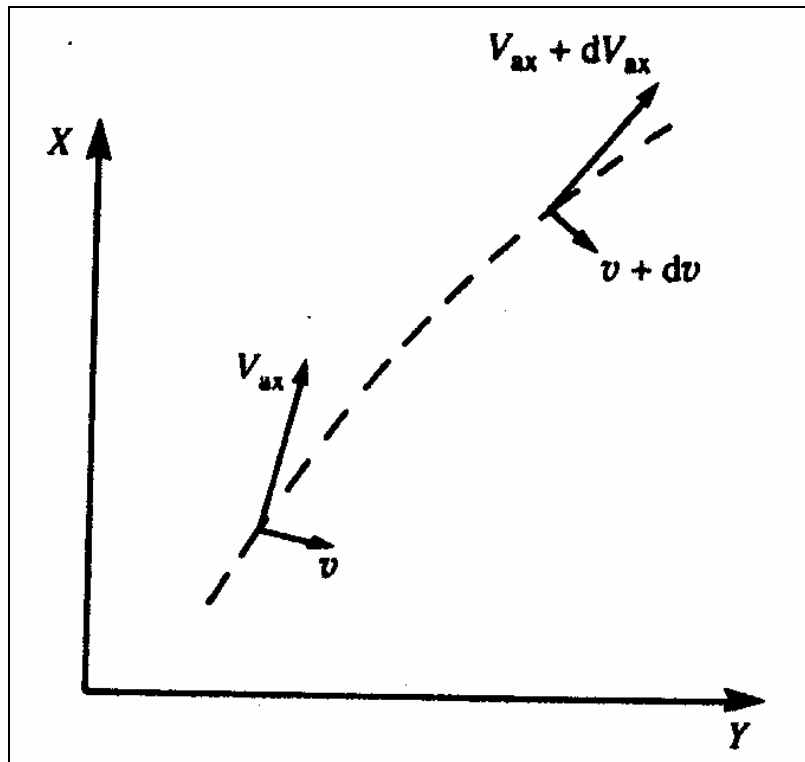


Figure 43 : Velocity components at path points [10]

Figure 43 shows the vehicle position and orientation at time t and $t + dt$. The relative rotation is $r dt$.

The absolute acceleration in the y direction is [10]

$$A_{ay} = dt = dv \cos(r dt) + V \sin(r dt)$$

$$\cong dv + V r dt \tag{13.4}$$

$$A_{ay} = \dot{v} + V$$

A free body diagram of the bicycle model, with the roll and load transfer neglected, are shown in Figure 44. The vehicle is considered in the accelerating vehicle-fixed axis, and the appropriate compensation force and moments are included. The vehicle has been subjected to a small disturbance, now having a lateral velocity component v . The attitude angle is [10]:

$$\beta = v / V_{ax} \cong v / V \tag{13.5}$$

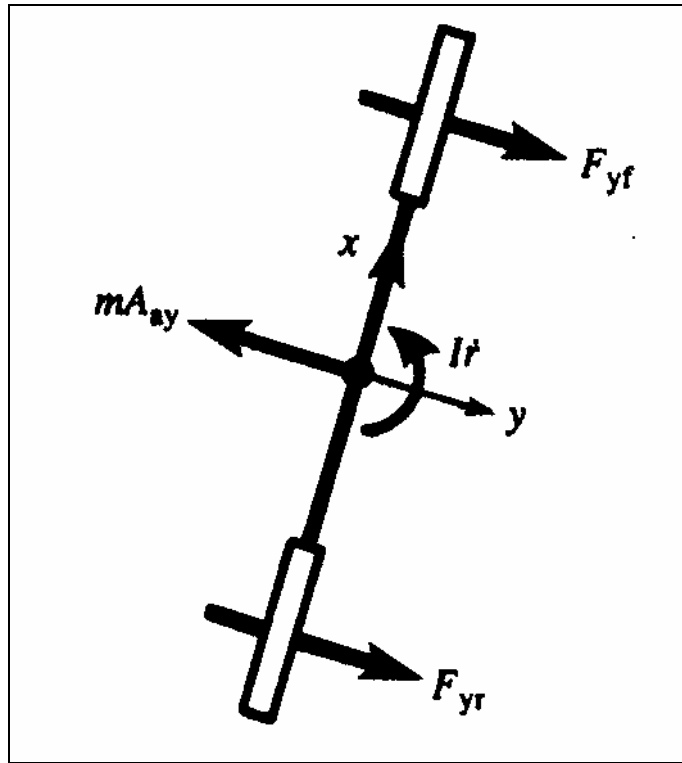


Figure 44 : Free body diagram [10]

The slip angles, allowing for the attitude angle and the yaw rotation speed r , is as follows [10]:

$$\alpha_f = v/V + ar/V \quad (13.6)$$

$$\alpha_r = v/V - br/V \quad (13.7)$$

Using a linear approximation for the tire forces, the forces from the front and rear tires are:

$$F_{yf} = 2 \alpha_f C_{\alpha f} \quad (13.8)$$

$$F_{yr} = 2 \alpha_r C_{\alpha r} \quad (13.9)$$

The acceleration in the vehicle fixed axis is zero, and the equations of motion can be described as [10]:

$$\sum F_y = F_{yf} + F_{yr} - M A_{ay} = 0 \quad (13.10)$$

$$\sum M = a.F_{yf} - b.F_{yr} - I dr/dt = 0 \quad (13.11)$$

Substituting F_{yf} and F_{yr} from above, the following equations can be derived:

$$\begin{pmatrix} \dot{v} \\ r \end{pmatrix} = \begin{pmatrix} A_{11} & A_{12} \\ A_{21} & A_{22} \end{pmatrix} \cdot \begin{pmatrix} v \\ r \end{pmatrix} \quad (13.12)$$

where:

$$A_{11} = \left(\frac{-2}{MV} \right) \cdot (C_{af} + C_{ar}) \quad (13.13)$$

$$A_{12} = - \left(V + \left(\frac{2}{MV} \right) \cdot (a \cdot C_{af} - b C_{ar}) \right) \quad (13.14)$$

$$A_{21} = \left(\frac{2}{IV} \right) \cdot (b \cdot C_{ar} - a \cdot C_{af}) \quad (13.15)$$

$$A_{22} = - \left(\frac{2}{IV} \right) \cdot (a^2 \cdot C_{af} + b^2 C_{ar}) \quad (13.16)$$

The above can be expanded further to include the steering angle δ , and the expanded equations can be shown to be:

$$\begin{pmatrix} \dot{v} \\ r \end{pmatrix} = \begin{pmatrix} A_{11} & A_{12} \\ A_{21} & A_{22} \end{pmatrix} \cdot \begin{pmatrix} v \\ r \end{pmatrix} + \begin{pmatrix} 2C_{af}/M \\ 2C_{af}/I \end{pmatrix} \cdot \begin{pmatrix} \delta \end{pmatrix} \quad (13.17)$$

The position of the vehicle on the road can be determined by calculating the X, Y and the heading angle ψ from:

$$\begin{aligned} X_t &= \int_{t_0}^t V_x(\tau) d\tau = \int_{t_0}^t (V \cos(\psi(\tau)) - v \sin(\psi(\tau))) d\tau \\ Y_t &= \int_{t_0}^t (V \sin(\psi(\tau)) - V(\tau) \cos(\psi(\tau))) d\tau \\ \psi_t &= \int_{t_0}^t r(\tau) d\tau \end{aligned} \quad (13.18)$$

13.2. Equations of motion, two degree of freedom model, four axles

The above equations can be expanded to a four-axle vehicle, steering with the first and second axles. Define the following:

F_{yf1} = Lateral (cornering) force at the first axle

F_{yf2} = Lateral (cornering) force at the second axle

- F_{yr1} = Lateral (cornering) force at the third axle
 F_{yr2} = Lateral (cornering) force at the fourth axle
 α_{f1} = Slip angle first axle
 α_{f2} = Slip angle second axle
 α_{r1} = Slip third first axle
 α_{r2} = Slip fourth first axle
 δ_1 = Steering angle first axle
 δ_2 = Steering angle second axle
 M = Mass of the vehicle
 V = Forward velocity
 R = Radius of the turn
 a = Distance between the first and second axle
 b = Distance between the second axle and centre of mass
 c = Distance between the centre of mass and third axle
 d = Distance between the third and fourth axle

The slip angles of the wheel combinations can be described by the equations below:

$$\alpha_{f1} = \frac{v}{V} + \frac{(a+b)r}{V} - \delta_1 \quad (13.18)$$

$$\alpha_{f2} = \frac{v}{V} + \frac{b.r}{V} - \delta_2 \quad (13.20)$$

$$\alpha_{r1} = \frac{v}{V} - \frac{c.r}{V} \quad (13.21)$$

$$\alpha_{r2} = \frac{v}{V} - \frac{(c+d).r}{V} \quad (13.22)$$

$\delta_2 = Sr.\delta_1$, where Sr is the steering ratio between the first and second axles.

$\sum F_Y = M_{ay}$ expanding to:

$$-2C_{af1}\alpha_{f1} - 2C_{af2}\alpha_{f2} - 2C_{ar1}\alpha_{r1} - 2C_{ar2}\alpha_{r2} = M \left(\dot{v} + Vr \right) \quad (13.23)$$

and

$\Sigma M_G = I_G \cdot \dot{r}$ expanding to:

$$-F_{yf1}(a+b) - F_{yf2}(b) + F_{yr1}(c) + F_{yr1}(c+d) = I_G \dot{r} \quad (13.24)$$

By substituting and regrouping, the equations can be written in matrix format as follows:

$$\begin{bmatrix} \cdot \\ \mathbf{v} \\ \cdot \\ r \end{bmatrix} = \begin{bmatrix} A_{11} & A_{12} \\ A_{21} & A_{22} \end{bmatrix} \begin{bmatrix} \cdot \\ \mathbf{v} \\ \cdot \\ r \end{bmatrix} + \begin{bmatrix} B_1 \\ B_2 \end{bmatrix} \cdot \delta \quad (13.25)$$

where:

$$A_{11} = \left(\frac{-2}{MV} \right) \cdot (C_{af1} + C_{af2} + C_{ar1} + C_{ar2}) \quad (13.26)$$

$$A_{12} = V + \frac{2}{MV} \cdot ((a+b) \cdot C_{af1} + b \cdot C_{af2} - c \cdot C_{ar1} - (c+d) \cdot C_{ar2}) \quad (13.27)$$

$$A_{21} = \left(\frac{2}{IV} \right) \cdot (c \cdot C_{ar1} + (c+d) \cdot C_{ar2} - (a+b) \cdot C_{af1} - b \cdot C_{af2}) \quad (13.28)$$

$$A_{22} = -\left(\frac{2}{IV} \right) \cdot ((a+b)^2 \cdot C_{af1} + b^2 \cdot C_{af2} + c^2 \cdot C_{ar1} + (c+d)^2 \cdot C_{ar2}) \quad (13.29)$$

$$B_1 = \left(\frac{1}{M} \right) \cdot (2 \cdot C_{af1} + 2 \cdot Sr \cdot C_{af2}) \quad (13.30)$$

$$B_2 = \left(\frac{1}{I} \right) \cdot (2 \cdot (a+b) \cdot C_{af1} + 2 \cdot Sr \cdot b \cdot C_{af2}) \quad (13.31)$$

The above system may be solved using Matlab Simulink. In this instance, Matlab 5.3.0.10183R11 was used, and solver were set to use ODE45 (Dormand Prince) variable step solver settings.

13.3. Equations of motion, two degree of freedom model, three axles

Since the 6x6 configuration was used to validate the model, using the above logic, it can be shown that the matrix values for a 6x6 configuration changes to:

$$A_{11} = \frac{-2}{MV} \cdot (C_{af1} + C_{af2} + C_{ar1}) \quad (13.32)$$

$$A_{12} = -V - \frac{2}{MV} \cdot ((aa) \cdot C_{af1} - bb \cdot C_{af2} - (bb+cc) \cdot C_{ar1}) \quad (13.33)$$

$$A_{21} = \frac{-2}{IV} \cdot \left(-(cc + bb) \cdot C_{ar1} + (aa) \cdot C_{af1} - bb \cdot C_{af2} \right) \quad (13.34)$$

$$A_{22} = \frac{-2}{IV} \cdot \left((aa)^2 \cdot C_{af1} + bb^2 C_{af2} + (cc + bb)^2 C_{ar1} \right) \quad (13.29)$$

$$B_1 = \left(\frac{1}{M} \right) \cdot \left(2 \cdot C_{af1} + 2 \cdot Sr \cdot C_{af2} \right) \quad (13.30)$$

$$B_1 = \frac{I}{I} \cdot \left(2 \cdot (aa) C_{af1} - 2 \cdot Sr \cdot bb \cdot C_{af2} \right) \quad (13.31)$$

where:

F_{yf1} = Lateral (cornering) force at the first axle

F_{yf2} = Lateral (cornering) force at the second axle

F_{yr1} = Lateral (cornering) force at the third axle

α_{f1} = Slip angle first axle

α_{f2} = Slip angle second axle

α_{r1} = Slip third first axle

δ_1 = Steering angle first axle

δ_2 = Steering angle second axle

M = Mass of the vehicle

V = Forward velocity

R = Radius of the turn

aa = Distance between the first and centre of mass

bb = Distance between the centre of mass and the second axle

cc = Distance between the second axle and third axle

14. Test track dimensions

The dimensions of the track (single lane change) and the track centreline used for the simulation is shown in Figure 45.

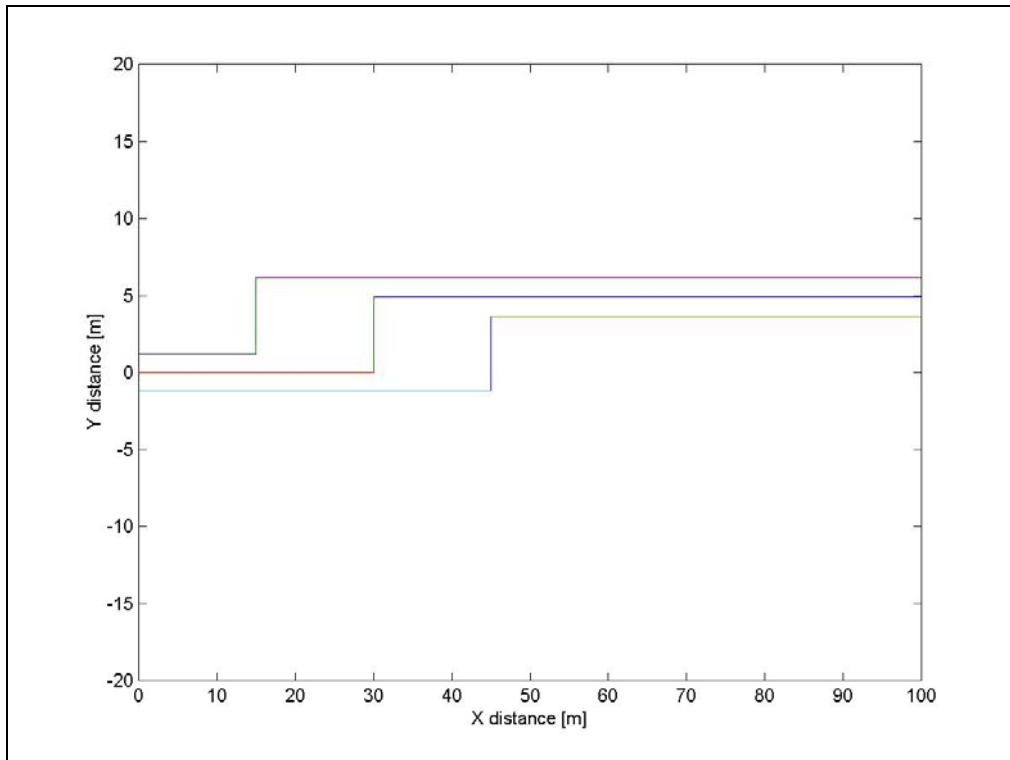


Figure 45 : Single lane change track dimensions

15. Driver/steering model

Various studies have been done on driver models and track followers for dynamic simulation [19, 20, 21] & [29]. The detail falls beyond the scope of this investigation.

A simple steering/driver model has been implemented to steer the vehicle through the single lane change track. The steering model receives as input the following:

- The vehicle speed (A constant speed is assumed).
- The centreline of the track that needs to be followed.
- The distance the driver is looking ahead of the vehicle (because speed is constant, distance is related to time).
- The distance to the side the driver is looking at (because speed is constant, distance is related to time).
- The calculated yaw angle of the vehicle in its current position.

A schematic layout of the driver model is shown in Figure 46.

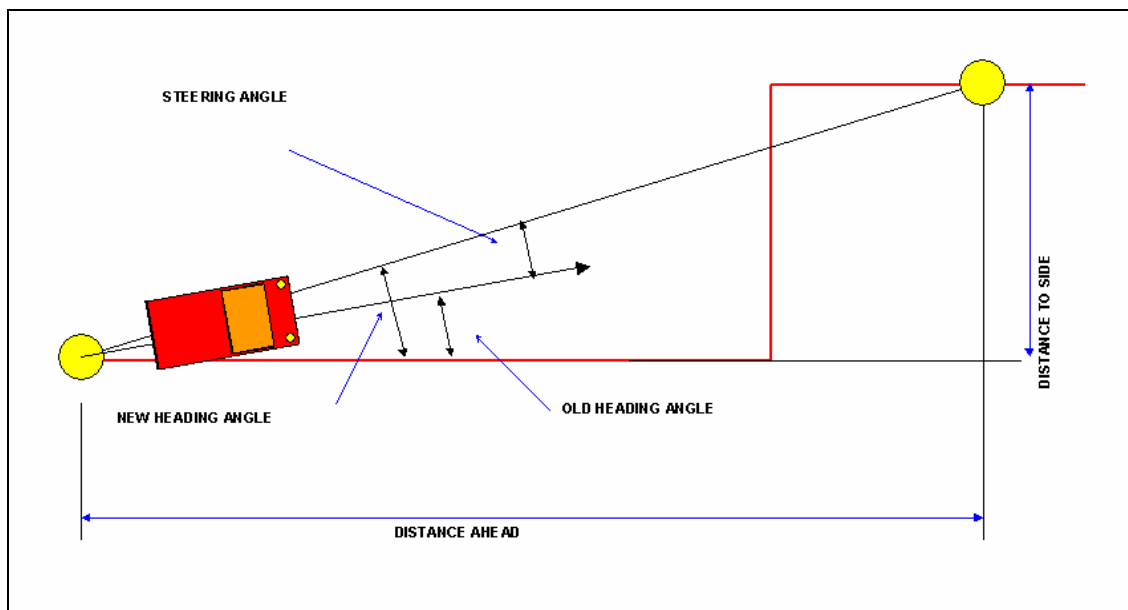


Figure 46 : Driver model

The implementation of the driver model in Matlab Simulink is shown in Figure 47. As can be seen, the predicted track position, and the current track position are added, after it is multiplied by a constant factor, in this case 0.5. Multiple runs of the simulation were done to determine the factor, changing the constant until acceptable results were obtained.

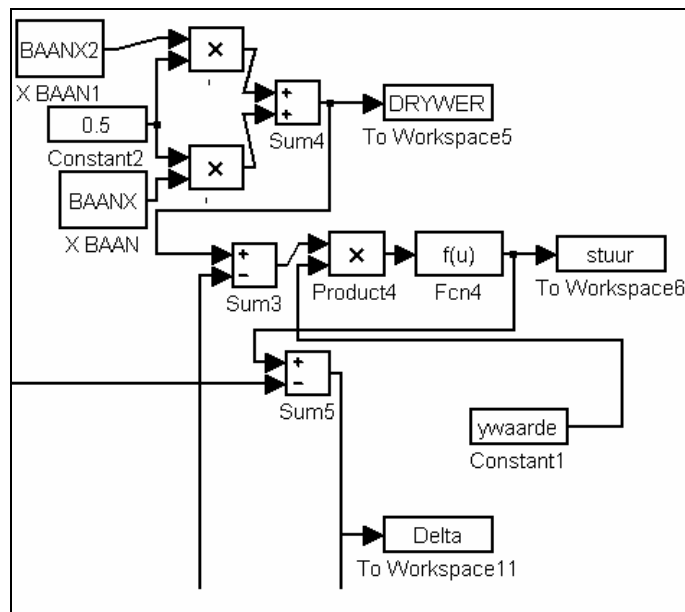


Figure 47 : Simulink driver model

It should be noted that the aim of the simulation is not to determine the absolute maximum speed the vehicle may attain during the single lane change, but to compare different steering geometry relationships, using the same control strategy to compare the effect on ratio changes.

16. Simulink model

The Simulink model used to solve the path of the vehicle and the slip angles of the individual axles are shown in Figure 48.

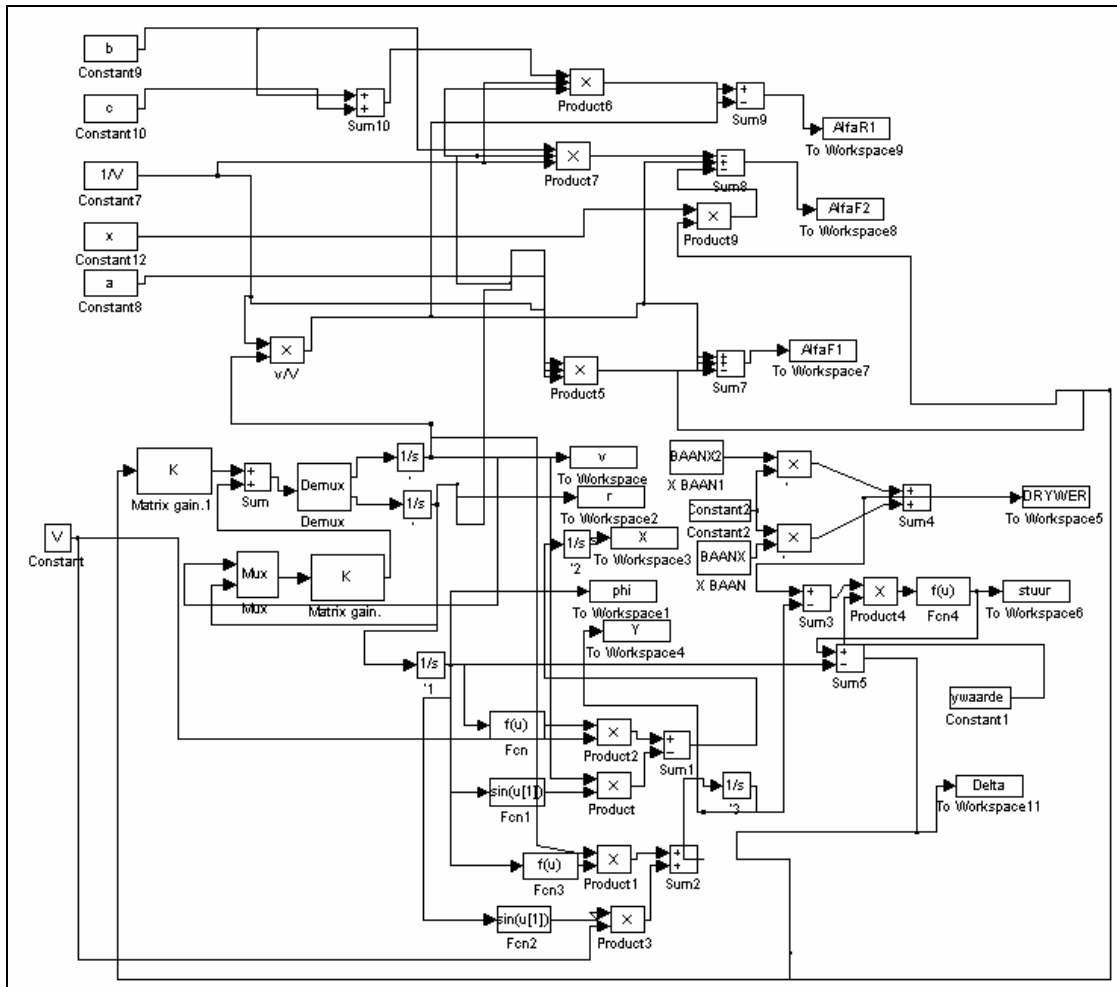


Figure 48 : Simulink diagram

Inputs to the model are listed below:

- Tire characteristics of the individual axles, $C_{\alpha f}$
- Geometry of the vehicle, axle distances
- Position of the centre of mass
- Yaw moment of inertia of the vehicle
- Mass of the vehicle
- Track geometry and centreline path the driver is looking at
- Initial steering angle input
- Distance the driver is looking ahead

- Distance the driver is looking to the side
- Ratio between the first axle and second axle steering angle
- Vehicle speed through the obstacle

As output, the following parameters are obtained:

- X and Y and heading angle ψ are displayed as a function of time
- Slip angles of the individual axles as a function of time
- Maximum slip angle per axle during the manoeuvre
- The length of the path the vehicle has followed, after a specific X distance
- The steering angle as a function of time for the first and second axles

A Matlab programme calculating the path as a function of time, as well as the tire characteristics is shown in Appendix B.

A Matlab programme plotting the data, and calculating the track length, and journey time is shown in Appendix C.

17. Simulink model simulation results

It should be noted that the aim of the simulation is not to find the absolute maximum speed that may be achieved through the lane change, but rather to use the results to investigate steering ratio tendencies. It may be possible to change the driver model to increase or decrease the speed of the vehicle through the obstacles, or improve the trajectory through the lane change. The driver models were set to ensure that the simulated results follow the measured results (as described in paragraph 18) as close as possible.

As a first attempt to compare the effect of the steering ratio on transient state handling, the steering ratio was varied from a ratio of 0.3 to a ratio of 1 between the first and second axles. The time required completing the lane change, for different vehicle speeds were calculated, and the times compared. In all instances, the exact same driver model for a specific speed was used. The results are shown in Figure 49.

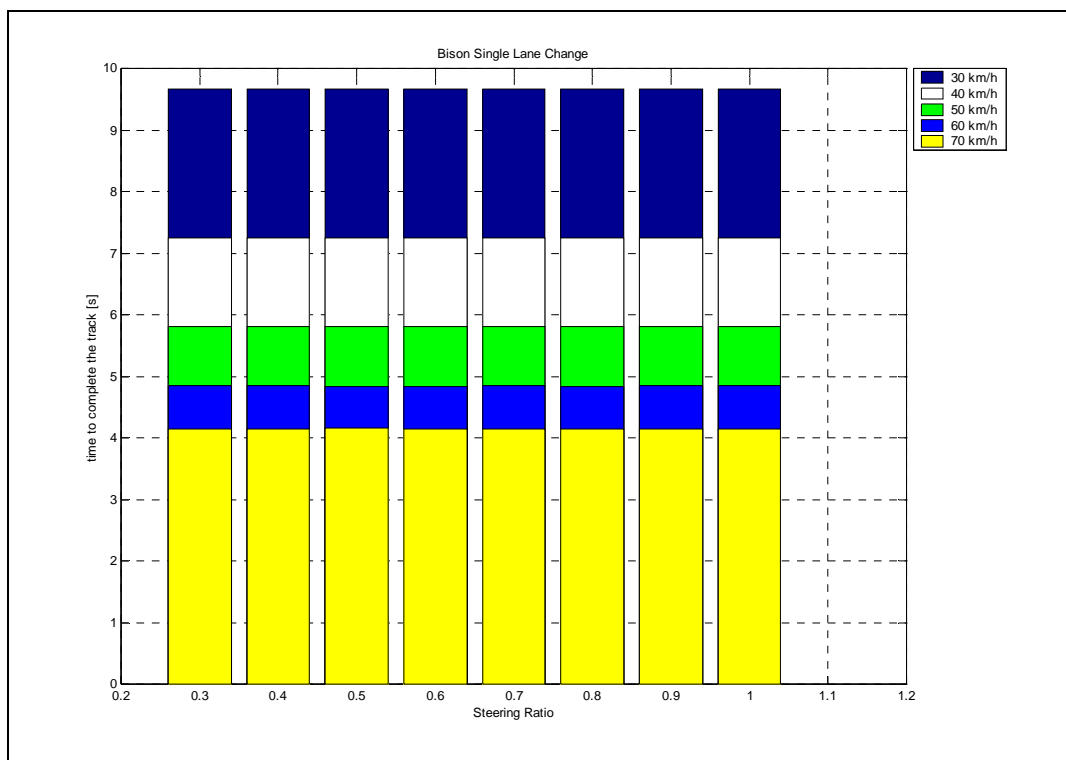


Figure 49 : Time to complete the maneuver

From the figure it is clear that no measurable time difference through the obstacle is achieved by changing the steering ratio, if the driver model is kept constant. In other words, a driver with the same “driving ability” will not achieve a quicker time through the lane change with a change in steering geometry.

A further factor that may be investigated is the slip angles that are induced between the tire and the road during the manoeuvre, for a specific steering ratio and speed. The maximum slip angle during the lane change manoeuvre is shown in Figure 50.

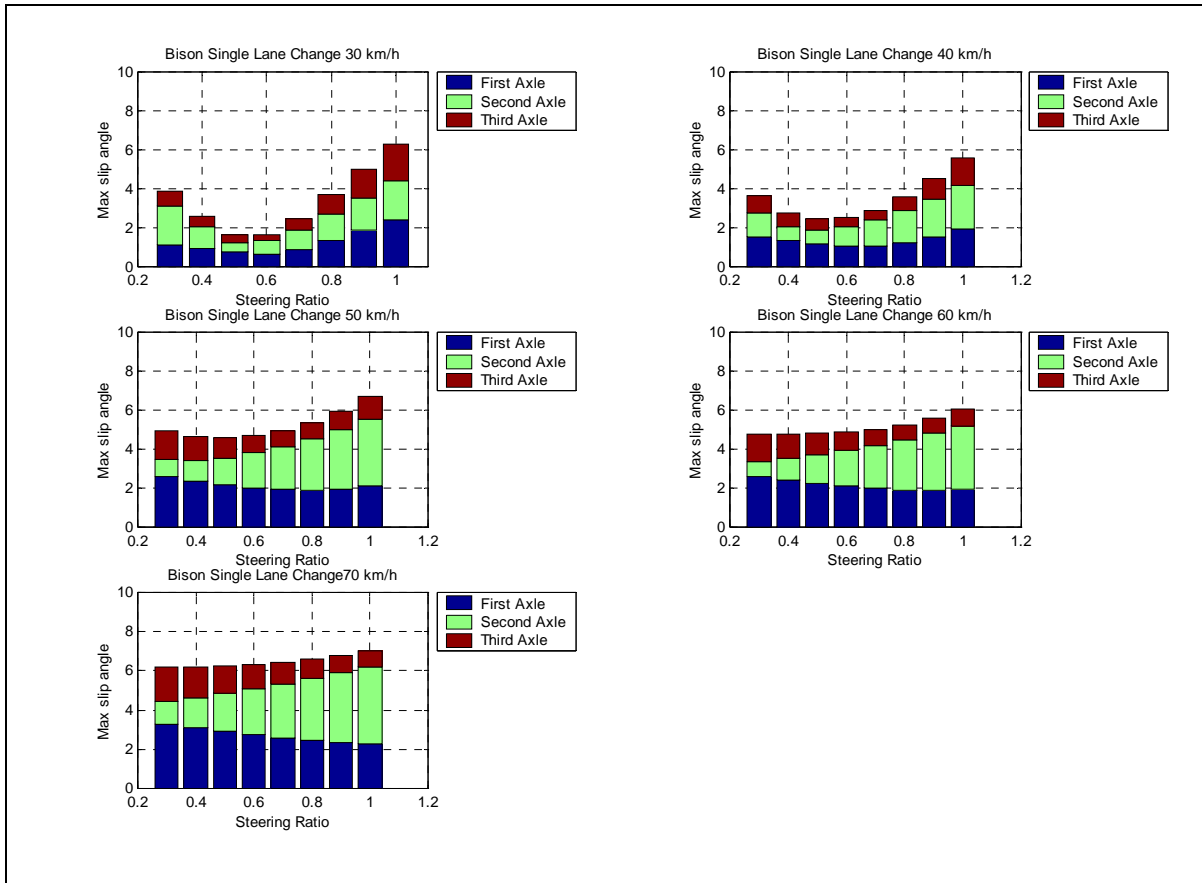


Figure 50 : Maximum slip angle

From the above, it can be seen that the maximum slip angle may be minimized when a steering ratio of 0.6 is used for low speed (30 km/h). For speeds above 50 km/h, the steering ratio will not minimize the maximum slip angle. The maximum slip angle is smaller for large steering ratios (less than 0.5), understandable since one axle is turned through an angle more than double the steering angle of the second axle.

When the simulated slip angles are plotted against time, it is clear that an “aggressive” driver model has been used. The model “reacts” to the step input at the beginning of the lane change (first peak), and has to compensate (again second peak) in order to complete the track. A more sophisticated model may have resulted in a smoother transition through the track. Since the aim of the study is not to determine the absolute maximum speed of the vehicle through the course, the results are deemed sufficient to investigate the problem on concept level.

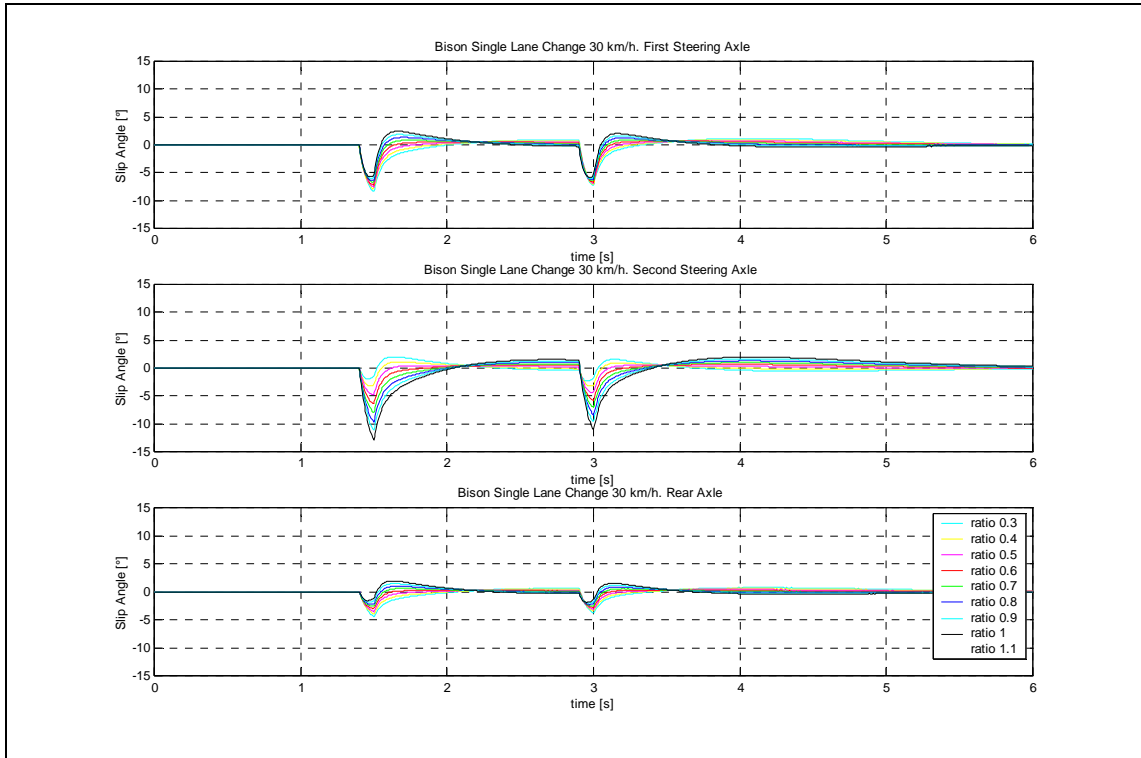


Figure 51 : Slip angles – 30 km/h

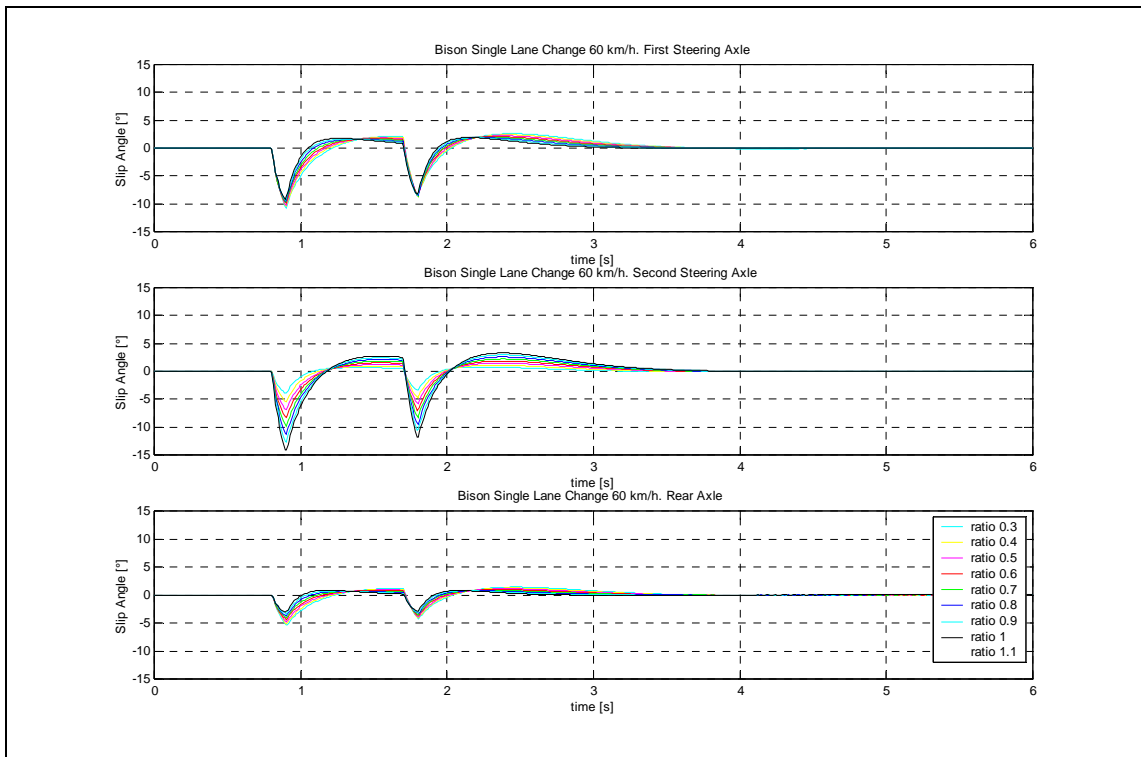


Figure 52 : Slip angles – 60 km/h

The above conclusions is also illustrated when the RMS of the slip angles are calculated, as shown in Figure 53.

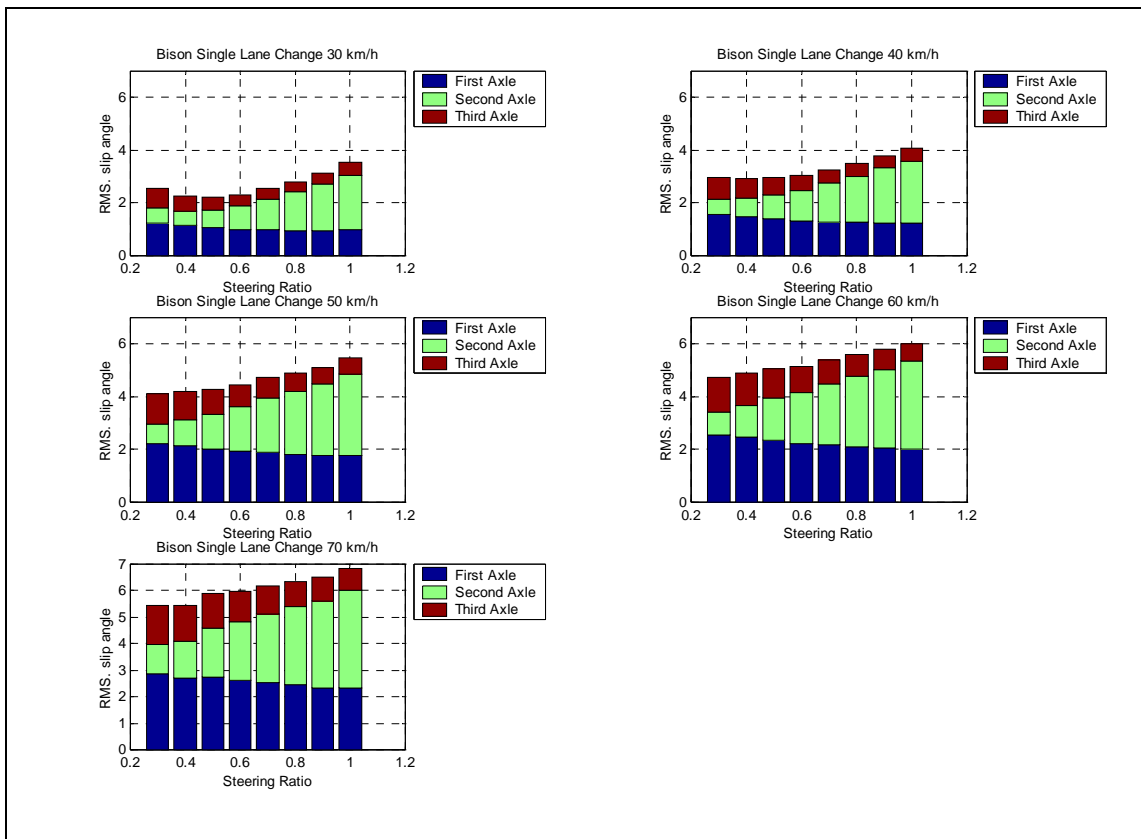


Figure 53 : RMS slip angles

The simulated trajectory through the lane change manoeuvre, for different steering ratios, and vehicle speeds are shown in Figure 54. As discussed above, the driver model ensures that the vehicle completes the track, but does not simulate the behaviour of a human driver, as will be shown in the following paragraphs when measured results are discussed.

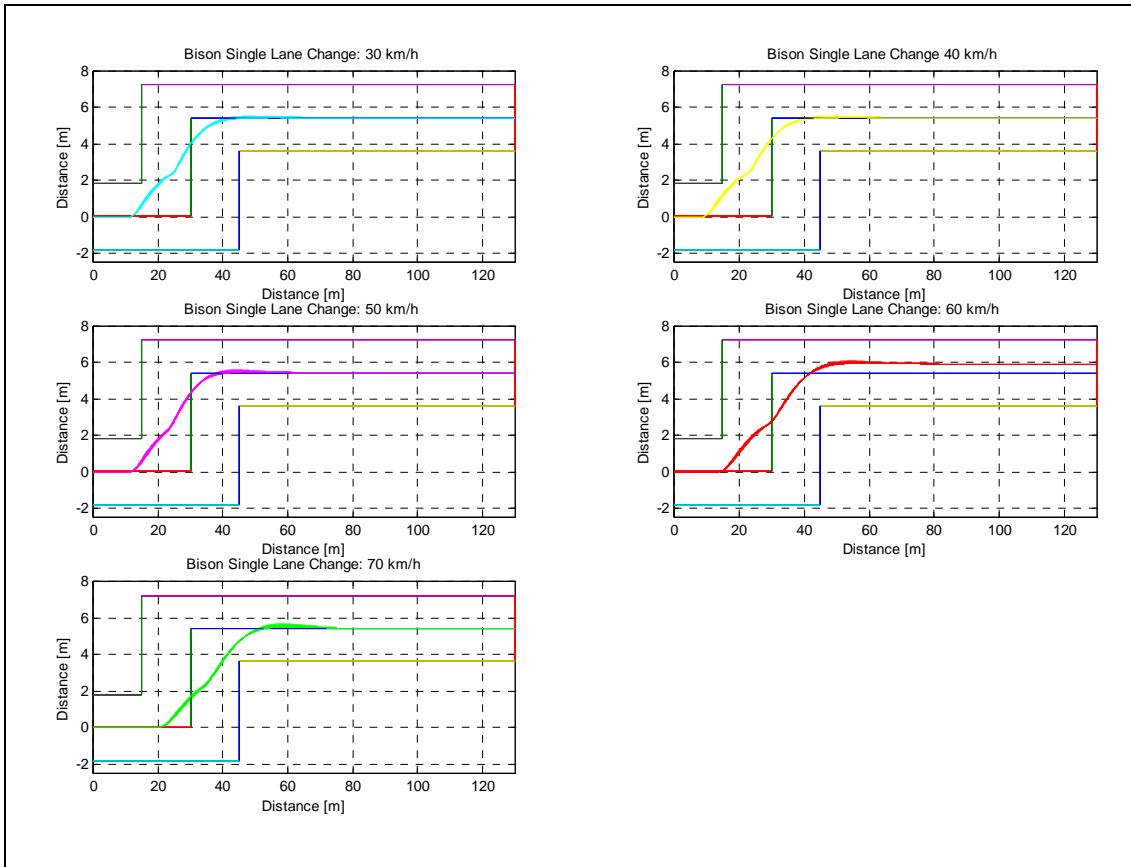


Figure 54 : Simulated trajectory

As a final example of typical output values that was achieved, the yaw angle of the simulated vehicle at 30 km/h is plotted in Figure 55. The effect of the aggressive driver model may be seen in the change in yaw rate to enable direction changes.

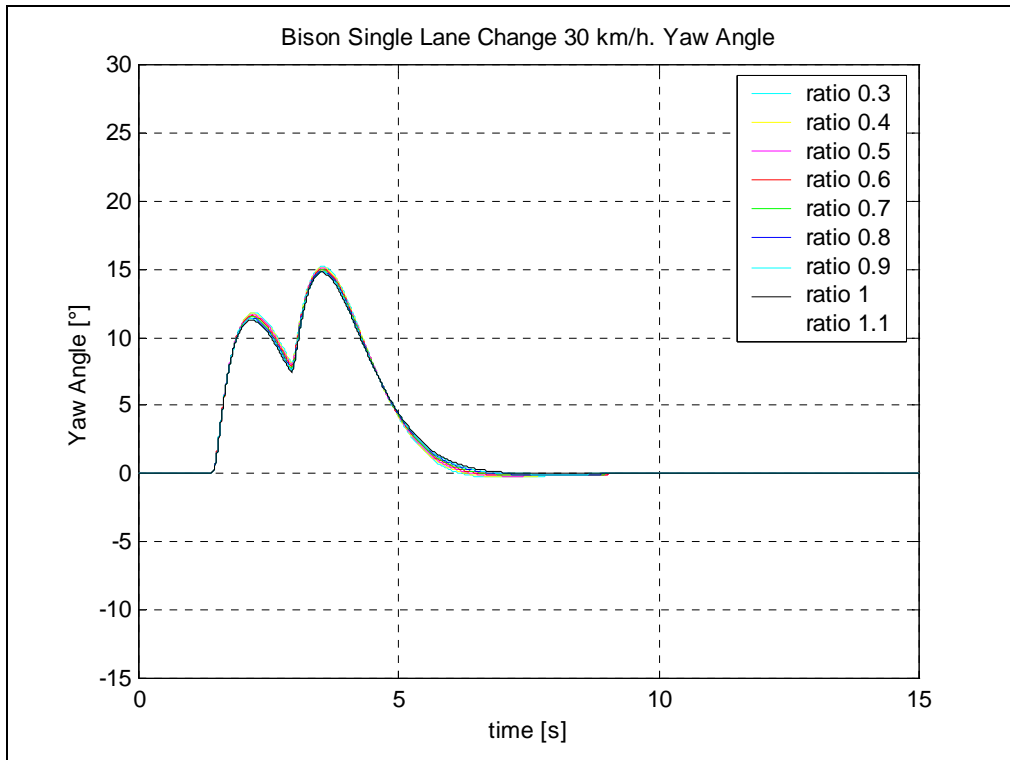


Figure 55 : Simulated yaw angle - 30 km/h

18. Vehicle measurements

18.1. Introduction

As a second phase of the investigation, track measurements were taken to verify and compare simulated results. Measured results would indicate the validity of the mathematical models, and the assumptions that was made.

The Bison vehicle was instrumented, and constant radius tests as well as single lane changes were performed as described below.

18.2. GPS measurements

During the planning phase of the vehicle tests, it was decided to investigate the use of dual GPS systems. With a GPS system mounted in the front of the vehicle, and a second GPS mounted on the rear of the vehicle, it should be possible, in theory, to determine the yaw angle of the vehicle at any time during the steady state and dynamic handling tests.

The yaw angle data and steering angle data may then be combined to evaluate the slip angles of any of the wheels. This information was previously difficult to calculate, since only the yaw *rate* is normally measured using a gyro. To obtain the yaw angle, the yaw rate needs to be numerically integrated to obtain the yaw angle. Numerical integration of measured data may result in drift, which needs to be corrected for.

18.3. Test equipment

The test equipment used is summarised in Table 4:

Table 4 : Measuring equipment

No	Description	Make	Model	Serial number
1.	Pitch gyro	Humphrey rate transducer	RT01-0101-1	H64
2.	Roll gyro	Humphrey rate transducer	RT01-0101-1	H66
3.	Yaw gyro	Humphrey rate transducer	RT01-0101-1	H65
4.	Optical pick-up (speed)	Banner	QS18VP6LV	0135F
5.	Frequency to voltage converter	Turck	MS25-Ui	MS25-Ui1
6.	Frequency to voltage converter	Turck	MS25-Ui	MS25-Ui2
7.	Position transducers	CELESCO	PT510-0040-111-1110	G1303685A
8.	Accelerometers	VTI Hamlin	5g	VOI 52
9.	GPS	RaceLogic	VBOX Pro -001	n/a
10.	Data acquisitioning system	DM5406 with 100Hz low pass filters LMT010	n/a	LMT DAQ001

18.4. Test vehicle and measurement positions

Figure 56 shows the instrumented vehicle performing a constant radius test on the Gerotek test track.



Figure 56 : Instrumented vehicle on the test track

The following was measured:

- Using wire displacement meters, the steering angle of the first and second axles were measured.
- The lateral acceleration of the vehicle body was measured.
- The vehicle speed was measured using a rotational pulse counter.
- The absolute position of the front of the vehicle was measured using a GPS.
- The absolute position of the rear of the vehicle was measured using a second GPS.
- The driver used a handheld GPS that was used to determine vehicle speed while performing the test.
- The roll and yaw velocities of the body was measured using gyros.

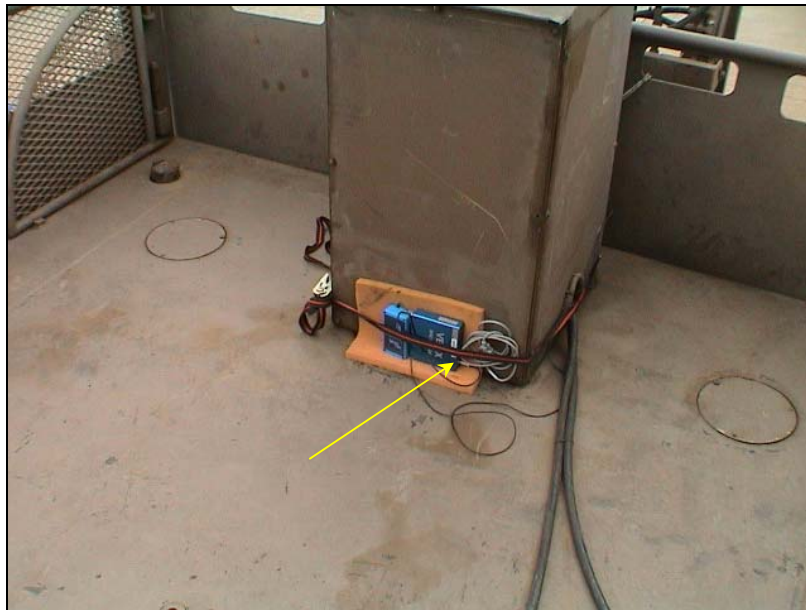


Figure 57 : Rear GPS



Figure 58 : Rear GPS antenna position

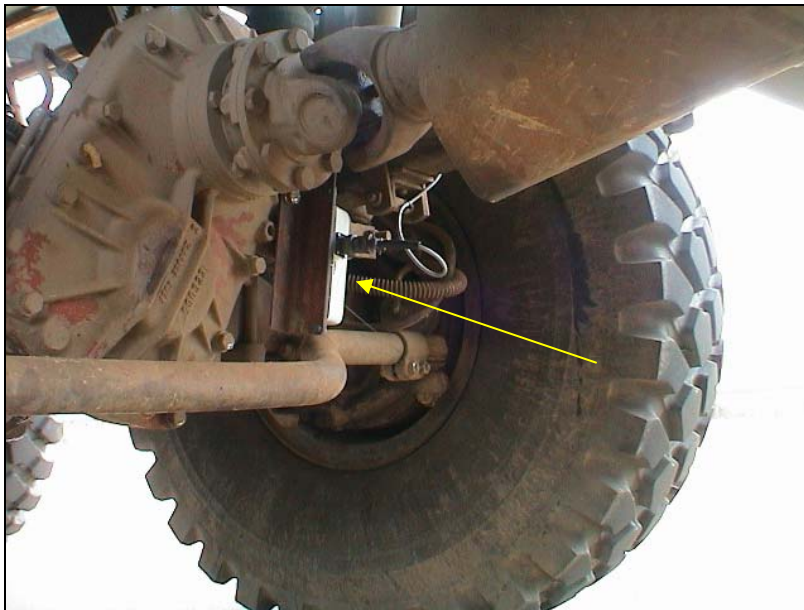


Figure 59 : First axle displacement meter position

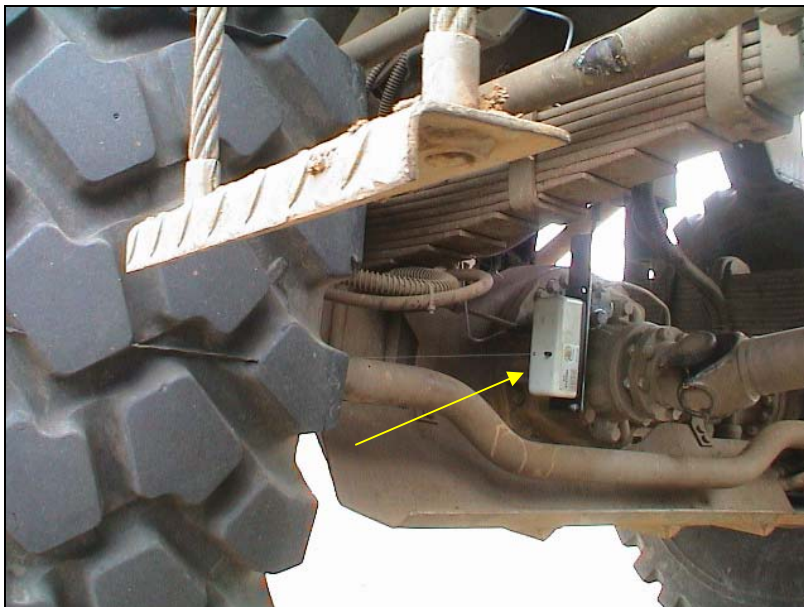


Figure 60 : Second axle displacement meter position



Figure 61 : Vehicle speed measurement



Figure 62 : Front GPS antenna position

18.5. Test procedure

The vehicle tires were inflated to 450 kPa all round, where after the wheel masses were measured, with the results indicated in Table 5:

Table 5 : Bison test wheel mass

Axle number	Left mass	Right mass	Axle total
1	2670 kg	2470 kg	5140 kg
2	2660 kg	2680 kg	5340 kg
3	2270 kg	2120 kg	4390 kg
		Total	14870 kg

The vehicle was driven to the test track, where the steering calibration was performed.

As a basis ISO 4138, steady state circular test procedure [30], and ISO 3888 for severe lane change manoeuvres [31] were used.

The vehicle was positioned at the skidpan track; the data capturing equipment was activated while the vehicle was stationary. The constant radius test was initiated, by first driving at a constant speed (against the engine governor to ensure a constant speed) in the gear closest to the required speed, around the track. After completion of a lap, the speed was increased. The procedure was completed clock-wise and anti-clockwise and the data capturing was ended after the vehicle came to a standstill.

A hand held GPS was used to record the actual vehicle speed as a reference.

A single lane change track was laid out on the Gerotek test facility long straight track. The track had the dimensions shown in Figure 63:

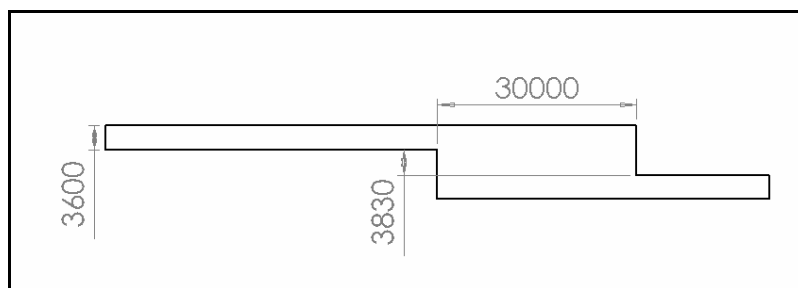


Figure 63 : Lane change track dimensions

Lane changes were performed at speeds of 28 km/h, 43 km/h, 51 km/h and 60 km/h.

The data capturing equipment was initiated, and the lane changes performed at a successive increase in speed.

After the vehicle came to a standstill, the measuring equipment was again switched off.

18.6. Steering calibration measurements

The steering angle calibration was done in two phases.

- The aim of the first phase was to determine the maximum measured steering angles of the first and second axles relative to the vehicle centreline, when the steering wheel is turned from lock to lock.
- The second phase was to determine the relationship between the linear displacement measured, and the absolute steering angles of the wheels, with the aim to determine the steering ratio between the first and second axles.

18.6.1. Steering calibration results: maximum steering angles

The vehicle was parked on a level surface, with the wheels at zero degrees. The steering wheel was rotated half a turn to the left, and the change in the angle between the wheel plane and the vehicle body was measured. The steering wheel was rotated another half a turn and the steering angle measured. The process was repeated until the end of travel stop was reached. The process was repeated turning the steering wheel to the left hand side, and the right hand side, for the left and right hand side wheels of the first and second axles.

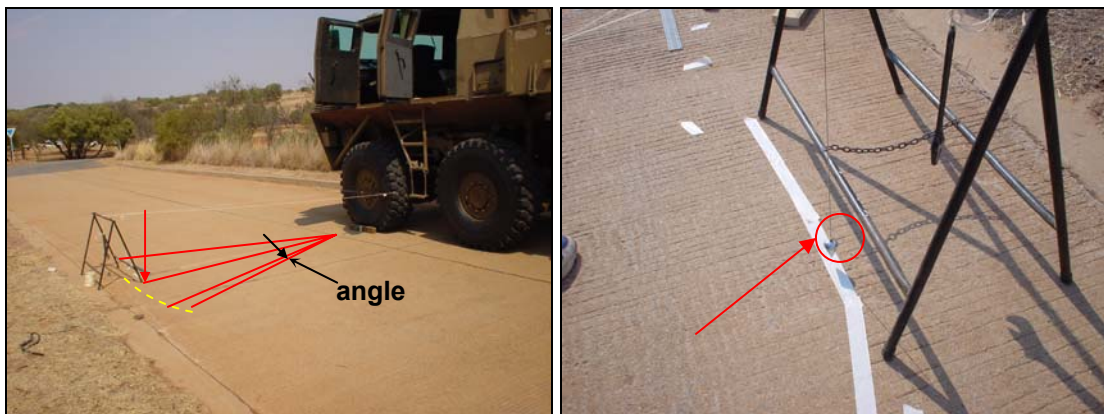


Figure 64 : Measuring steering angles. The position of the plumb line are shown

Figure 64 shows the measurement of steering angles. A plumb line, perpendicular to the wheel plane was used to scribe the position of the tire angle relative to the direction of travel, for the steering wheel increments. A long distance between the wheel and measuring point was used to reduce measuring errors. The process was repeated for the 4 wheels of the first and second axles.

18.6.2. Steering calibration results linear to angles

The second phase was the measurement of the steering angles using linear displacement meters on the first and second axles. From the neutral position, the steering was first turned to left lock, and then to right lock.

The wheel angle relative to the vehicle chassis measurement could be derived once the linear measurements were transformed to angular values.

The linear displacements measured, are shown in Figure 65.

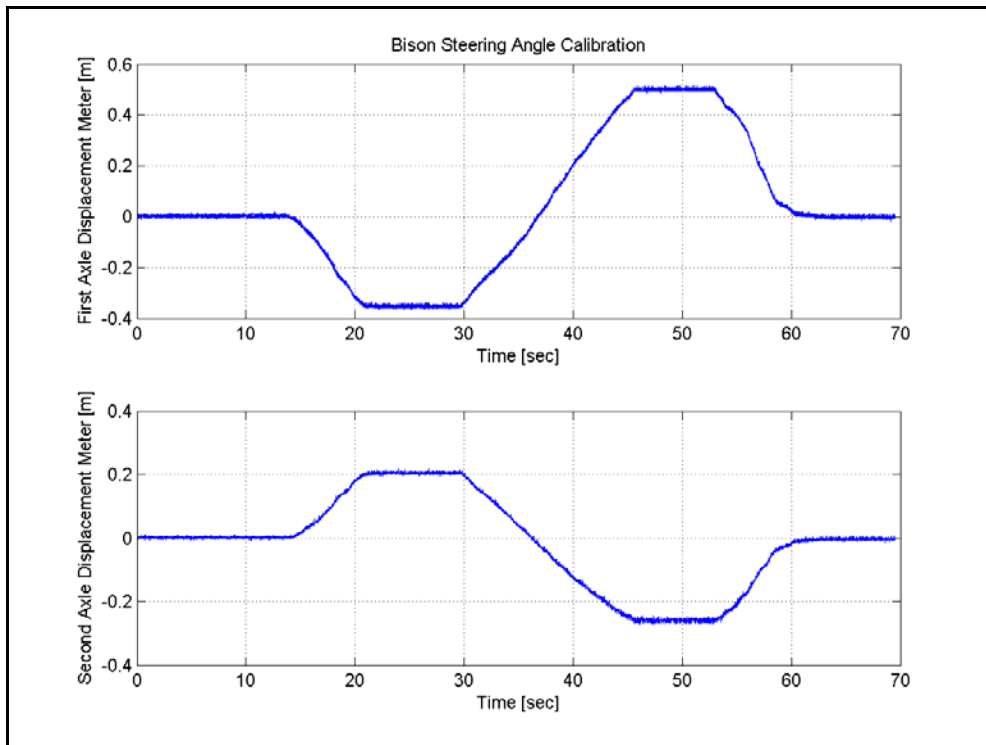


Figure 65 : Steering angle calibration, measured data

In order to transform the linear displacements to angular values (as required by the simulations), the actual wheel angles was measured, as described above.

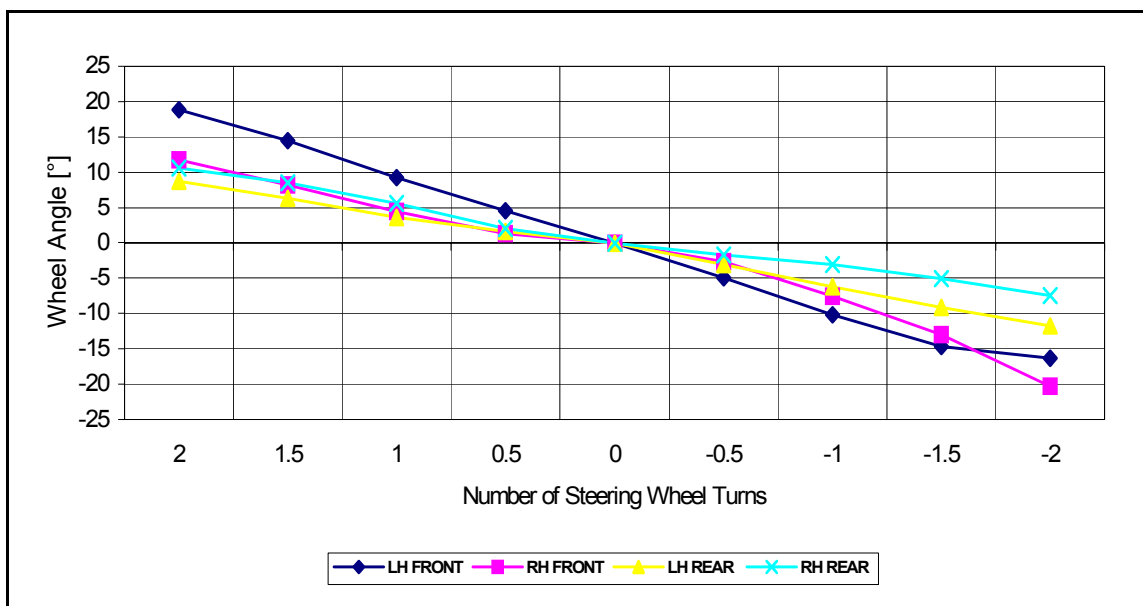


Figure 66 : Measured steering angles for steering wheel positions

From Figure 66 it is clear that the steering system is not symmetrical. As the system will be simplified to a bicycle model, the average of the left and right wheels are determined.

The angles used are shown in Table 6.

Table 6 : Measured wheel angles

	Counter clockwise	Clockwise
Maximum angle: 1 st axle left	-16°	18°
Maximum angle: 1 st axle right	-20°	12°
Maximum angle: 2 nd axle left	-12°	9°
Maximum angle: 2 nd axle right	-7°	10°
Average 1st axle	-18°	15°
Average 2nd axle	-9.5°	9.5°

A Matlab subroutine (Appendix A) converts the measured linear displacements to angular displacements. The results are shown in Figure 67 and Figure 68.

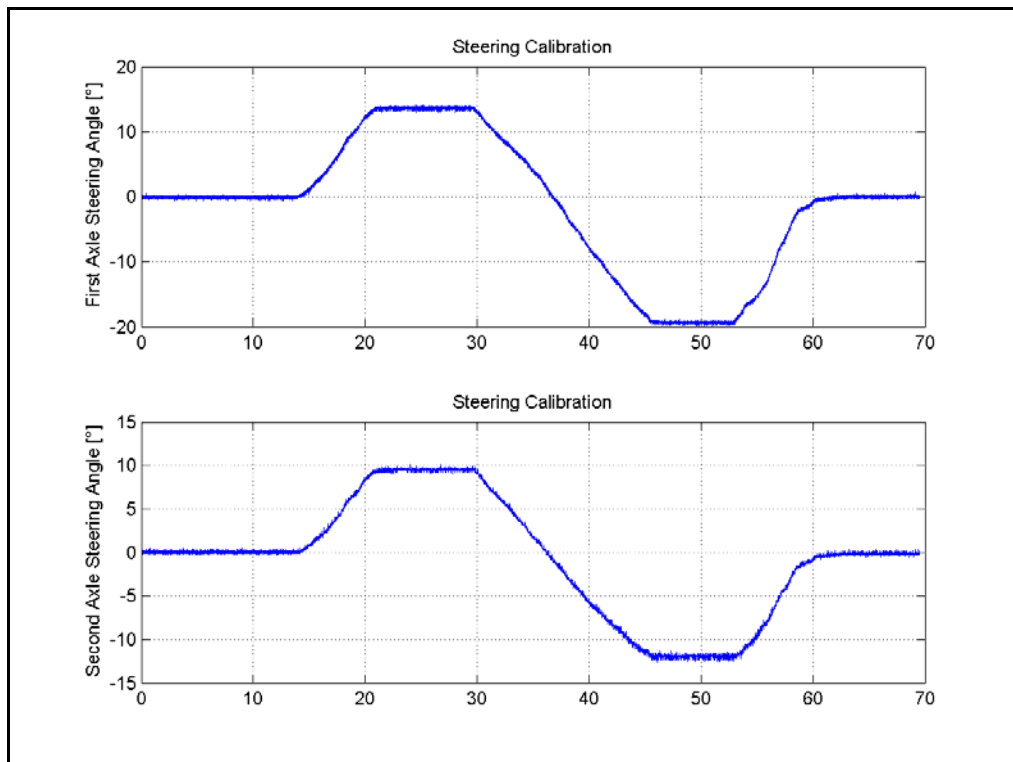


Figure 67 : Calibrated steering angle

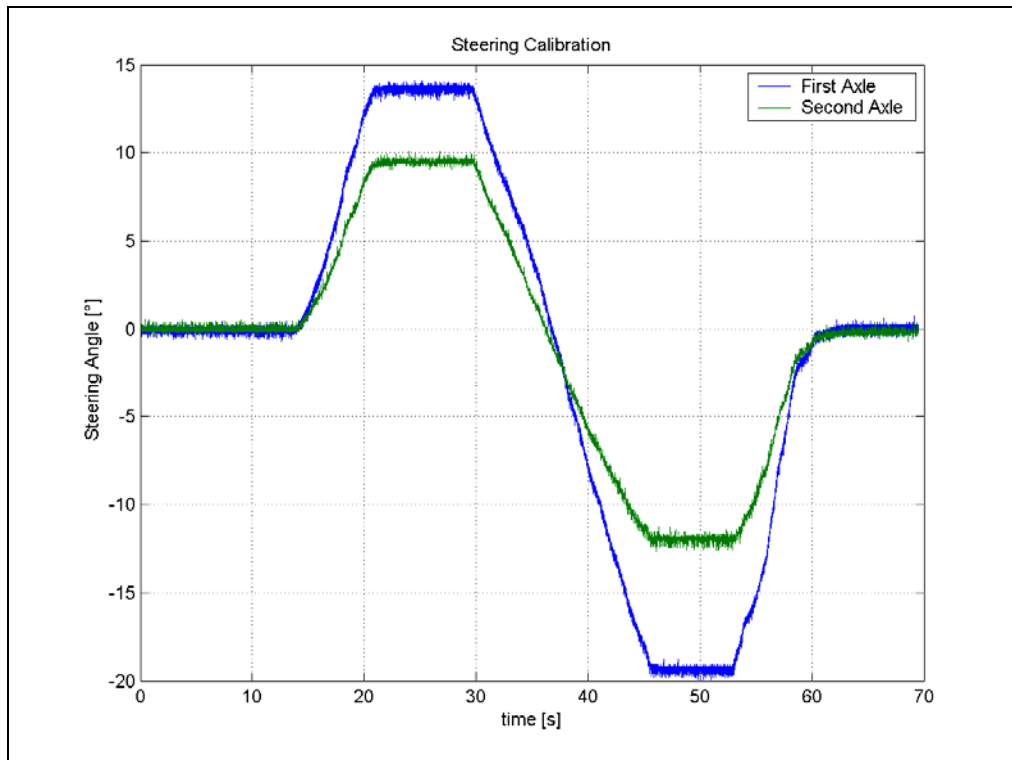


Figure 68 : First and second axle calibrated steering angles

Lines may be fitted through the first and second axle measurements, taken from time 30 seconds to time 45 seconds, representing full lock left to full lock right turn. The steering ratio between the first and second axle may be calculated, and is shown in Figure 69.

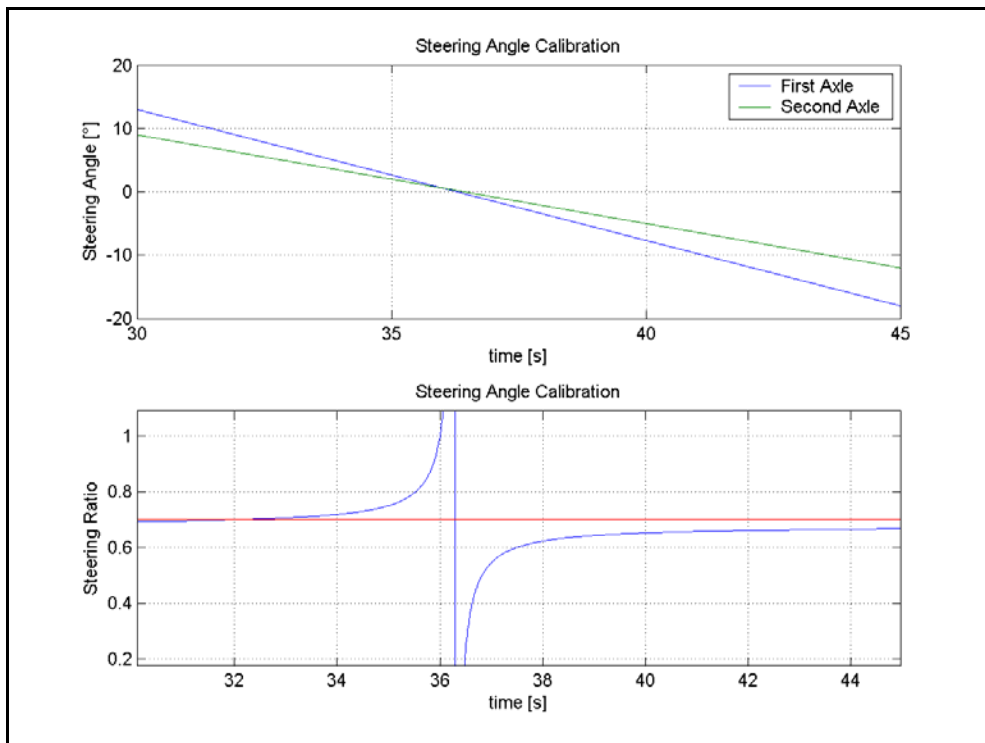


Figure 69 : Steering ratio, 0.7

The data in Figure 69 shows that the steering ratio between the first and second axle may be approximated as 0.7, for large steering angles. Small steering angles close to zero, results in an infinite ratio since the ratio calculation divides by zero.

18.7. GPS measurements

As mentioned, two GPS systems were used to plot the position of the vehicle at all times. It was found that the data was not accurate enough to determine the vehicle heading to such an extent that slip angles could be determined.

As an example, when the data of the constant radius test from the first and second GPS is overlaid, a result shown in Figure 70 is obtained.

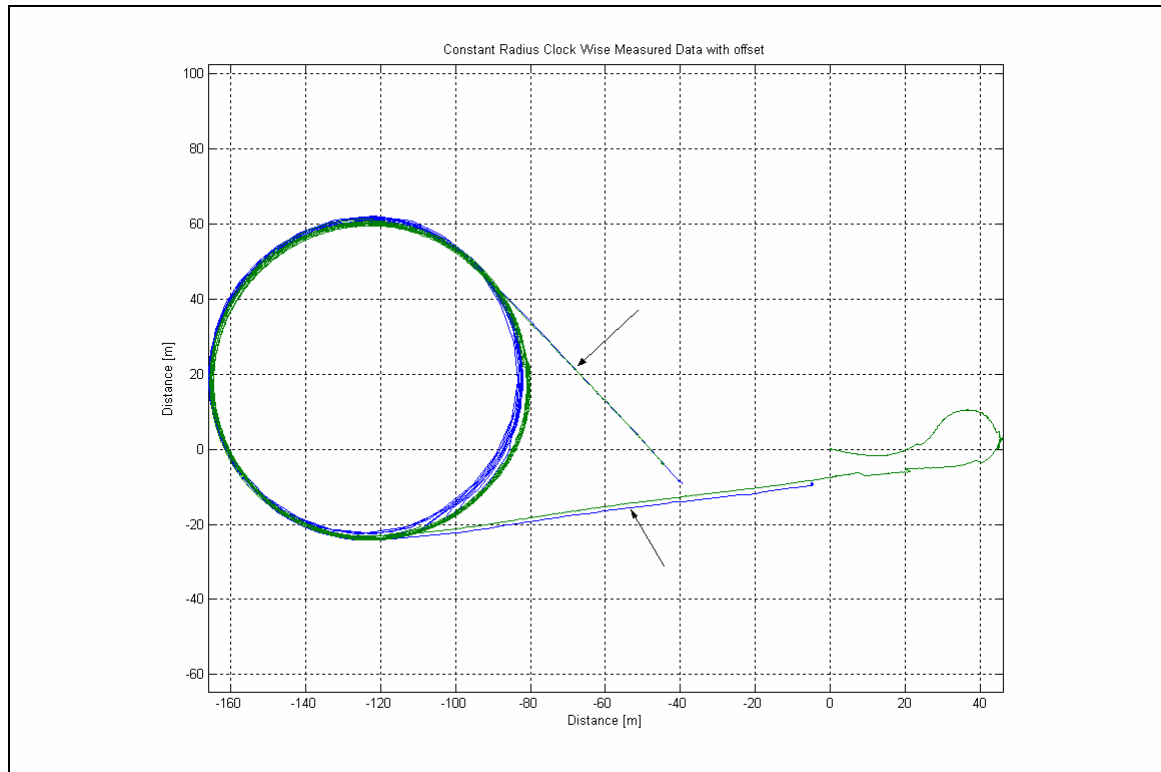


Figure 70 : Front and rear GPS data

It was expected that the approach and departure lines to and from the circle would have been plotted over one another, since the vehicle travelled in a straight line. The arrows in Figure 70 indicate the problem areas. From the above, it is clear that inaccurate slip angle data will be calculated, if the GPS data was used. A similar result for the lane change data is shown in Figure 71.

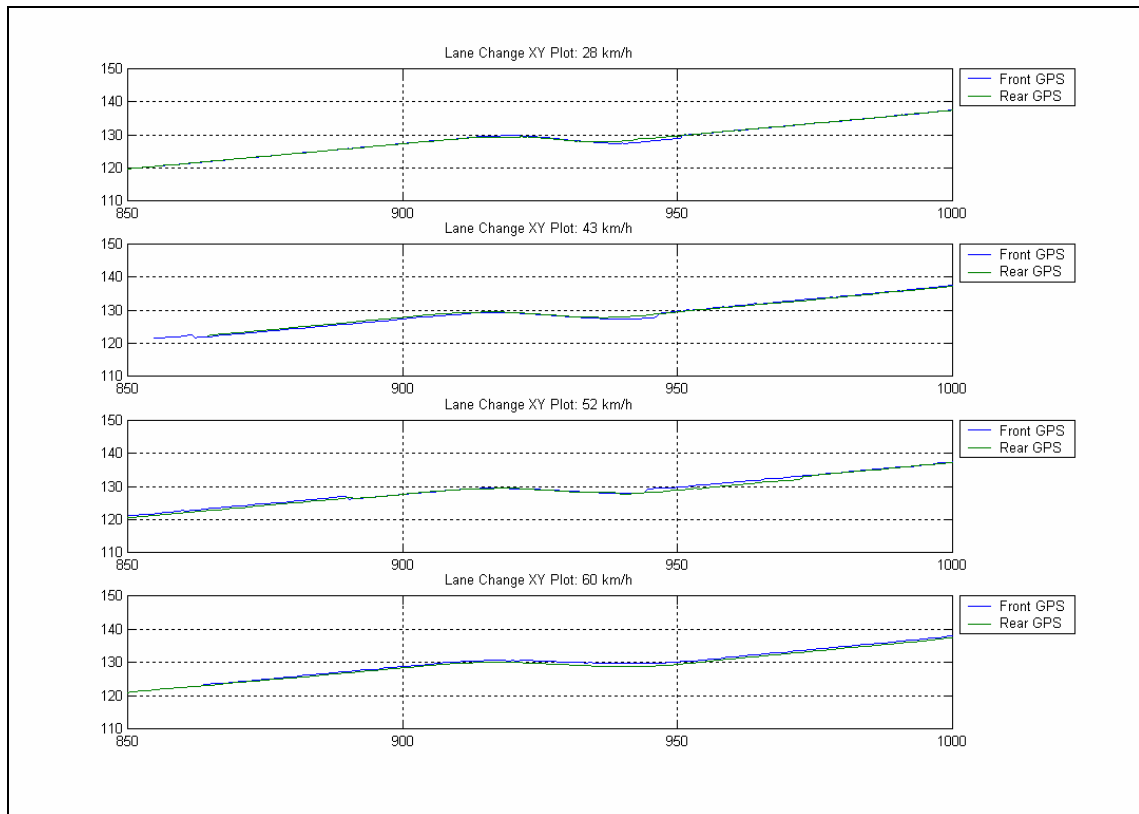


Figure 71 : GPS lane change data, front and rear GPS, 4 vehicle speeds

The inaccurate results may be contributed, amongst other things, to the GPS systems switching between satellites during the test. A further problem may have been the surrounding walls of the test track, deflecting satellite signals away from the equipment.

The GPS data was used to determine the trajectory through the lane change, but could not be used to calculate slip angles, as can be seen in Figure 71.

18.8. Test results, constant radius test

The skidpan track at the Gerotek test facility [32] was used to perform constant radius tests. The constant radius manoeuvre was first completed clockwise, at measured speeds of 10 km/h, 17.9 km/h, 27 km/h, 37 km/h and 40 km/h. The tests were repeated counter clockwise, at the same speeds. The radius of the test was typically 55 meters.

The results of the constant radius tests are shown below. The lateral acceleration, yaw rate and roll rate are shown as a function of time. During the test, the speed of the vehicle was increased, while the data was captured. Figure 72 to Figure 76 indicates the filtered measured values.

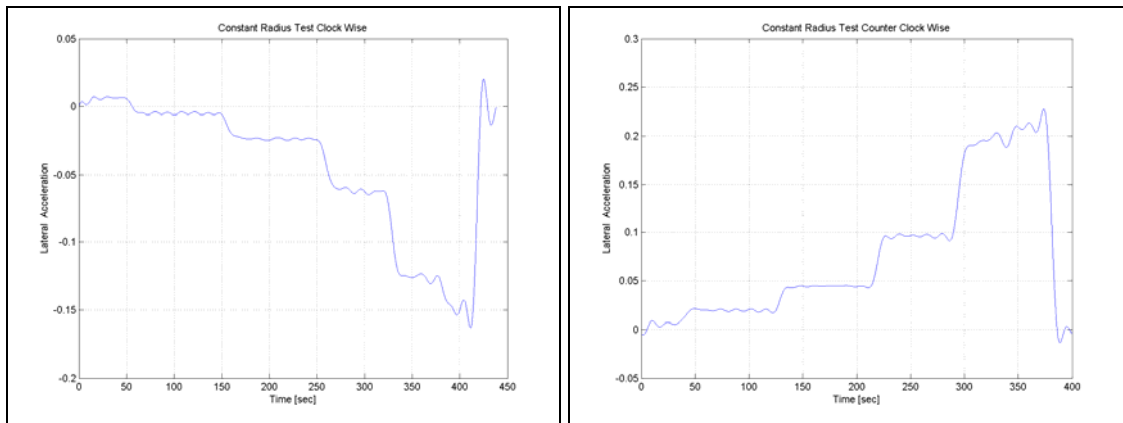


Figure 72 : Lateral acceleration, constant radius test

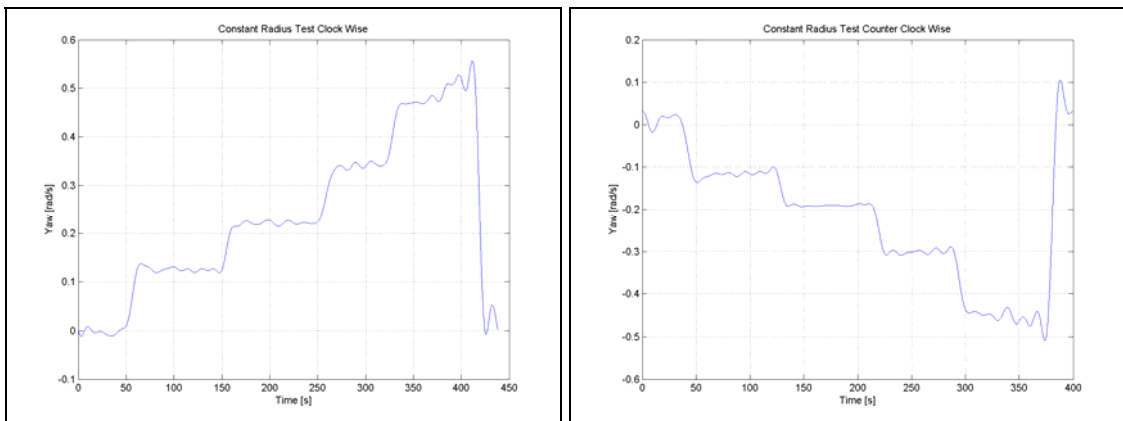


Figure 73 : Yaw rate, constant radius test

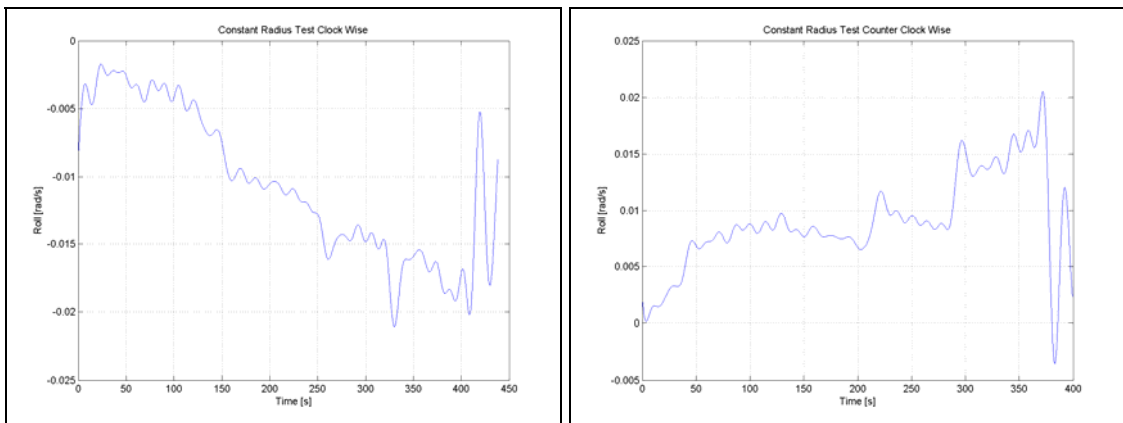


Figure 74 : Roll, constant radius test

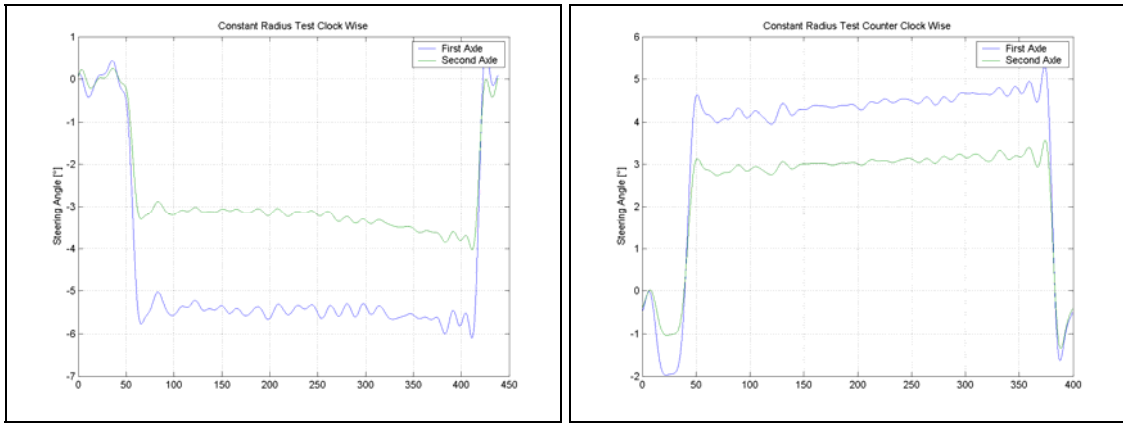


Figure 75 : Steering angle comparison, constant radius test

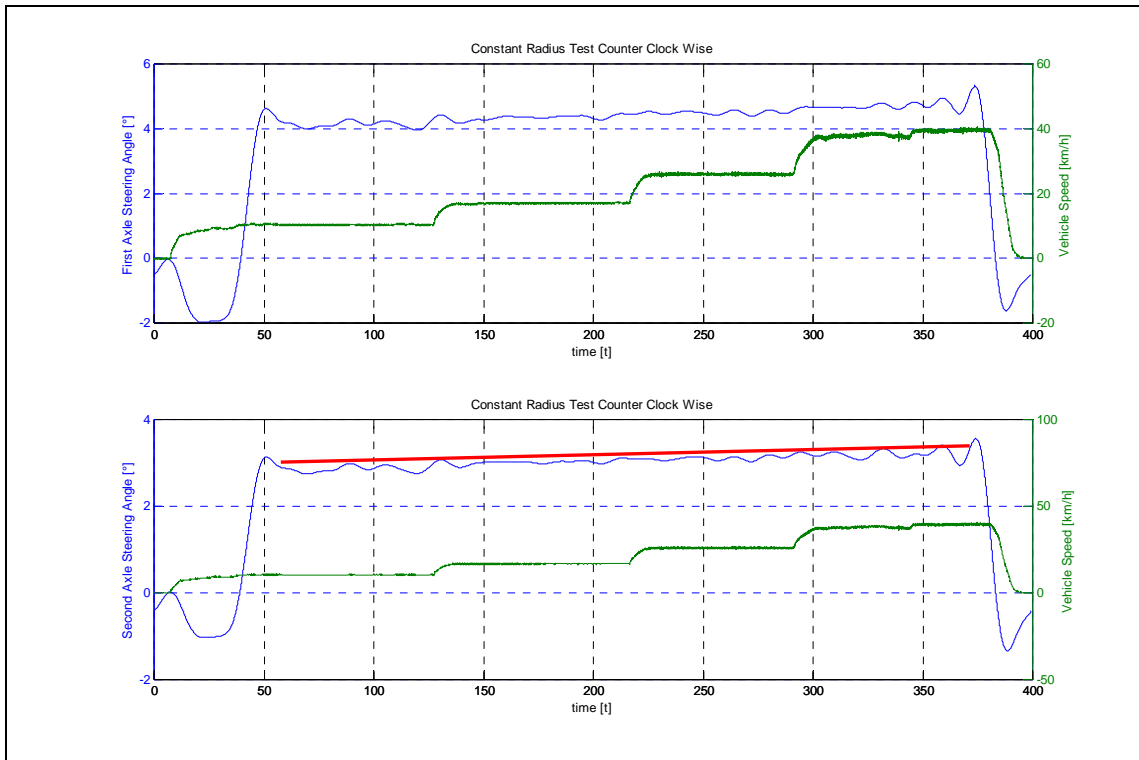


Figure 76 : Steering single and speed comparison, constant radius test

As expected, an increase in steering angle is required to keep the vehicle on the same radius at an increased speed. A detailed comparison of the measured and simulated results is given in paragraph 20.

19. Test results, single lane change

An example of measurements obtained from the single lane change manoeuvre is shown in Figure 77 to Figure 79. The lateral acceleration, yaw and roll velocities and wheel steering angles are shown.

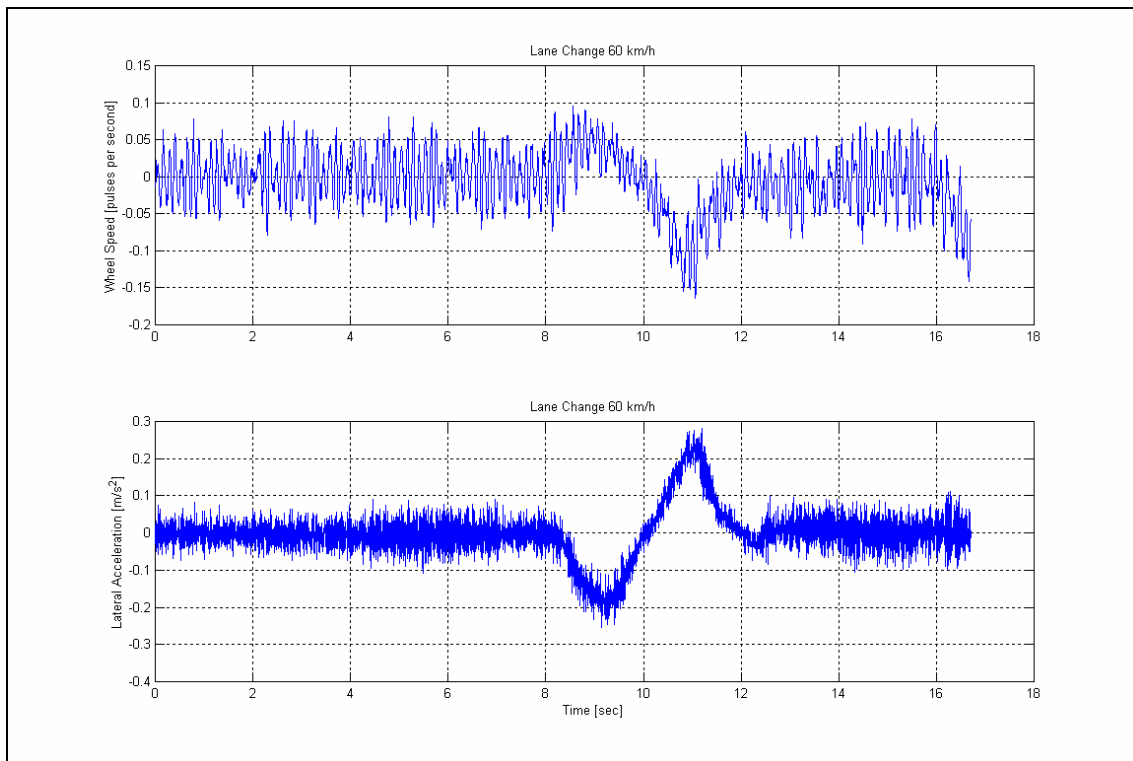


Figure 77 : Measured first axle wheel speed and lateral acceleration - 28 km/h

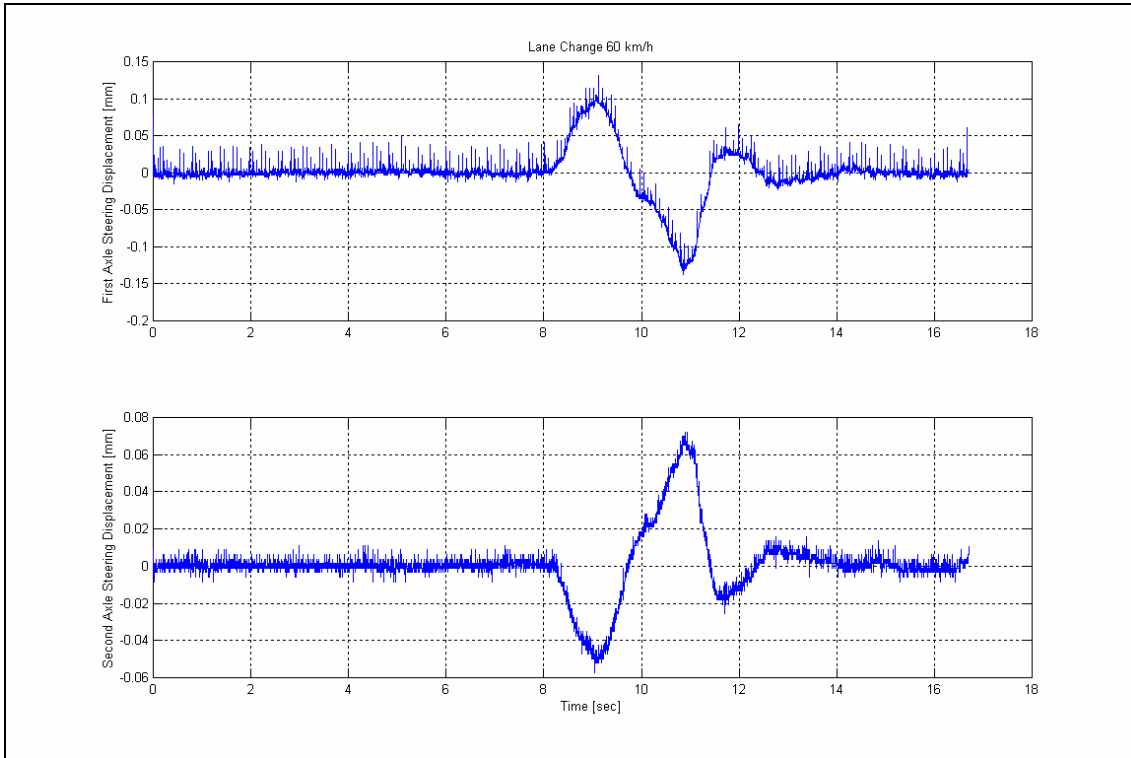


Figure 78 : Steering angles on first and second axles measured data - 28 km/h

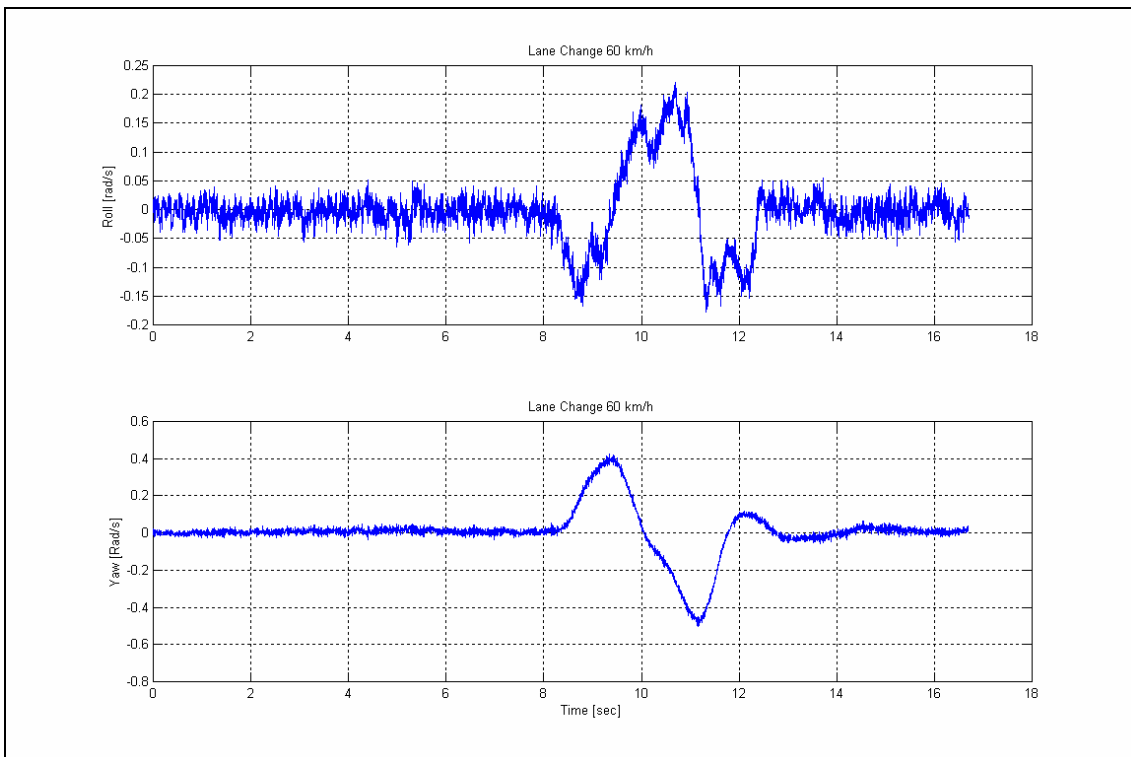


Figure 79 : Roll and yaw measured data - 28 km/h

20. Simulated vs. measured results

20.1. Introduction

The aim of the measurements described in the paragraphs above, was to determine the correlation between simulated and measured results. A correlation will confirm the mathematical model, and will provide confidence in performance improvements, effected by changing the steering system geometry of the vehicle.

20.2. Constant radius test

Correlation is obtained when the measured and simulated results are compared. Results of previous figures are combined and shown as Figure 80.

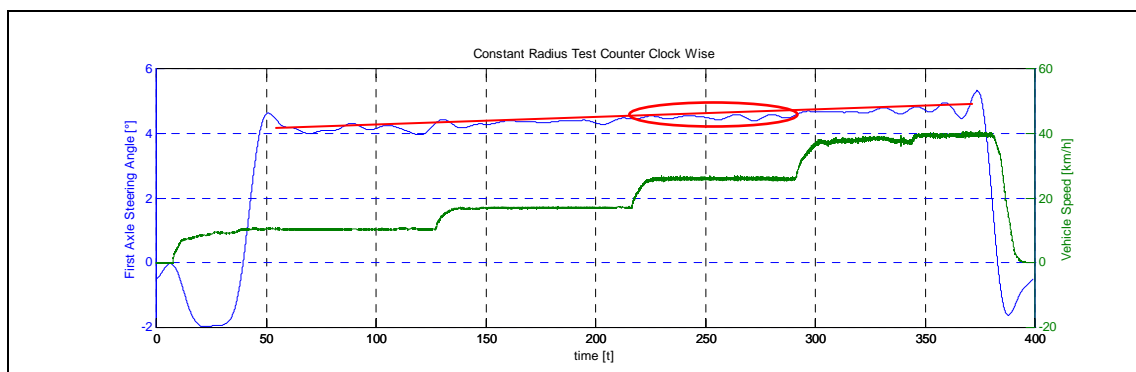
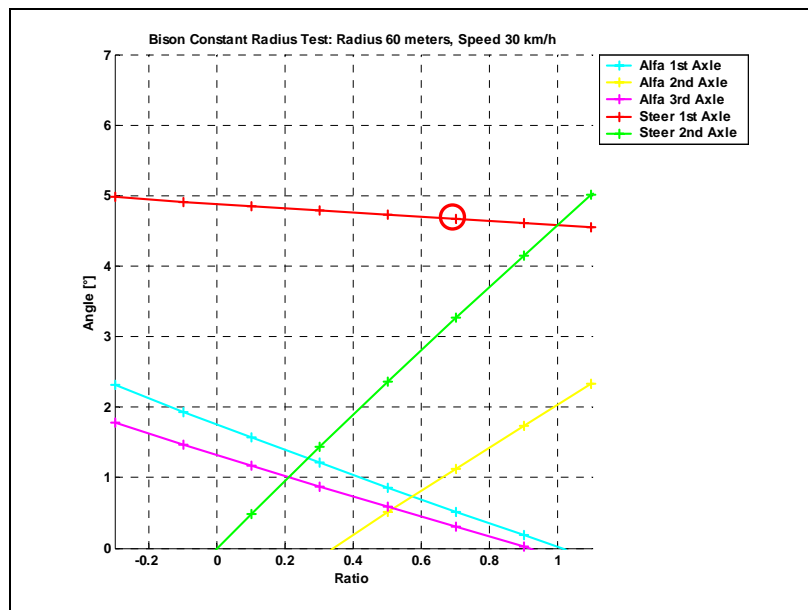


Figure 80 : (Result of Figure 34 and Figure 76)

Figure 34 (repeated as Figure 80) indicates the simulated first axle steering angle for a 60 meter radius test at 30 km/h (for a steering ratio of 0.7) equates to 4.8 degrees. Figure 75 and Figure 76 indicates a measured angle of 5.3 degrees clockwise and 4.2 degrees anti-clockwise. An average of the clockwise and anti-clockwise data is 4.75 degrees, similar to the calculated value of 4.8. The simulated angle for the second axle is 3.5 degrees, and the measured angle is 3 degrees at 30 km/h.

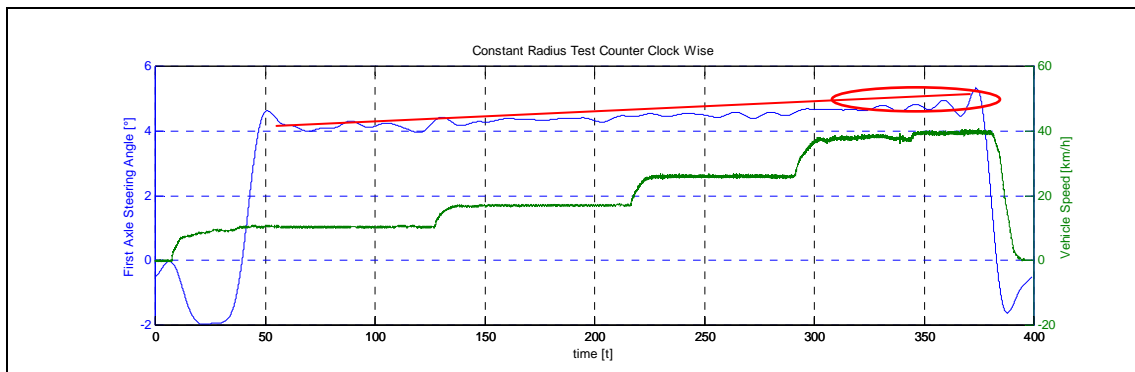
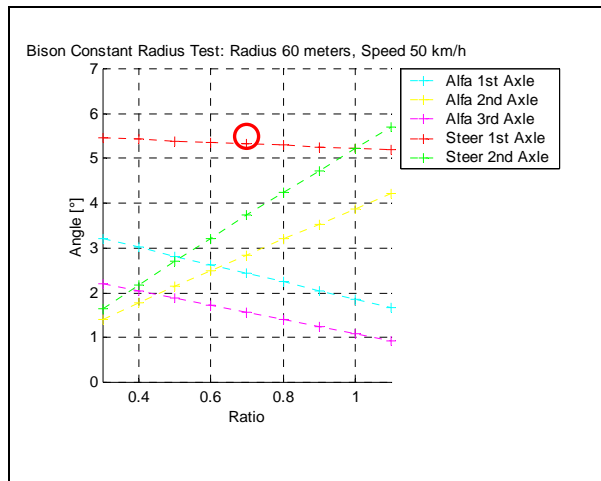


Figure 81 : (Result of Figure 34 and Figure 76)

Figure 34 indicates the simulated steering angle for a 60 meter radius test at 50 km/h (for a steering ratio of 0.7) equates to 5.3 degrees. Figure 75 and Figure 76 indicates a measured angle of 5.6 degrees clockwise and 5.3 degrees anti-clockwise. Once again the average of 5.45 degrees corresponds with the calculated 5.3 degrees. The simulated angle for the second axle is 4 degrees, and the measured angle is 3.5 and 3.2 degrees for clockwise and anti-clockwise tests, an average of 3.35 compared to 4 degrees at 50 km/h.

20.3. Single lane change

The simulated path that the vehicle followed through the single lane change obstacle course, at different vehicle speeds, are compared with the measured path of the vehicle through the single lane change (front and rear GPS data) in Figure 82. Also included in Figure 82 is the simulated trajectories predicted for the vehicle when the steering ratio between the front and rear axle is varied from 0.5 to 1.1.

Once again the problem with the GPS changing satellite reference may be seen in the results.

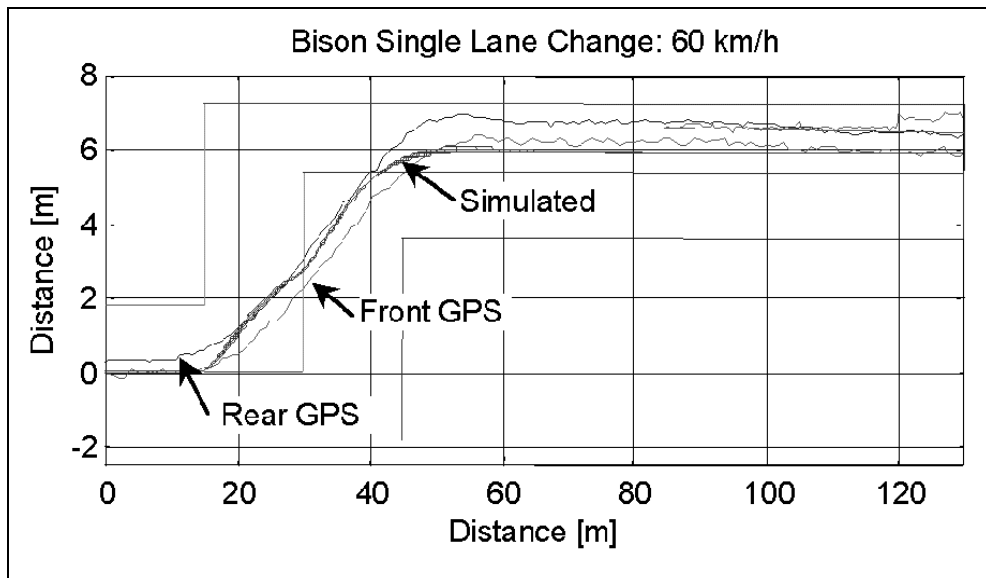
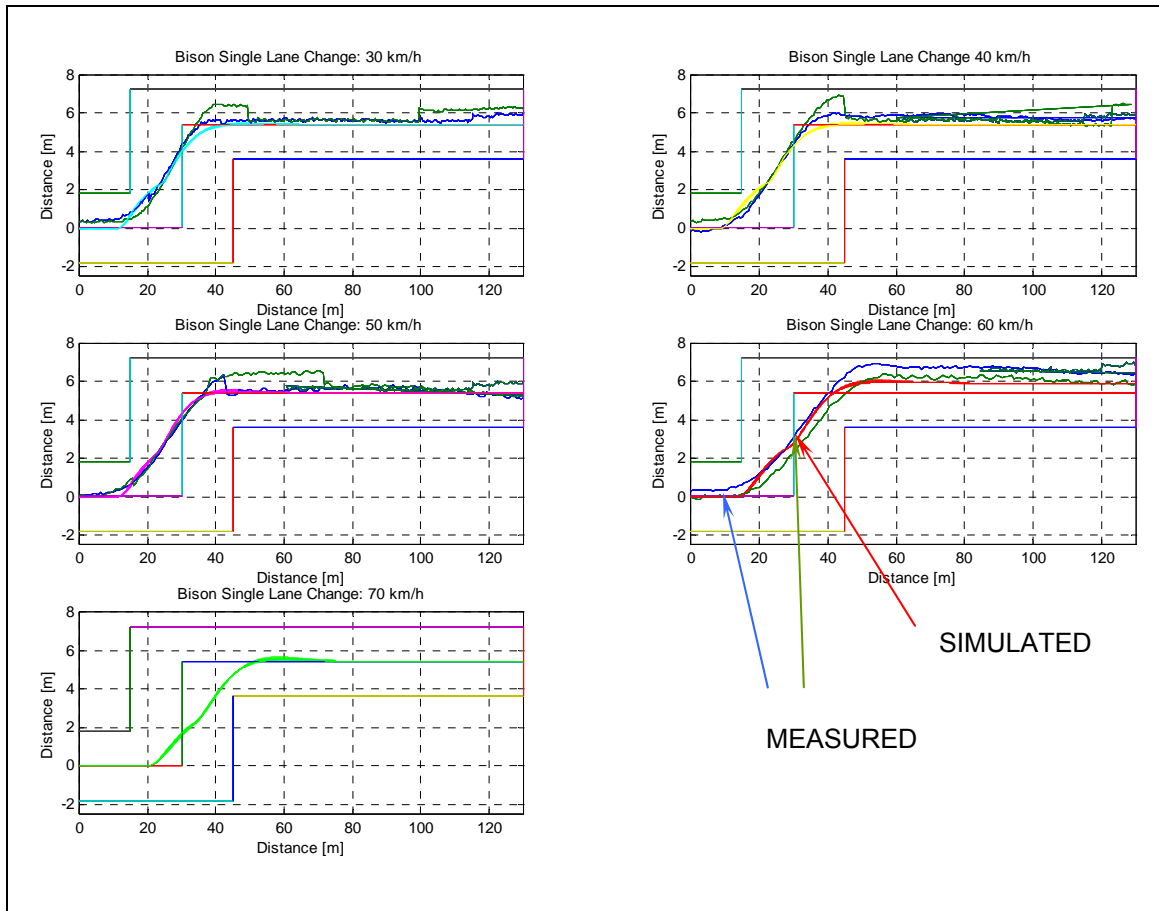


Figure 82 : Single lane change measured vs. simulated trajectories

The following conclusions may be drawn from the above:

- The simulated results match the measured results accurately during the approach, lane change and exit of the course.

- The simulated driver model is more aggressive, resulting in increased slip angles because of larger steer movements.
- For the same driver model, a change in the steering ratio at any practical speed will not have a noticeable effect on the path that the vehicle will follow through the lane change.

As a second comparison, the measured and simulated steering angles for the 43 km/h lane change are shown in Figure 83 and Figure 84. As mentioned in the preceding paragraphs, the simulation driver model is more aggressive than the test driver. The rate of change of steering angle for the test driver is 2 degrees per second, and the simulation results show a steering rate change of 15 degrees per second in some instances. However, the vehicle trajectory, and journey time correlates with measured results.

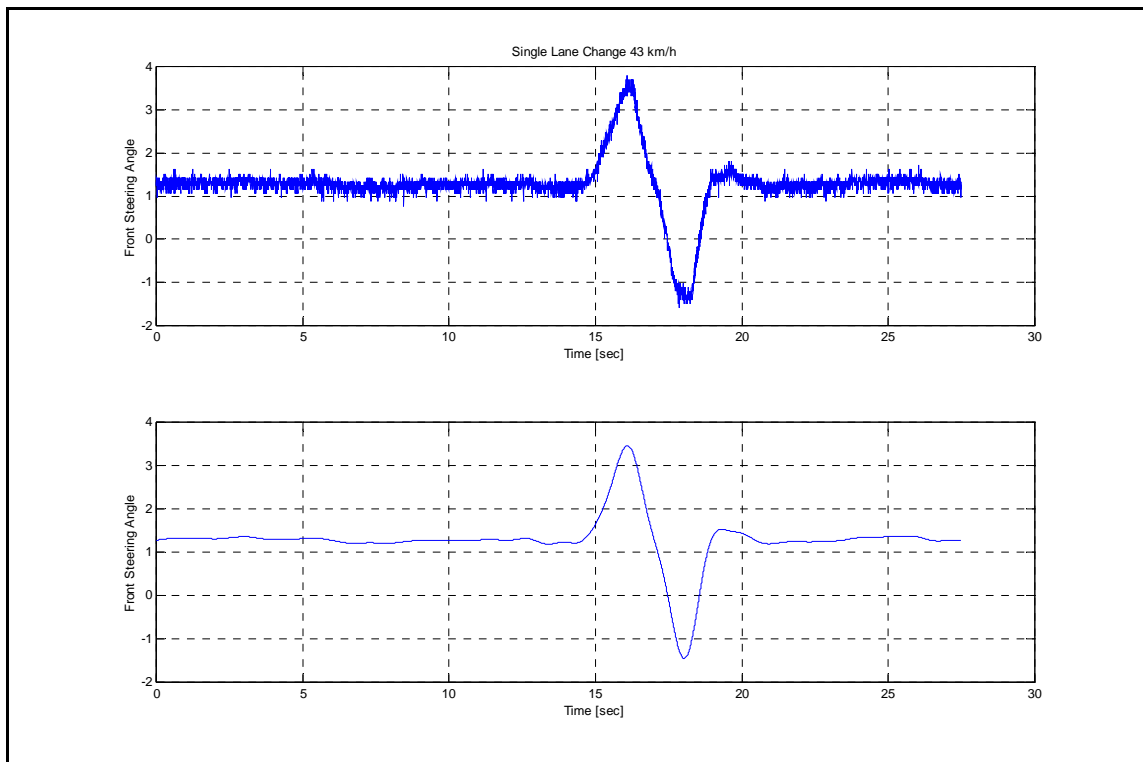


Figure 83 : Measured steering angle single lane change - 43 km/h

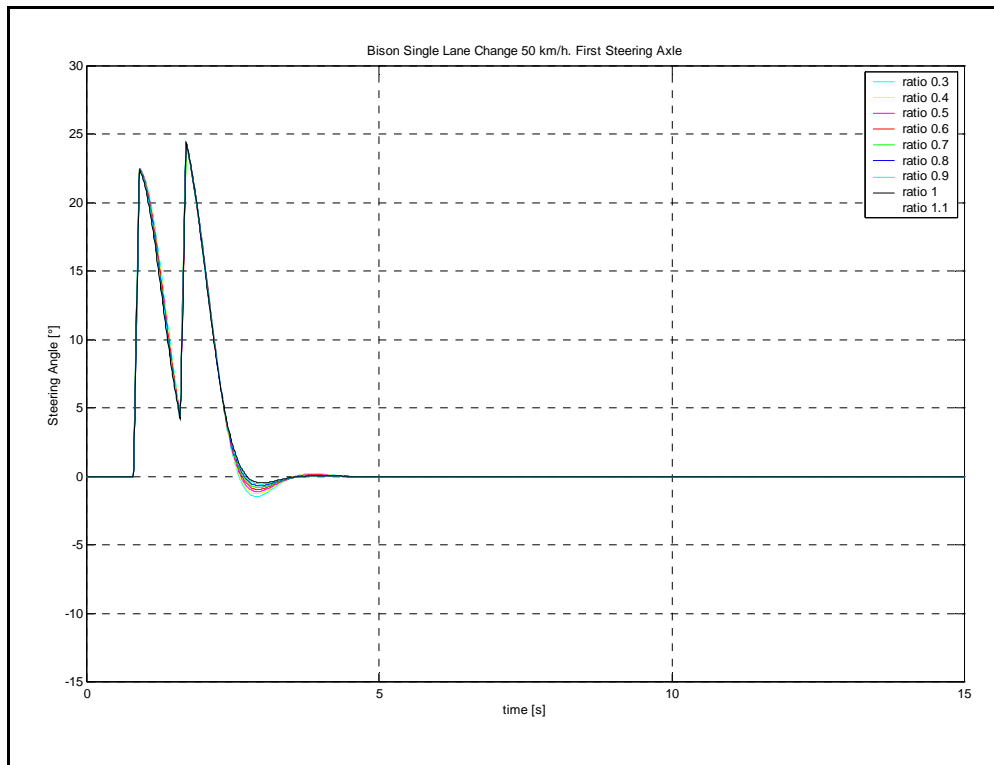


Figure 84 : Simulated steering angle single lane change - 50 km/h

21. Vehicle specific characteristics

Reasons for the small improvement in handling, that have been measured and simulated in the preceding paragraphs, may be explained summarised as follows:

21.1. Vehicle geometry

The Bison vehicle is a 6x6 vehicle, steering with the first and second axles. The third axle is not steerable, but acts as a reaction to the steering forces generated by the first and second axles. The tires on the three axles are the same, and the centre of mass of the vehicle is close to the second axle. (The vehicle was tested in the unladen condition.) As measured before the tests commenced, the axle load on the first and second axles are approximately 5 tonnes for first and second, and only 3.9 tonnes on the rear axle.

Based on these assumptions, the following may be postulated:

- The side force of the front axle and rear axle is balanced around the centre of mass, with the second axle (with a short lever arm close to the centre of mass) having little effect on the moment equilibrium of the vehicle.
- Therefore, by changing the steering ratio within practical ranges (to ensure manoeuvrability at low speed), the effect on the vehicle system, at normal operating speeds have little effect.
- Following on the above, it may be concluded that the effect of changing the steering ratio may be more pronounced in vehicles with long wheelbases, and vehicles with a centre of mass further away from the second steering axle, as was the case with Bison.

To illustrate the above, the single lane change simulation was repeated for a fictitious 6x6 vehicle with the dimensions shown in Figure 85.

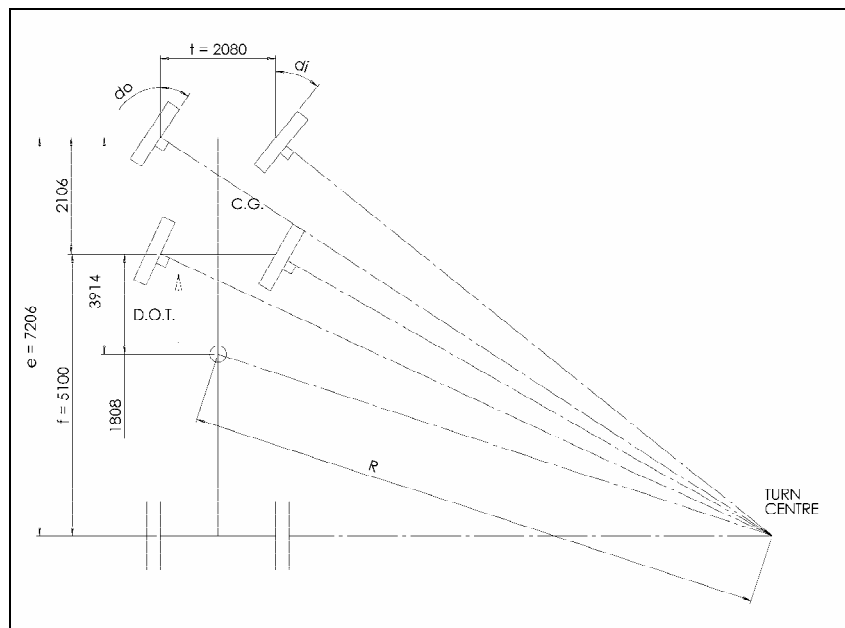


Figure 85 : LWB vehicle

When the slip angles for the same driver model of Bison is compared to a vehicle with the same mass, but different axle spacing, it can be seen that for a Long Wheel Base (LWB) vehicle, a steering ratio may be chosen to minimize the slip angles for a specific speed. The results are compared in the following figures. Figure 86 shows the simulated slip angles on three axles for a single lane change at 40 km/h for a LWB vehicle, and Figure 87 shows the slip angles for Bison.

The slip angles for a LWB vehicle may be minimized, because of the better force and lever arm relations that exist. For the instance calculated, a 0.7 steering ratio the slip angles of the first and second axles are minimized for 30 km/h. Figure 88 illustrates the above concept when slip angles may be reduced by a factor of more than two for all vehicle speeds simulated. When the results of Bison is evaluated, it may be seen that steering ratio changes have little effect on the slip angles that are generated by the first axle, and to a lesser extend the second axle.

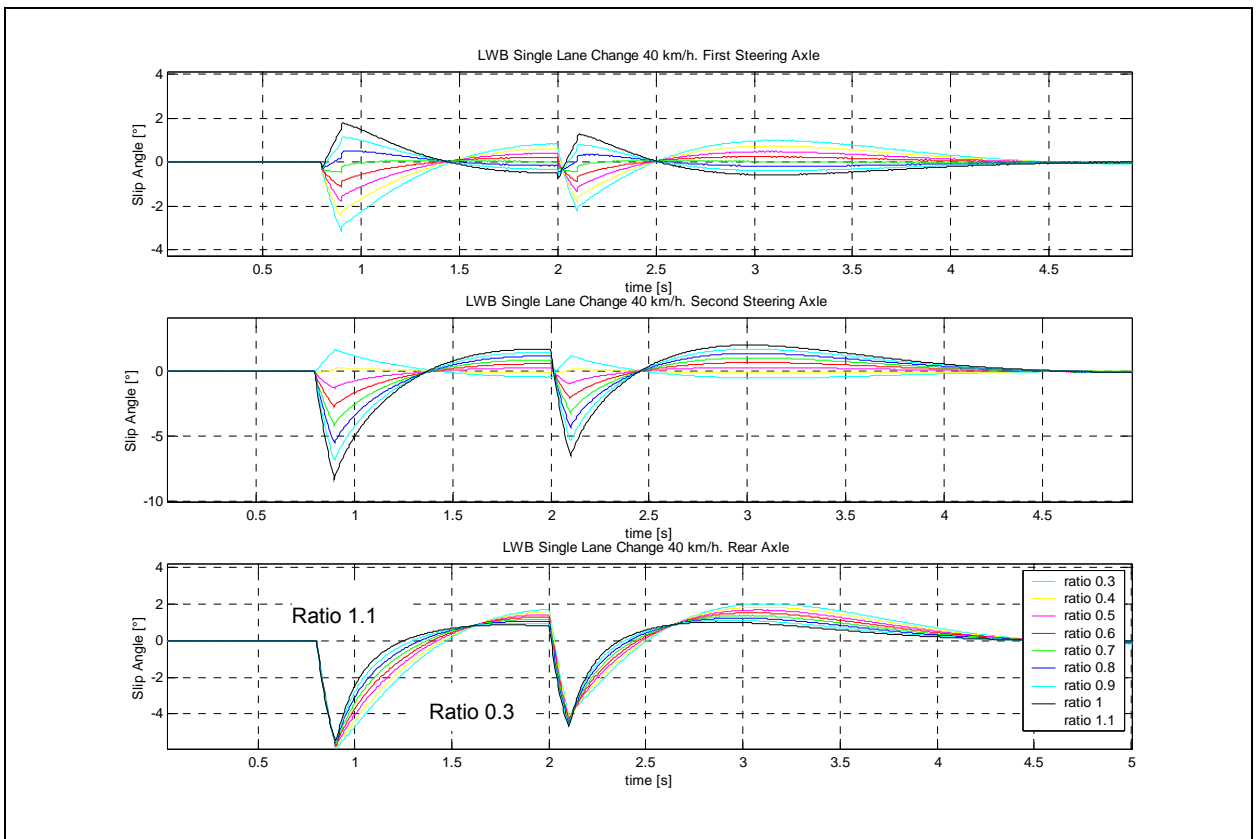


Figure 86 : LWB slip angles

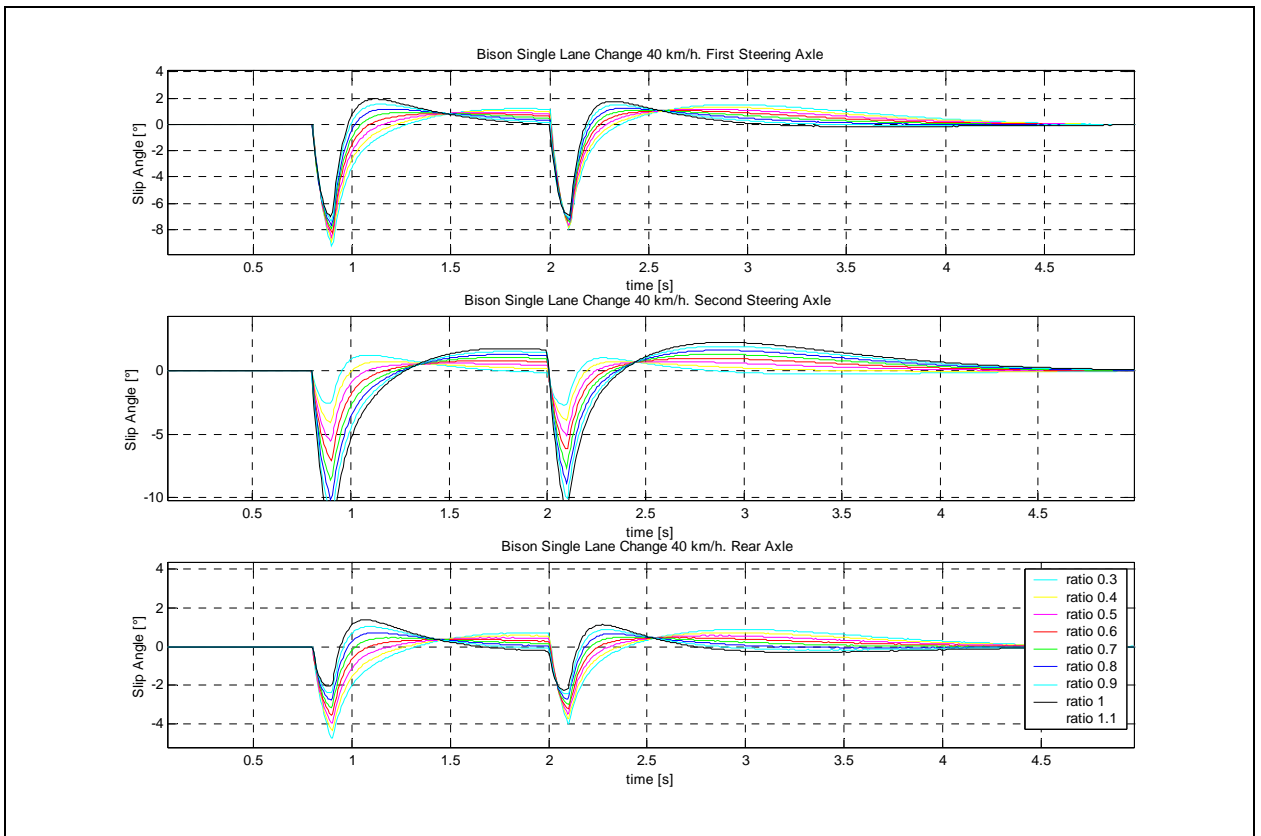


Figure 87 : Bison slip angles

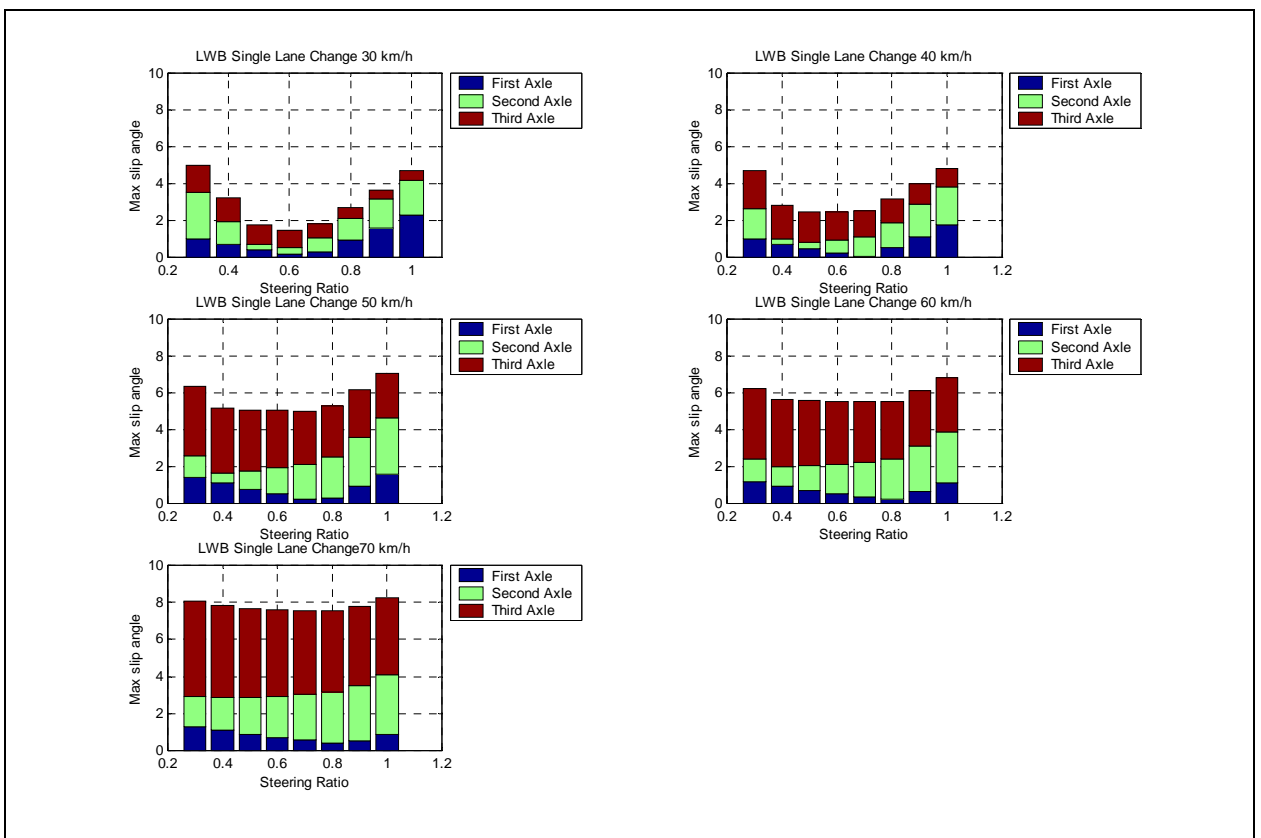


Figure 88 : LWB vehicle, maximum slip angles

The above conclusion may be expanded to 8x8 vehicles as shown in Figure 89. Once again the vehicle has a long wheelbase, with the centre of mass close to the middle of the vehicle. Due to the dual rear axles, spaced close together far from the centre of mass, the change in steering ratio for this vehicle may have a smaller effect, than on a similar 6x6 configuration, steering with two axles.



Figure 89 : 8x8 MAN

21.2. Tire and driver model

A further characteristic of the Bison vehicle is a stiff spring pack and limited wheel travel, compared to similar vehicles in its class. At low speed, these factors reduce body roll and may increase load transfer. Load transfer, combined with a linear tire model may be expanded in future work to improve results.

21.3. Speed ranges

The aim of the study was to investigate the improvement of vehicle handling during normal road use, to see if a marked improvement can be found. In other words, a marked improvement in handling of a variable ratio system, during normal use, may convince a potential customer to select a variable ratio steering system above a normal system, only if improvement can be shown.

The test speeds that were used, were selected to reduce the risk of vehicle and accident damage, and represent realistic road manoeuvres that may be performed by normal road users. The aim was not to improve the maximum lane change speed of the vehicle or on the edge handling, even though upper limit handling improvement may be a life saving feature.

21.4. Tire wear

The theoretical study indicated that selecting a speed specific steering ratio might reduce the slip angles. Improved tire wear should be traded off against the user profile of the vehicle. If, for example, the vehicle will be used predominantly off-road and in sandy conditions, reduced tire scrub may not on its own justify the added cost of a variable ratio steering system. On the other hand, if tight manoeuvring on tar roads is done, or long distances covered, tire wear and tire cost may justify the increased cost of a variable ratio steering system.

22. Conclusion

The following is concluded:

- i. For the specific vehicle and tire characteristics, simplified mathematical models for steady and transient handling was developed and produced acceptable results and correlation for the purpose of this investigation.
- ii. The simulation results enabled the evaluation of the feasibility of changing the steering system of the test vehicle to a variable ratio steering system.
- iii. The Matlab models that were developed, gave valuable insight into the handling of the test vehicle during steady state constant radius tests, and transient state single lane change manoeuvres.
- iv. A further characteristic of the test vehicle is a stiff spring pack and limited wheel travel, compared to similar vehicles in its class. At low speed, these factors reduces body roll and may increase load transfer. Load transfer, combined with a non-linear tire model may be expanded in future work to improve results.
- v. It is not recommended to implement a variable ratio steering system in the test vehicle, since it was determined that no measurable improvement in the steady-state or transient-state handling will be achieved.
- vi. Based on the results of a similar study done on a 6x6 all-wheel steer vehicle [4], for the same level of mechanical complexity, a far greater improvement in vehicle handling, manoeuvrability and tire wear may be achieved by changing the vehicle to steer with the first and last axle, compared to the effect of changing the steering system to a variable ratio type steering system for the first and second axles.
- vii. Tire wear is a function of vehicle speed and slip angle amongst other parameters. It is possible (at least in theory) to select a steering ratio to reduce tire wear at a specific vehicle speed. For low speed manoeuvres, the Ackerman ratio may be selected to reduce tire wear.
- viii. The Ackerman ratio selected for low speeds may be adjusted at higher vehicle speeds, by selecting a steering ratio between the first and second axles that is closer to one. This steering ratio may be selected to increase the side force that can be generated by the second axle, and improve the vehicle response to steering inputs. A downside may be increased tire wear.
- ix. Steering ratio changes, and the dynamic adjustment of steering ratios may however have a measurable effect on vehicles with specific geometry. It was shown that the wheelbase, distance to centre of mass, and axle loading plays a role in the response of a vehicle to steering ratio changes.
- x. It would be possible to integrate a simple mechanical adjustment on the test vehicle, to perform further testing if required.

23. Recommendations

The following can be recommended:

- i. That an 8x8 vehicle be investigated further, to determine the effect on a long wheelbase vehicle with a centre of mass in the geometric centre of the vehicle.
- ii. That the use of GPS systems to measure slip angles be investigated further, as this technology will eliminate inaccuracies in the conventional measuring chain.
- iii. The Simulink driver model should be developed further in order to obtain a smoother “human” approach tendency through the single lane change.
- iv. The effect of load transfer during both the lane change and constant radius manoeuvres should be investigated and included in future simulation models.
- v. The available measured tire data should be used with the aim to include non-linear tire characteristics, especially when load transfer is investigated.

24. References

1. Allen, J., **Four-Wheel-Steer Jeeps, 4x4x4**, JP Magazine, Primedia Magazines Inc, www.jpmagazine.com, accessed 2 August 2004.
2. Anon, **EMAS Automatic Hydraulic Steering**, www.v-s-e.nl/rechts.htm, accessed 28 January 2005.
3. Kleine, S., **Active control of a four-wheel-steered vehicle**, University of Pretoria, August 1996.
4. Nell, S., **The influence of all-wheel steer (6x6) on vehicle handling and tire wear**, Ermetek, 7th European ISTVS Conference, Ferrara, Italy, October 1997.
5. Anon, **Patria Vehicles**, www.patria.fi, accessed Desember 2004.
6. Anon, **BPW Axles**, www.BPW.de, accessed 1 February 2005.
7. Anon, **Multidrive Limited**, North Yorkshire YO7 3BX, UK, www.multidrive.co.uk, accessed 12 January 2005.
8. Giliomee, C.L., **RSA-MIL-STD for Mobility: Software Validation (Milestone 10)**, Reumech Ermetek, R0015195-0626, March 1999.
9. Gillespie, T.D., **Fundamentals of Vehicle Dynamics**, Society of Automotive Engineers, Warrenville, 1994
10. Dixon, **Tires, Suspension and Handling**, Second Edition, Society for Automotive Engineers, 1996.
11. Wetall, T.T., **Fighting vehicles**, Brassey's New Battlefield Weapons Systems and Technology Series, Volume 1, 1991
12. Pacejka, H.B., **Modelling of the Pneumatic Tire and its impact on vehicle dynamic behaviour**, CCG-Lehrgang V2.03, Carl-Cranz-Gesellschaft e. V., Oberpfaffenhofen, 1986.
13. Bakker, E., **The Magic Formula Tire Model**, 1st International Colloquium on Tire models for Vehicle Dynamic Analysis, Netherlands, 21-22October, 1991.
14. Dugoff, H., Fancher, P.S. and Segel, L., **An analysis of tire traction properties and their influence on vehicle dynamic performance**, 1970 International Automobile Safety Compendium, FISITA/SAE, Brussels, June 1970, SAE no 700377.
15. Pacejka, H.B., and Fancher, P.S, **Hybrid simulation of shear force development of a tire experiencing longitudinal and lateral slip**, Proceedings XIVth FISITA Congress, London, June 1972, p 3/78.
16. Savkoor, A.R., **The lateral flexibility of pneumatic tires and its application to the lateral rolling contact problem**, SAE paper 700378, FISITA/SAE Congress, 1970 (Brussels).

17. Pacejka, H.B., **Some recent investigations into dynamics and frictional behaviour of pneumatic tires, the Physics of Tire traction**, eds D.F. Hays and A.L. Browne, Procedures of symposium held at General Motors Research Lab. (Mich. 1973), Plenum Press, New York 1974.
18. Nordeen, D.L., and Cortese, A.D., **Force and Moment Characteristics of Rolling Tires**, SAE paper no 640028 (713A), 1963, 13p.
19. Hirano, Y. et al, **Development of Integrated System of 4WS and 4WD by H_∞ Control**, SAE Paper 930267, 1993.
20. Metz, L.D. et al, **Transient and Steady state performance characteristics of a two wheel and four-wheel steer vehicle model**, SAE Paper 911926, 1991.
21. Yu, S. et al, **A Global approach to vehicle control: Coordination of four-wheel steering and wheel torque's**, Journal of Dynamic Systems, Measurement, and Control, vol 116, Dec 1994, pp 659-667.
22. Copley, OH, **1991 Yearbook, The tire and Rim Association Inc.**, 1991.
23. Anon, **Michelin Tire**, www.michelintruck.com, accessed 2 February 2005.
24. Anon, **SupaQuick**, www.supaquick.co.za, accessed 2 February 2005.
25. Anon, **Yokohama Tires**, www.yokohama.co.za, accessed 2 February 2005.
26. Anon, **Dunlop Tire**, www.dunlopng.com/care.htm, accessed 2 February 2005.
27. Anon, **Continental Tire**, www.continental.co.za, accessed 2 February 2005.
28. Nell, S., **Die implemetering van 'n aandryfmodel en baanvolger stuurmodel in DADS (The Implementation of a drive and track follower model in DADS)**, Ermetek, 0119305-0679-001, 1991.
29. Sledge, N.H. Jr and Marshek, K.M, **Comparison of Ideal Vehicle Lane Change Trajectories**, SAE, 971062.
30. Anon, **Road vehicles, Steady state circular test procedure**, ISO4138, first edition, International Organization for Standardization, 1982.
31. Anon, **Road vehicles, Test track for a severe lane-change manoeuvre – part 2**, ISO 3888, Second Edition, International Organization for Standardization, 2002.
32. Anon, **Gerotek**, www.gerotek.co.za, accessed 2 May 2004.
33. Strauss, L., **Inleindende Fisika**, Universiteit van Pretoria, 1st ed, 1980.

Appendix A

Matlab routine to convert linear measured displacement to angular displacements

% Subroutine converts measured linear wheel displacements to Angular Displacements

clear all

close all

fname = 'strcal';

eval(['a = loadlmt_4('',fname, '.lmt');']);

time=0:0.003333:(length(a)-1)*0.003333;

figure(1)

subplot(2,1,1);

plot(time,(a(:,1)-mean(a(1:100,1)))*1,'b');% check cal values

ylabel('First Axle Displacement Meter [m]');

title('Bison Steering Angle Calibration');

xlabel('Time [sec]');

grid on

zoom on

subplot(2,1,2);

plot(time,(a(:,2)-mean(a(1:100,2)))*1,'b');

ylabel('Second Axle Displacement Meter [m]');

xlabel('Time [sec]');

grid on

zoom on

figure (2)

subplot(2,1,1);

plot(time,(a(:,3)-mean(a(1:100,3)))*1,'b');

ylabel('Wheel Speed');

title('Carl Test')

grid on

zoom on

figure (2)

subplot(2,1,2);

plot(time,(a(:,4)-mean(a(1:100,4)))*1,'b');

ylabel('Lat Acc');

xlabel('Time [sec]');

grid on

zoom on

%gem hoek van die linker en regter wiel word gebruik om die as se hoek te gee

%1e as: lk 18° -16° rk 12° -20° avg -18° 15°

%2e as: lk 9° -12° rk 10° -7° avg -9.5° 9.5°

q=polyfit([-0.355 0.5],[15 -18],1);

s=polyfit([0.204 -0.206],[9.5 -9.5],1);

%meter=-0.355

%degree=q(1,1)*meter+q(1,2)

%meter=0.5

%degree=q(1,1)*meter+q(1,2)

caldata(:,1)=q(1,2)+q(1,1)*((a(:,1)-mean(a(1:100,1))))*1;

caldata(:,2)=s(1,2)+s(1,1)*((a(:,2)-mean(a(1:100,2))))*1;

caldata(:,3)=(a(:,3)-mean(a(1:100,3)))*1;

caldata(:,4)=(a(:,4)-mean(a(1:100,4)))*1;

figure;

subplot(2,1,1);

plot(time,caldata(:,1));

ylabel('First Axle Steering Angle [°]');

title('Steering Calibration')

grid on

zoom on

subplot(2,1,2);

plot(time,caldata(:,2));

ylabel('Second Axle Steering Angle [°]');

title('Steering Calibration')

grid on

zoom on

figure;

subplot(2,1,1);

```
plot(time,clgfilt(time,calddata(:,1),0.5,'blue'));  
ylabel('First Axle Steering Angle [°]');  
title('Steering Calibration')  
  
grid on  
  
zoom on  
  
subplot(2,1,2);  
plot(time,clgfilt(time,calddata(:,2),0.5,'red'));  
ylabel('Second Axle Steering Angle [°]');  
title('Steering Calibration')  
  
grid on  
  
zoom on
```

Appendix B

Measured CCW plot data manipulation

Measured CCW Plot data manipulation

```

clear all
close all
fname = 'ccw';
eval(['a = loadlmt_6('',fname, '.lmt');']);
time=0:0.003333:(length(a)-1)*0.003333;
q=polyfit([-0.355 0.5],[15 -18],1);
s=polyfit([0.204 -0.206],[9.5 -9.5],1);
caldata(:,1)=q(1,2)+q(1,1)*((a(:,1)-mean(a(1:100,1))))*1;
caldata(:,2)=s(1,2)+s(1,1)*((a(:,2)-mean(a(1:100,2))))*1;
caldata(:,3)=(a(:,3)-mean(a(1:100,3)))*1;
caldata(:,4)=(a(:,4)-mean(a(1:100,4)))*1;
figure;
subplot(2,1,1);
plot(time,caldata(:,1));
ylabel('First Axle Steering Angle [°]');
title('Steering Calibration')
grid on
zoom on
subplot(2,1,2);
plot(time,caldata(:,2));
ylabel('Second Axle Steering Angle [°]');
title('Steering Calibration')
grid on
zoom on
subplot(2,1,1);
plot(time,(a(:,1)-mean(a(1:100,1)))*1,'b');% check cal values
ylabel('Front Str Ang');
title('Carl Test')
grid on
zoom on
subplot(2,1,2);
plot(time,(a(:,2)-mean(a(1:100,2)))*1,'b');
ylabel('Second Str Ang');
xlabel('Time [sec]');
grid on
zoom on
figure (2)
subplot(2,1,1);
plot(time,60*(a(:,3)-mean(a(1:100,3))),'b');
ylabel('Wheel Speed');
title('Carl Test')
grid on
zoom on
figure (2)
subplot(2,1,2);
plot(time,(a(:,4)-mean(a(1:100,4)))*1,'b');
ylabel('Lat Acc');
xlabel('Time [sec]');
grid on
zoom on
figure(3)
subplot(2,1,1);
plot(time,(a(:,5)-mean(a(1:100,5)))*1,'b');% check cal values
ylabel('Roll');
title('Carl Test')
grid on
zoom on
subplot(2,1,2);
plot(time,(a(:,6)-mean(a(1:100,6)))*1,'b');
ylabel('Yaw');
xlabel('Time [sec]');
grid on
zoom on

```

```

figure;
yaw=(a(:,6)-mean(a(1:100,6)))*1;
latacc=(a(:,4)-mean(a(1:100,4)))*1;
roll=(a(:,5)-mean(a(1:100,5)))*1;
plot(time,clgfilt(time,yaw,0.07,'b'),'b');
title('Constant Radius Test Counter Clock Wise')
ylabel('Yaw [rad/s]');
xlabel('Time [s]');
grid on
zoom on
figure
plot(time,clgfilt(time,latacc,0.07,'b'),'b');
title('Constant Radius Test Counter Clock Wise')
ylabel('Lateral Acceleration');
xlabel('Time [sec]');
grid on
zoom on
figure
plot(time,clgfilt(time,roll,0.07,'b'),'b');% check cal values
ylabel('Roll [rad/s]');
xlabel('Time [s]');
title('Constant Radius Test Counter Clock Wise')
grid on
zoom on
figure;
%Kalibreer Data
%gem hoek van die linker en regter wiel word gebruik om die
as se hoek te gee
%1e as: lk 18° -16° rk 12° -20° avg -18° 15°
%2e as: lk 9° -12° rk 10° -7° avg -9.5° 9.5°
q=polyfit([-0.355 0.5],[15 -18],1);
s=polyfit([0.204 -0.206],[9.5 -9.5],1);
caldata1(:,1)=q(1,2)+q(1,1)*(a(:,1));
caldata1(:,2)=s(1,2)+s(1,1)*(a(:,2));
caldata(:,1)=caldata1(:,1)-mean(caldata1(1:100,1))*1;
caldata(:,2)=caldata1(:,2)-mean(caldata1(1:100,2))*1;
caldata(:,3)=(a(:,3)-mean(a(1:100,3)))*14.54;
caldata(:,4)=(a(:,4)-mean(a(1:100,4)))*1;
%Filter data
caldata(:,1)=clgfilt(time,caldata(:,1),0.07,'b');
caldata(:,2)=clgfilt(time,caldata(:,2),0.07,'b');
figure;
subplot(2,1,1);
[AX,H1,H2] = plotyy(time,caldata(:,1),time,caldata(:,3),'plot');
set(get(AX(1),'Ylabel'),'String','First Axle Steering Angle [°]')
set(get(AX(2),'Ylabel'),'String','Vehicle Speed [km/h]')
title('Constant Radius Test Counter Clock Wise')
grid on
zoom on
subplot(2,1,2);
[AX,H1,H2] = plotyy(time,caldata(:,2),time,caldata(:,3),'plot');
set(get(AX(1),'Ylabel'),'String','Second Axle Steering Angle [°]')
set(get(AX(2),'Ylabel'),'String','Vehicle Speed [km/h]')
title('Constant Radius Test Counter Clock Wise')
grid on
zoom on
pack;
figure
plot(time,caldata(:,1),time,caldata(:,2))
title('Constant Radius Test Counter Clock Wise');
ylabel('Steering Angle [°]');
legend('First Axle','Second Axle');
grid on
zoom on
pack;

```

Appendix C

Constant radius test – Matlab M file

```
clear;  
close all;  
%*****  
%18 June 2003
```

```
%BISON CONST RADIUS TEST  
%Updated 21 June 2004 - Diameter 84 meters  
%Update 28 June 2004
```

```
%*****VEHICLE
PARAMETERS*****
g=9.81;
ratio=0.8;
M=14210;%kg
w=2.325;%width

%*****TIRE
DATA *****
x2370_600=[0 2 4 6 8 10]/57.3;
y2370_600=[-2000 6000 12000 15000 17000 18000];

x2370_400=[0 2 4 6 8 10]/57.3;
y2370_400=[-2000 7000 13500 16500 17500 19000];

x4020_600=[0 2 4 6 8 10]/57.3;
y4020_600=[-4000 5050 15000 21000 24000 25500];

x4020_400=[0 2 4 6 8 10]/57.3;
y4020_400=[-4000 5000 16000 22500 25000 27000];
%*****ZERO TIRE
DATA *****
offset1=y2370_600(1,1);
offset2=y2370_400(1,1);
offset3=y4020_600(1,1);
offset4=y4020_400(1,1);

for i = 1:6,
    y2370_600(i)=y2370_600(i)-offset1;
    y2370_400(i)=y2370_400(i)-offset2;
    y4020_600(i)=y4020_600(i)-offset3;
    y4020_400(i)=y4020_400(i)-offset4;

end;
%*****FIT
PLOT*****
a2370_600=polyfit(x2370_600,y2370_600,2);
a2370_400=polyfit(x2370_400,y2370_400,2);
a4020_600=polyfit(x4020_600,y4020_600,2);
a4020_400=polyfit(x4020_400,y4020_400,2);

for i = 1:6,

y1(i,1)=(a2370_600(1,1)*(x2370_600(1,i))^2+a2370_600(1,2)*
x2370_600(1,i))+a2370_600(1,3);

y2(i,1)=(a2370_400(1,1)*(x2370_400(1,i))^2+a2370_400(1,2)*
x2370_400(1,i))+a2370_400(1,3);

y3(i,1)=(a4020_600(1,1)*(x4020_600(1,i))^2+a4020_600(1,2)*
x4020_600(1,i))+a4020_600(1,3);

y4(i,1)=(a4020_400(1,1)*(x4020_400(1,i))^2+a4020_400(1,2)*
x4020_400(1,i))+a4020_400(1,3);

%*****CORNERING
STIFFNESS*****

Cy1(i,1)=(2*a2370_600(1,1)*(x2370_600(1,i))+a2370_600(1,2)
);

Cy2(i,1)=(2*a2370_400(1,1)*(x2370_400(1,i))+a2370_400(1,2)
);

Cy3(i,1)=(2*a4020_600(1,1)*(x4020_600(1,i))+a4020_600(1,2)
);

Cy3(i,1)=(2*a4020_400(1,1)*(x4020_400(1,i))+a4020_400(1,2)
);

end;
%*****use 2370 kg @ 4 bar for CORNERING
STIFFNESS*****

CyF1=2*Cy1(1,1);
CyF2=2*Cy1(1,1);
```

```
CyR1=2*Cy1(1,1);

a=1.937;%DISTANCE FIRST AXLE TO CENTRE OF MASS
b=0.169;%DISTANCE CENTRE OF MASS TO SECOND
AXLE
c=2.550;%DISTANCE SECOND AXLE TO THIRD AXLE

t=2.080;

R=15;
v=5/3.6;

A(1,1)=0;
A(1,2)=0;
A(1,3)=CyF1;
A(1,4)=CyF2;
A(1,5)=CyR1;
A(2,1)=0;
A(2,2)=0;
A(2,3)=a*CyF1;
A(2,4)=-b*CyF2;
A(2,5)=-1*(b+c)*CyR1;
A(3,1)=1;
A(3,2)=0;
A(3,3)=-1;
A(3,4)=0;
A(3,5)=1;
A(4,1)=0;
A(4,2)=1;
A(4,3)=0;
A(4,4)=-1;
A(4,5)=1;
A(5,2)=-1;
A(5,3)=0;
A(5,4)=0;
A(5,5)=0;

B(2,1)=0;
B(5,1)=0;
%=====generate matrix for
plotting=====

maxR=10;

R=10;
v=0.5;%m/s
ry=0;
ratio=0.2;

%Parameters to vary R,v,ratio
for countRatio = 1:10,
    ratio=ratio+0.1;
    R=10;
    for countR = 1:10,
        R=R+5;%meter
        v=(30/3.6)-2.7778;
        for countv = 1:9,
            ry=ry+1;
            v=v+2.7778;%m/s
            A(5,1)=ratio;
            B(1,1)=M*(v)^2/(R)+0;
            B(4,1)=c/R;
            B(3,1)=(a+b+c)/R;
            C=inv(A);
            Slip=C*B*57.3;
            Antw(ry,1)=fix(v*3.6);%speed
            Antw(ry,2)=R;%radius
            Antw(ry,3)=ratio;
            Antw(ry,4)=Slip(3);%Alfa1st
            Antw(ry,5)=Slip(4);%Alfa2nd
            Antw(ry,6)=Slip(5);%Alfa3rd
            Antw(ry,7)=Slip(1);%Delta1
            Antw(ry,8)=Slip(2);%Delta2

        end;
    end;
```



```
%***** plot radius 20 rms slip
angles*****
figure;
subplot(3,3,1);
radius=20;
spoed=30;
hold on;
eval(['plot(data_R_',num2str(radius),'_v_',num2str(spoed),'(:,1)
,data_R_',num2str(radius),'_v_',num2str(spoed),'(:,9),'c+:"');]);
eval(['title("Bison Const.R Test: Radius ',num2str(radius),'
meters, Speed ',num2str(spoed),' km/h")']);
xlabel('Steering Ratio');
ylabel('RMS Slip Angle [°]');
axis([0.3 1.1 0 10]);
grid;
subplot(3,3,2);
radius=20;
spoed=40;
hold on;
eval(['plot(data_R_',num2str(radius),'_v_',num2str(spoed),'(:,1)
,data_R_',num2str(radius),'_v_',num2str(spoed),'(:,9),'c+:"');]);
eval(['title("Bison Const.R Test: Radius ',num2str(radius),'
meters, Speed ',num2str(spoed),' km/h")']);
xlabel('Steering Ratio');
ylabel('RMS Slip Angle [°]');
axis([0.3 1.1 0 10]);;
grid;
subplot(3,3,3);
radius=20;
spoed=60;
hold on;
eval(['plot(data_R_',num2str(radius),'_v_',num2str(spoed),'(:,1)
,data_R_',num2str(radius),'_v_',num2str(spoed),'(:,9),'c+:"');]);
eval(['title("Bison Const.R Test: Radius ',num2str(radius),'
meters, Speed ',num2str(spoed),' km/h")']);
xlabel('Steering Ratio');
ylabel('RMS Slip Angle [°]');
axis([0.3 1.1 0 10]);;
grid;
subplot(3,3,4);
radius=40;
spoed=30;
hold on;
eval(['plot(data_R_',num2str(radius),'_v_',num2str(spoed),'(:,1)
,data_R_',num2str(radius),'_v_',num2str(spoed),'(:,9),'c+:"');]);
eval(['title("Bison Const.R Test: Radius ',num2str(radius),'
meters, Speed ',num2str(spoed),' km/h")']);
xlabel('Steering Ratio');
ylabel('RMS Slip Angle [°]');
axis([0.3 1.1 0 6]);;
grid;
subplot(3,3,5);
radius=40;
spoed=40;
hold on;
eval(['plot(data_R_',num2str(radius),'_v_',num2str(spoed),'(:,1)
,data_R_',num2str(radius),'_v_',num2str(spoed),'(:,9),'c+:"');]);
eval(['title("Bison Const.R Test: Radius ',num2str(radius),'
meters, Speed ',num2str(spoed),' km/h")']);
xlabel('Steering Ratio');
ylabel('RMS Slip Angle [°]');
axis([0.3 1.1 0 6]);;
grid;
subplot(3,3,6);
radius=40;
spoed=60;
hold on;
eval(['plot(data_R_',num2str(radius),'_v_',num2str(spoed),'(:,1)
,data_R_',num2str(radius),'_v_',num2str(spoed),'(:,9),'c+:"');]);
eval(['title("Bison Const.R Test: Radius ',num2str(radius),'
meters, Speed ',num2str(spoed),' km/h")']);
xlabel('Steering Ratio');
ylabel('RMS Slip Angle [°]');
axis([0.3 1.1 0 6]);;
grid;
subplot(3,3,7);
```

```
radius=60;
spoed=30;
hold on;
eval(['plot(data_R_',num2str(radius),'_v_',num2str(spoed),'(:,1)
,data_R_',num2str(radius),'_v_',num2str(spoed),'(:,9),'c+:"');]);
eval(['title("Bison Const.R Test: Radius ',num2str(radius),'
meters, Speed ',num2str(spoed),' km/h")']);
xlabel('Steering Ratio');
ylabel('RMS Slip Angle [°]');
axis([0.3 1.1 0 6]);;

grid;
subplot(3,3,8);
radius=60;
spoed=40;
hold on;
eval(['plot(data_R_',num2str(radius),'_v_',num2str(spoed),'(:,1)
,data_R_',num2str(radius),'_v_',num2str(spoed),'(:,9),'c+:"');]);
eval(['title("Bison Const.R Test: Radius ',num2str(radius),'
meters, Speed ',num2str(spoed),' km/h")']);
xlabel('Steering Ratio');
ylabel('RMS Slip Angle [°]');
axis([0.3 1.1 0 6]);;

grid;
subplot(3,3,9);
radius=60;
spoed=60;
hold on;
eval(['plot(data_R_',num2str(radius),'_v_',num2str(spoed),'(:,1)
,data_R_',num2str(radius),'_v_',num2str(spoed),'(:,9),'c+:"');]);
eval(['title("Bison Const.R Test: Radius ',num2str(radius),'
meters, Speed ',num2str(spoed),' km/h")']);
xlabel('Steering Ratio');
ylabel('RMS Slip Angle [°]');
axis([0.3 1.1 0 6]);;

grid;
%***** plot radius 20 rms steering
angles*****
figure;
subplot(3,3,1);
radius=20;
spoed=30;
hold on;
eval(['plot(data_R_',num2str(radius),'_v_',num2str(spoed),'(:,1)
,data_R_',num2str(radius),'_v_',num2str(spoed),'(:,10),'c+:"');]);
eval(['title("Bison Const.R Test: Radius ',num2str(radius),'
meters, Speed ',num2str(spoed),' km/h")']);
xlabel('Steering Ratio');
ylabel('RMS Steering Angle [°]');
axis([0.3 1.1 0 12]);;
grid;
subplot(3,3,2);
radius=20;
spoed=40;
hold on;
eval(['plot(data_R_',num2str(radius),'_v_',num2str(spoed),'(:,1)
,data_R_',num2str(radius),'_v_',num2str(spoed),'(:,10),'c+:"');]);
eval(['title("Bison Const.R Test: Radius ',num2str(radius),'
meters, Speed ',num2str(spoed),' km/h")']);
xlabel('Steering Ratio');
ylabel('RMS Steering Angle [°]');
axis([0.3 1.1 0 12]);;
grid;
subplot(3,3,3);
radius=20;
spoed=60;
hold on;
eval(['plot(data_R_',num2str(radius),'_v_',num2str(spoed),'(:,1)
,data_R_',num2str(radius),'_v_',num2str(spoed),'(:,10),'c+:"');]);
eval(['title("Bison Const.R Test: Radius ',num2str(radius),'
meters, Speed ',num2str(spoed),' km/h")']);
xlabel('Steering Ratio');
ylabel('RMS Steering Angle [°]');
axis([0.3 1.1 0 12]);;
grid;
```

```

subplot(3,3,4);
radius=40;
spoed=30;
hold on;
eval(['plot(data_R_',num2str(radius),'_v_',num2str(spoed),':(:,1)
,data_R_',num2str(radius),'_v_',num2str(spoed),':(:,10),"c+");']);
eval(['title("Bison Const.R Test: Radius ',num2str(radius),'
meters, Speed ',num2str(spoed),' km/h)");
xlabel('Steering Ratio');
ylabel('RMS Steering Angle [°]');
axis([0.3 1.1 0 12]);
grid;
subplot(3,3,5);
radius=40;
spoed=40;
hold on;
eval(['plot(data_R_',num2str(radius),'_v_',num2str(spoed),':(:,1)
,data_R_',num2str(radius),'_v_',num2str(spoed),':(:,10),"c+");']);
eval(['title("Bison Const.R Test: Radius ',num2str(radius),'
meters, Speed ',num2str(spoed),' km/h)");
xlabel('Steering Ratio');
ylabel('RMS Steering Angle [°]');
axis([0.3 1.1 0 12]);
grid;
subplot(3,3,6);
radius=40;
spoed=60;
hold on;
eval(['plot(data_R_',num2str(radius),'_v_',num2str(spoed),':(:,1)
,data_R_',num2str(radius),'_v_',num2str(spoed),':(:,10),"c+");']);
eval(['title("Bison Const.R Test: Radius ',num2str(radius),'
meters, Speed ',num2str(spoed),' km/h)");
xlabel('Steering Ratio');
ylabel('RMS Steering Angle [°]');
axis([0.3 1.1 0 12]);
grid;
subplot(3,3,7);
radius=60;
spoed=30;
hold on;
eval(['plot(data_R_',num2str(radius),'_v_',num2str(spoed),':(:,1)
,data_R_',num2str(radius),'_v_',num2str(spoed),':(:,10),"c+");']);
eval(['title("Bison Const.R Test: Radius ',num2str(radius),'
meters, Speed ',num2str(spoed),' km/h)");
xlabel('Steering Ratio');
ylabel('RMS Steering Angle [°]');
axis([0.3 1.1 0 12]);
grid;
subplot(3,3,8);
radius=60;
spoed=40;
hold on;
eval(['plot(data_R_',num2str(radius),'_v_',num2str(spoed),':(:,1)
,data_R_',num2str(radius),'_v_',num2str(spoed),':(:,10),"c+");']);
eval(['title("Bison Const.R Test: Radius ',num2str(radius),'
meters, Speed ',num2str(spoed),' km/h)");
xlabel('Steering Ratio');
ylabel('RMS Steering Angle [°]');
axis([0.3 1.1 0 12]);
grid;
subplot(3,3,9);
radius=60;
spoed=60;
hold on;
eval(['plot(data_R_',num2str(radius),'_v_',num2str(spoed),':(:,1)
,data_R_',num2str(radius),'_v_',num2str(spoed),':(:,10),"c+");']);
eval(['title("Bison Const.R Test: Radius ',num2str(radius),'
meters, Speed ',num2str(spoed),' km/h)");
xlabel('Steering Ratio');
ylabel('RMS Steering Angle [°]');
axis([0.3 1.1 0 12]);
grid;

hold off;
%%***** plot radius 20 rms slip angle and
steering*****
figure;

```

```

subplot(3,3,1);
radius=20;
spoed=30;
hold on;
eval(['plot(data_R_',num2str(radius),'_v_',num2str(spoed),':(:,1)
,data_R_',num2str(radius),'_v_',num2str(spoed),':(:,9),"r+");']);
eval(['plot(data_R_',num2str(radius),'_v_',num2str(spoed),':(:,1)
,data_R_',num2str(radius),'_v_',num2str(spoed),':(:,10),"b+");']);
eval(['title("Bison Const.R Test: Radius ',num2str(radius),'
meters, Speed ',num2str(spoed),' km/h)");
xlabel('Steering Ratio');
ylabel('RMS Angle [°]');
legend('Slip Angle','Steering Angle');
%axis([0.3 1.1 0 200]);
grid;
subplot(3,3,2);
radius=20;
spoed=40;
hold on;
eval(['plot(data_R_',num2str(radius),'_v_',num2str(spoed),':(:,1)
,data_R_',num2str(radius),'_v_',num2str(spoed),':(:,9),"r+");']);
eval(['plot(data_R_',num2str(radius),'_v_',num2str(spoed),':(:,1)
,data_R_',num2str(radius),'_v_',num2str(spoed),':(:,10),"b+");']);
eval(['title("Bison Const.R Test: Radius ',num2str(radius),'
meters, Speed ',num2str(spoed),' km/h)");
xlabel('Steering Ratio');
ylabel('RMS Angle [°]');
legend('Slip Angle','Steering Angle');
%axis([0.3 1.1 0 200]);
grid;
subplot(3,3,3);
radius=20;
spoed=60;
hold on;
eval(['plot(data_R_',num2str(radius),'_v_',num2str(spoed),':(:,1)
,data_R_',num2str(radius),'_v_',num2str(spoed),':(:,9),"r+");']);
eval(['plot(data_R_',num2str(radius),'_v_',num2str(spoed),':(:,1)
,data_R_',num2str(radius),'_v_',num2str(spoed),':(:,10),"b+");']);
eval(['title("Bison Const.R Test: Radius ',num2str(radius),'
meters, Speed ',num2str(spoed),' km/h)");
xlabel('Steering Ratio');
ylabel('RMS Angle [°]');
legend('Slip Angle','Steering Angle');
%axis([0.3 1.1 0 200]);
grid;
subplot(3,3,4);
radius=40;
spoed=30;
hold on;
eval(['plot(data_R_',num2str(radius),'_v_',num2str(spoed),':(:,1)
,data_R_',num2str(radius),'_v_',num2str(spoed),':(:,9),"r+");']);
eval(['plot(data_R_',num2str(radius),'_v_',num2str(spoed),':(:,1)
,data_R_',num2str(radius),'_v_',num2str(spoed),':(:,10),"b+");']);
eval(['title("Bison Const.R Test: Radius ',num2str(radius),'
meters, Speed ',num2str(spoed),' km/h)");
xlabel('Steering Ratio');
ylabel('RMS Angle [°]');
legend('Slip Angle','Steering Angle');
%axis([0.3 1.1 0 200]);
grid;
subplot(3,3,5);
radius=40;
spoed=40;
hold on;
eval(['plot(data_R_',num2str(radius),'_v_',num2str(spoed),':(:,1)
,data_R_',num2str(radius),'_v_',num2str(spoed),':(:,9),"r+");']);
eval(['plot(data_R_',num2str(radius),'_v_',num2str(spoed),':(:,1)
,data_R_',num2str(radius),'_v_',num2str(spoed),':(:,10),"b+");']);
eval(['title("Bison Const.R Test: Radius ',num2str(radius),'
meters, Speed ',num2str(spoed),' km/h)");
xlabel('Steering Ratio');
ylabel('RMS Angle [°]');
legend('Slip Angle','Steering Angle');
%axis([0.3 1.1 0 200]);
grid;
subplot(3,3,6);
radius=40;

```

```

spoed=60;
hold on;
eval(['plot(data_R_',num2str(radius),'_v_',num2str(spoed),'(:,1)
,data_R_',num2str(radius),'_v_',num2str(spoed),'(:,9),"r+");']);
eval(['plot(data_R_',num2str(radius),'_v_',num2str(spoed),'(:,1)
,data_R_',num2str(radius),'_v_',num2str(spoed),'(:,10),"b+");']);
eval(['title("Bison Const.R Test: Radius ',num2str(radius),'
meters, Speed ',num2str(spoed),' km/h")']);
xlabel('Steering Ratio');
ylabel('RMS Angle [°]')
legend('Slip Angle','Steering Angle')
%axis([0.3 1.1 0 200]);
grid;
subplot(3,3,7);
radius=60;
spoed=30;
hold on;
eval(['plot(data_R_',num2str(radius),'_v_',num2str(spoed),'(:,1)
,data_R_',num2str(radius),'_v_',num2str(spoed),'(:,9),"r+");']);
eval(['plot(data_R_',num2str(radius),'_v_',num2str(spoed),'(:,1)
,data_R_',num2str(radius),'_v_',num2str(spoed),'(:,10),"b+");']);
eval(['title("Bison Const.R Test: Radius ',num2str(radius),'
meters, Speed ',num2str(spoed),' km/h")']);
xlabel('Steering Ratio');
ylabel('RMS Angle [°]');
legend('Slip Angle','Steering Angle')
%axis([0.3 1.1 0 200]);
grid;
subplot(3,3,8);
radius=60;
spoed=40;
hold on;
eval(['plot(data_R_',num2str(radius),'_v_',num2str(spoed),'(:,1)
,data_R_',num2str(radius),'_v_',num2str(spoed),'(:,9),"r+");']);
eval(['plot(data_R_',num2str(radius),'_v_',num2str(spoed),'(:,1)
,data_R_',num2str(radius),'_v_',num2str(spoed),'(:,10),"b+");']);
eval(['title("Bison Const.R Test: Radius ',num2str(radius),'
meters, Speed ',num2str(spoed),' km/h")']);
xlabel('Steering Ratio');
ylabel('RMS Angle [°]')
legend('Slip Angle','Steering Angle')
%axis([0.3 1.1 0 200]);
grid;
subplot(3,3,9);
radius=60;
spoed=60;
hold on;
eval(['plot(data_R_',num2str(radius),'_v_',num2str(spoed),'(:,1)
,data_R_',num2str(radius),'_v_',num2str(spoed),'(:,9),"r+");']);
eval(['plot(data_R_',num2str(radius),'_v_',num2str(spoed),'(:,1)
,data_R_',num2str(radius),'_v_',num2str(spoed),'(:,10),"b+");']);
eval(['title("Bison Const.R Test: Radius ',num2str(radius),'
meters, Speed ',num2str(spoed),' km/h")']);
legend('Slip Angle','Steering Angle')
xlabel('Steering Ratio');
ylabel('RMS Angle [°]')
%axis([0.3 1.1 0 200]);
grid;
%*****
**
$$$$$$$$$$$$$$$$$$$$$$$$$$$$$$$$$$$$$$$$$$$$$$$$$$$$$$$$$$$$
$$$$$$$$$$$$$$$$$$$$$$$$$$$$$$$$$$$$$$$$$$$$$$$$$$$$$$$$$$$$
$$$$$$$$$$

%*****
**
%***** plot radius 20
*****

figure;
subplot(2,2,1);
radius=20;
spoed=30;
hold on;
eval(['plot(data_R_',num2str(radius),'_v_',num2str(spoed),'(:,1)
,data_R_',num2str(radius),'_v_',num2str(spoed),'(:,2),"c+");']);

```

```

eval(['plot(data_R_',num2str(radius),'_v_',num2str(spoed),'(:,1)
,data_R_',num2str(radius),'_v_',num2str(spoed),'(:,3),"y+");']);
eval(['plot(data_R_',num2str(radius),'_v_',num2str(spoed),'(:,1)
,data_R_',num2str(radius),'_v_',num2str(spoed),'(:,4),"m+");']);
eval(['plot(data_R_',num2str(radius),'_v_',num2str(spoed),'(:,1)
,data_R_',num2str(radius),'_v_',num2str(spoed),'(:,5),"r+");']);
eval(['plot(data_R_',num2str(radius),'_v_',num2str(spoed),'(:,1)
,data_R_',num2str(radius),'_v_',num2str(spoed),'(:,6),"g+");']);
eval(['title("Bison Constant Radius Test: Radius
',num2str(radius),' meters, Speed ',num2str(spoed),' km/h")'])
axis([0.3 1.1 0 20]);
xlabel('Ratio');
ylabel('Angle [°]');
grid;
legend('Alfa 1st Axle','Alfa 2nd Axle','Alfa 3rd Axle','Steer 1st
Axle','Steer 2nd Axle',-1);
hold off;
%*****
**
subplot(2,2,2);
radius=20;
spoed=40;
hold on;
eval(['plot(data_R_',num2str(radius),'_v_',num2str(spoed),'(:,1)
,data_R_',num2str(radius),'_v_',num2str(spoed),'(:,2),"c+");']);
eval(['plot(data_R_',num2str(radius),'_v_',num2str(spoed),'(:,1)
,data_R_',num2str(radius),'_v_',num2str(spoed),'(:,3),"y+");']);
eval(['plot(data_R_',num2str(radius),'_v_',num2str(spoed),'(:,1)
,data_R_',num2str(radius),'_v_',num2str(spoed),'(:,4),"m+");']);
eval(['plot(data_R_',num2str(radius),'_v_',num2str(spoed),'(:,1)
,data_R_',num2str(radius),'_v_',num2str(spoed),'(:,5),"r+");']);
eval(['plot(data_R_',num2str(radius),'_v_',num2str(spoed),'(:,1)
,data_R_',num2str(radius),'_v_',num2str(spoed),'(:,6),"g+");']);
eval(['title("Bison Constant Radius Test: Radius
',num2str(radius),' meters, Speed ',num2str(spoed),' km/h")'])
axis([0.3 1.1 0 20]);
xlabel('Ratio');
ylabel('Angle [°]');
grid;
legend('Alfa 1st Axle','Alfa 2nd Axle','Alfa 3rd Axle','Steer 1st
Axle','Steer 2nd Axle',-1);
hold off;
%*****
**
subplot(2,2,3);
radius=20;
spoed=50;
hold on;
eval(['plot(data_R_',num2str(radius),'_v_',num2str(spoed),'(:,1)
,data_R_',num2str(radius),'_v_',num2str(spoed),'(:,2),"c+");']);
eval(['plot(data_R_',num2str(radius),'_v_',num2str(spoed),'(:,1)
,data_R_',num2str(radius),'_v_',num2str(spoed),'(:,3),"y+");']);
eval(['plot(data_R_',num2str(radius),'_v_',num2str(spoed),'(:,1)
,data_R_',num2str(radius),'_v_',num2str(spoed),'(:,4),"m+");']);
eval(['plot(data_R_',num2str(radius),'_v_',num2str(spoed),'(:,1)
,data_R_',num2str(radius),'_v_',num2str(spoed),'(:,5),"r+");']);
eval(['plot(data_R_',num2str(radius),'_v_',num2str(spoed),'(:,1)
,data_R_',num2str(radius),'_v_',num2str(spoed),'(:,6),"g+");']);
eval(['title("Bison Constant Radius Test: Radius
',num2str(radius),' meters, Speed ',num2str(spoed),' km/h")'])
axis([0.3 1.1 0 20]);
xlabel('Ratio');
ylabel('Angle [°]');
grid;
legend('Alfa 1st Axle','Alfa 2nd Axle','Alfa 3rd Axle','Steer 1st
Axle','Steer 2nd Axle',-1);
hold off;
%*****
**
subplot(2,2,4);
radius=20;
spoed=60;
hold on;
eval(['plot(data_R_',num2str(radius),'_v_',num2str(spoed),'(:,1)
,data_R_',num2str(radius),'_v_',num2str(spoed),'(:,2),"c+");']);
eval(['plot(data_R_',num2str(radius),'_v_',num2str(spoed),'(:,1)
,data_R_',num2str(radius),'_v_',num2str(spoed),'(:,3),"y+");']);

```



```

eval(['plot(data_R_',num2str(radius),'_v_',num2str(spoed),':(,1)
,data_R_',num2str(radius),'_v_',num2str(spoed),':(,2),"c+:"');
eval(['plot(data_R_',num2str(radius),'_v_',num2str(spoed),':(,1)
,data_R_',num2str(radius),'_v_',num2str(spoed),':(,3),"y+:"');
eval(['plot(data_R_',num2str(radius),'_v_',num2str(spoed),':(,1)
,data_R_',num2str(radius),'_v_',num2str(spoed),':(,4),"m+:"');
eval(['plot(data_R_',num2str(radius),'_v_',num2str(spoed),':(,1)
,data_R_',num2str(radius),'_v_',num2str(spoed),':(,5),"r+:"');
eval(['plot(data_R_',num2str(radius),'_v_',num2str(spoed),':(,1)
,data_R_',num2str(radius),'_v_',num2str(spoed),':(,6),"g+:"');
eval(['title("Bison Constant Radius Test: Radius
',num2str(radius),' meters, Speed ',num2str(spoed),' km/h'')
axis([0.3 1.1 0 7]);
xlabel('Ratio');
ylabel('Angle [°]');

grid;
legend('Alfa 1st Axle','Alfa 2nd Axle','Alfa 3rd Axle','Steer 1st
Axle','Steer 2nd Axle',-1);
hold off;
%*****
**
subplot(2,2,3);
radius=60;
spoed=50;
hold on;
eval(['plot(data_R_',num2str(radius),'_v_',num2str(spoed),':(,1)
,data_R_',num2str(radius),'_v_',num2str(spoed),':(,2),"c+:"');
eval(['plot(data_R_',num2str(radius),'_v_',num2str(spoed),':(,1)
,data_R_',num2str(radius),'_v_',num2str(spoed),':(,3),"y+:"');
eval(['plot(data_R_',num2str(radius),'_v_',num2str(spoed),':(,1)
,data_R_',num2str(radius),'_v_',num2str(spoed),':(,4),"m+:"');
eval(['plot(data_R_',num2str(radius),'_v_',num2str(spoed),':(,1)
,data_R_',num2str(radius),'_v_',num2str(spoed),':(,5),"r+:"');
eval(['plot(data_R_',num2str(radius),'_v_',num2str(spoed),':(,1)
,data_R_',num2str(radius),'_v_',num2str(spoed),':(,6),"g+:"');
eval(['title("Bison Constant Radius Test: Radius
',num2str(radius),' meters, Speed ',num2str(spoed),' km/h'')
axis([0.3 1.1 0 7]);
xlabel('Ratio');
ylabel('Angle [°]');
grid;
legend('Alfa 1st Axle','Alfa 2nd Axle','Alfa 3rd Axle','Steer 1st
Axle','Steer 2nd Axle',-1);
hold off;
%*****
**
subplot(2,2,4);
radius=60;
spoed=60;
hold on;
eval(['plot(data_R_',num2str(radius),'_v_',num2str(spoed),':(,1)
,data_R_',num2str(radius),'_v_',num2str(spoed),':(,2),"c+:"');
eval(['plot(data_R_',num2str(radius),'_v_',num2str(spoed),':(,1)
,data_R_',num2str(radius),'_v_',num2str(spoed),':(,3),"y+:"');
eval(['plot(data_R_',num2str(radius),'_v_',num2str(spoed),':(,1)
,data_R_',num2str(radius),'_v_',num2str(spoed),':(,4),"m+:"');
eval(['plot(data_R_',num2str(radius),'_v_',num2str(spoed),':(,1)
,data_R_',num2str(radius),'_v_',num2str(spoed),':(,5),"r+:"');
eval(['plot(data_R_',num2str(radius),'_v_',num2str(spoed),':(,1)
,data_R_',num2str(radius),'_v_',num2str(spoed),':(,6),"g+:"');
eval(['title("Bison Constant Radius Test: Radius
',num2str(radius),' meters, Speed ',num2str(spoed),' km/h'')
axis([0.3 1.1 0 7]);
xlabel('Ratio');
ylabel('Angle [°]');
grid;
legend('Alfa 1st Axle','Alfa 2nd Axle','Alfa 3rd Axle','Steer 1st
Axle','Steer 2nd Axle',-1);
hold off;
%#####
#####
#####
%plot ratio vs speed for a specific slip angle and turning radius

```

```

%#####
#####
#####
%#####radius
20#####
s=20;
a=0;
b=0;
c=0;
d=0;
e=0;
f=0;
g=0;
h=0;
j=0;
for w = 1:8
    s=s+10;
    for i=1:10
        eval(['temp=data_R_20_v_',num2str(s),'(i,1)'];)
        if temp <= 0.32
            a=a+1;
        end;
        eval(['leer_rad_20_ratio_03(a,:)=data_R_20_v_',num2str(s),'(i,
7) data_R_20_v_',num2str(s),'(i,2)
data_R_20_v_',num2str(s),'(i,3)
data_R_20_v_',num2str(s),'(i,4)
data_R_20_v_',num2str(s),'(i,5)
data_R_20_v_',num2str(s),'(i,6)
data_R_20_v_',num2str(s),'(i,1)'];);
    end;
    if temp <= 0.42
        b=b+1;
    end;
    if temp >= 0.32
        b=b+1;
    end;
    eval(['leer_rad_20_ratio_04(b,:)=data_R_20_v_',num2str(s),'(i,
7) data_R_20_v_',num2str(s),'(i,2)
data_R_20_v_',num2str(s),'(i,3)
data_R_20_v_',num2str(s),'(i,4)
data_R_20_v_',num2str(s),'(i,5)
data_R_20_v_',num2str(s),'(i,6)
data_R_20_v_',num2str(s),'(i,1)'];);
    end;
    if temp <= 0.52
        c=c+1;
    end;
    if temp >= 0.42
        c=c+1;
    end;
    eval(['leer_rad_20_ratio_05(c,:)=data_R_20_v_',num2str(s),'(i,
7) data_R_20_v_',num2str(s),'(i,2)
data_R_20_v_',num2str(s),'(i,3)
data_R_20_v_',num2str(s),'(i,4)
data_R_20_v_',num2str(s),'(i,5)
data_R_20_v_',num2str(s),'(i,6)
data_R_20_v_',num2str(s),'(i,1)'];);
    end;
    if temp <= 0.62
        d=d+1;
    end;
    if temp >= 0.52
        d=d+1;
    end;
    eval(['leer_rad_20_ratio_06(d,:)=data_R_20_v_',num2str(s),'(i,
7) data_R_20_v_',num2str(s),'(i,2)
data_R_20_v_',num2str(s),'(i,3)
data_R_20_v_',num2str(s),'(i,4)
data_R_20_v_',num2str(s),'(i,5)
data_R_20_v_',num2str(s),'(i,6)
data_R_20_v_',num2str(s),'(i,1)'];);
    end;
    if temp <= 0.72
        e=e+1;
    end;
    if temp >= 0.62
        e=e+1;
    end;
    eval(['leer_rad_20_ratio_07(e,:)=data_R_20_v_',num2str(s),'(i,
7) data_R_20_v_',num2str(s),'(i,2)
data_R_20_v_',num2str(s),'(i,3)

```

```

data_R_20_v_',num2str(s),'(i,4)
data_R_20_v_',num2str(s),'(i,5)
data_R_20_v_',num2str(s),'(i,6)
data_R_20_v_',num2str(s),'(i,1)'];]);
end;
end;
if temp <= 0.82
if temp >= 0.72
f=f+1;

eval(['leer_rad_20_ratio_08(f,:)=data_R_20_v_',num2str(s),'(i,
7) data_R_20_v_',num2str(s),'(i,2)
data_R_20_v_',num2str(s),'(i,3)
data_R_20_v_',num2str(s),'(i,4)
data_R_20_v_',num2str(s),'(i,5)
data_R_20_v_',num2str(s),'(i,6)
data_R_20_v_',num2str(s),'(i,1)'];]);
end;
end;
if temp <= 0.92
if temp >= 0.82
g=g+1;

eval(['leer_rad_20_ratio_09(g,:)=data_R_20_v_',num2str(s),'(i,
7) data_R_20_v_',num2str(s),'(i,2)
data_R_20_v_',num2str(s),'(i,3)
data_R_20_v_',num2str(s),'(i,4)
data_R_20_v_',num2str(s),'(i,5)
data_R_20_v_',num2str(s),'(i,6)
data_R_20_v_',num2str(s),'(i,1)'];]);
end;
end;
if temp <= 1.02
if temp >= 0.92
h=h+1;

eval(['leer_rad_20_ratio_10(b,:)=data_R_20_v_',num2str(s),'(i,
7) data_R_20_v_',num2str(s),'(i,2)
data_R_20_v_',num2str(s),'(i,3)
data_R_20_v_',num2str(s),'(i,4)
data_R_20_v_',num2str(s),'(i,5)
data_R_20_v_',num2str(s),'(i,6)
data_R_20_v_',num2str(s),'(i,1)'];]);
end;
end;
if temp <= 1.12
if temp >= 1.02
j=j+1;

eval(['leer_rad_20_ratio_11(b,:)=data_R_20_v_',num2str(s),'(i,
7) data_R_20_v_',num2str(s),'(i,2)
data_R_20_v_',num2str(s),'(i,3)
data_R_20_v_',num2str(s),'(i,4)
data_R_20_v_',num2str(s),'(i,5)
data_R_20_v_',num2str(s),'(i,6)
data_R_20_v_',num2str(s),'(i,1)'];]);
end;
end;
end;
#####radius
40#####
s=20;
a=0;
b=0;
c=0;
d=0;
e=0;
f=0;
g=0;
h=0;
j=0;
for w = 1:8
s=s+10;
for i=1:10
eval(['temp=data_R_40_v_',num2str(s),'(i,1)'];]);
if temp <= 0.32
a=a+1;

eval(['leer_rad_40_ratio_03(a,:)=data_R_40_v_',num2str(s),'(i,
7) data_R_40_v_',num2str(s),'(i,2)
data_R_40_v_',num2str(s),'(i,3)
data_R_40_v_',num2str(s),'(i,4)
data_R_40_v_',num2str(s),'(i,5)
data_R_40_v_',num2str(s),'(i,6)
data_R_40_v_',num2str(s),'(i,1)'];]);
end;
end;
if temp <= 0.42
if temp >= 0.32
b=b+1;

eval(['leer_rad_40_ratio_04(b,:)=data_R_40_v_',num2str(s),'(i,
7) data_R_40_v_',num2str(s),'(i,2)
data_R_40_v_',num2str(s),'(i,3)
data_R_40_v_',num2str(s),'(i,4)
data_R_40_v_',num2str(s),'(i,5)
data_R_40_v_',num2str(s),'(i,6)
data_R_40_v_',num2str(s),'(i,1)'];]);
end;
end;
if temp <= 0.52
if temp >= 0.42
c=c+1;

eval(['leer_rad_40_ratio_05(c,:)=data_R_40_v_',num2str(s),'(i,
7) data_R_40_v_',num2str(s),'(i,2)
data_R_40_v_',num2str(s),'(i,3)
data_R_40_v_',num2str(s),'(i,4)
data_R_40_v_',num2str(s),'(i,5)
data_R_40_v_',num2str(s),'(i,6)
data_R_40_v_',num2str(s),'(i,1)'];]);
end;
end;
if temp <= 0.62
if temp >= 0.52
d=d+1;

eval(['leer_rad_40_ratio_06(d,:)=data_R_40_v_',num2str(s),'(i,
7) data_R_40_v_',num2str(s),'(i,2)
data_R_40_v_',num2str(s),'(i,3)
data_R_40_v_',num2str(s),'(i,4)
data_R_40_v_',num2str(s),'(i,5)
data_R_40_v_',num2str(s),'(i,6)
data_R_40_v_',num2str(s),'(i,1)'];]);
end;
end;
if temp <= 0.72
if temp >= 0.62
e=e+1;

eval(['leer_rad_40_ratio_07(e,:)=data_R_40_v_',num2str(s),'(i,
7) data_R_40_v_',num2str(s),'(i,2)
data_R_40_v_',num2str(s),'(i,3)
data_R_40_v_',num2str(s),'(i,4)
data_R_40_v_',num2str(s),'(i,5)
data_R_40_v_',num2str(s),'(i,6)
data_R_40_v_',num2str(s),'(i,1)'];]);
end;
end;
if temp <= 0.82
if temp >= 0.72
f=f+1;

eval(['leer_rad_40_ratio_08(f,:)=data_R_40_v_',num2str(s),'(i,
7) data_R_40_v_',num2str(s),'(i,2)
data_R_40_v_',num2str(s),'(i,3)
data_R_40_v_',num2str(s),'(i,4)
data_R_40_v_',num2str(s),'(i,5)
data_R_40_v_',num2str(s),'(i,6)
data_R_40_v_',num2str(s),'(i,1)'];]);
end;
end;
if temp <= 0.92
if temp >= 0.82

```



```

data_R_60_v_',num2str(s),'(i,6)
data_R_60_v_',num2str(s),'(i,1)'];
end;
end;
if temp <= 1.12
if temp >= 1.02
j=j+1;

eval(['leer_rad_60_ratio_11(b,:)=data_R_60_v_',num2str(s),'(i,
7) data_R_60_v_',num2str(s),'(i,2)
data_R_60_v_',num2str(s),'(i,3)
data_R_60_v_',num2str(s),'(i,4)
data_R_60_v_',num2str(s),'(i,5)
data_R_60_v_',num2str(s),'(i,6)
data_R_60_v_',num2str(s),'(i,1)'];)
end;
end;
end;
end;

```

```

figure
subplot(3,1,1);
hold on;
plot(leer_rad_20_ratio_03(:,1),leer_rad_20_ratio_03(:,2),leer_r
ad_20_ratio_03(:,1),leer_rad_20_ratio_03(:,3),leer_rad_20_rati
o_03(:,1),leer_rad_20_ratio_03(:,4));
plot(leer_rad_20_ratio_04(:,1),leer_rad_20_ratio_04(:,2),leer_r
ad_20_ratio_04(:,1),leer_rad_20_ratio_04(:,3),leer_rad_20_rati
o_04(:,1),leer_rad_20_ratio_04(:,4));
plot(leer_rad_20_ratio_05(:,1),leer_rad_20_ratio_05(:,2),leer_r
ad_20_ratio_05(:,1),leer_rad_20_ratio_05(:,3),leer_rad_20_rati
o_05(:,1),leer_rad_20_ratio_05(:,4));
plot(leer_rad_20_ratio_06(:,1),leer_rad_20_ratio_06(:,2),leer_r
ad_20_ratio_06(:,1),leer_rad_20_ratio_06(:,3),leer_rad_20_rati
o_06(:,1),leer_rad_20_ratio_06(:,4));
plot(leer_rad_20_ratio_07(:,1),leer_rad_20_ratio_07(:,2),leer_r
ad_20_ratio_07(:,1),leer_rad_20_ratio_07(:,3),leer_rad_20_rati
o_07(:,1),leer_rad_20_ratio_07(:,4));
plot(leer_rad_20_ratio_08(:,1),leer_rad_20_ratio_08(:,2),leer_r
ad_20_ratio_08(:,1),leer_rad_20_ratio_08(:,3),leer_rad_20_rati
o_08(:,1),leer_rad_20_ratio_08(:,4));
plot(leer_rad_20_ratio_09(:,1),leer_rad_20_ratio_09(:,2),leer_r
ad_20_ratio_09(:,1),leer_rad_20_ratio_09(:,3),leer_rad_20_rati
o_09(:,1),leer_rad_20_ratio_09(:,4));
plot(leer_rad_20_ratio_10(:,1),leer_rad_20_ratio_10(:,2),leer_r
ad_20_ratio_10(:,1),leer_rad_20_ratio_10(:,3),leer_rad_20_rati
o_10(:,1),leer_rad_20_ratio_10(:,4));
plot(leer_rad_20_ratio_11(:,1),leer_rad_20_ratio_11(:,2),leer_r
ad_20_ratio_11(:,1),leer_rad_20_ratio_11(:,3),leer_rad_20_rati
o_11(:,1),leer_rad_20_ratio_11(:,4));
legend('First Axle','Second Axle','Third Axle',-1);
title('Bison Constant Radius Test, Radius 20 meters');
xlabel('Vehicle Speed [km/h]');
ylabel('Slip Angle [°]');
grid;
axis([30 60 0 15]);

```

```

subplot(3,1,2);
hold on;
plot(leer_rad_40_ratio_03(:,1),leer_rad_40_ratio_03(:,2),leer_r
ad_40_ratio_03(:,1),leer_rad_40_ratio_03(:,3),leer_rad_40_rati
o_03(:,1),leer_rad_40_ratio_03(:,4));
plot(leer_rad_40_ratio_04(:,1),leer_rad_40_ratio_04(:,2),leer_r
ad_40_ratio_04(:,1),leer_rad_40_ratio_04(:,3),leer_rad_40_rati
o_04(:,1),leer_rad_40_ratio_04(:,4));
plot(leer_rad_40_ratio_05(:,1),leer_rad_40_ratio_05(:,2),leer_r
ad_40_ratio_05(:,1),leer_rad_40_ratio_05(:,3),leer_rad_40_rati
o_05(:,1),leer_rad_40_ratio_05(:,4));
plot(leer_rad_40_ratio_06(:,1),leer_rad_40_ratio_06(:,2),leer_r
ad_40_ratio_06(:,1),leer_rad_40_ratio_06(:,3),leer_rad_40_rati
o_06(:,1),leer_rad_40_ratio_06(:,4));
plot(leer_rad_40_ratio_07(:,1),leer_rad_40_ratio_07(:,2),leer_r
ad_40_ratio_07(:,1),leer_rad_40_ratio_07(:,3),leer_rad_40_rati
o_07(:,1),leer_rad_40_ratio_07(:,4));
plot(leer_rad_40_ratio_08(:,1),leer_rad_40_ratio_08(:,2),leer_r
ad_40_ratio_08(:,1),leer_rad_40_ratio_08(:,3),leer_rad_40_rati
o_08(:,1),leer_rad_40_ratio_08(:,4));

```

```

plot(leer_rad_40_ratio_09(:,1),leer_rad_40_ratio_09(:,2),leer_r
ad_40_ratio_09(:,1),leer_rad_40_ratio_09(:,3),leer_rad_40_rati
o_09(:,1),leer_rad_40_ratio_09(:,4));
plot(leer_rad_40_ratio_10(:,1),leer_rad_40_ratio_10(:,2),leer_r
ad_40_ratio_10(:,1),leer_rad_40_ratio_10(:,3),leer_rad_40_rati
o_10(:,1),leer_rad_40_ratio_10(:,4));
plot(leer_rad_40_ratio_11(:,1),leer_rad_40_ratio_11(:,2),leer_r
ad_40_ratio_11(:,1),leer_rad_40_ratio_11(:,3),leer_rad_40_rati
o_11(:,1),leer_rad_40_ratio_11(:,4));
legend('First Axle','Second Axle','Third Axle',-1);
title('Bison Constant Radius Test, Radius 40 meters');
xlabel('Vehicle Speed [km/h]');
grid;
axis([30 60 0 15]);

```

```

ylabel('Slip Angle [°]');subplot(3,1,3); hold on;
plot(leer_rad_60_ratio_03(:,1),leer_rad_60_ratio_03(:,2),leer_r
ad_60_ratio_03(:,1),leer_rad_60_ratio_03(:,3),leer_rad_60_rati
o_03(:,1),leer_rad_60_ratio_03(:,4));
plot(leer_rad_60_ratio_04(:,1),leer_rad_60_ratio_04(:,2),leer_r
ad_60_ratio_04(:,1),leer_rad_60_ratio_04(:,3),leer_rad_60_rati
o_04(:,1),leer_rad_60_ratio_04(:,4));
plot(leer_rad_60_ratio_05(:,1),leer_rad_60_ratio_05(:,2),leer_r
ad_60_ratio_05(:,1),leer_rad_60_ratio_05(:,3),leer_rad_60_rati
o_05(:,1),leer_rad_60_ratio_05(:,4));
plot(leer_rad_60_ratio_06(:,1),leer_rad_60_ratio_06(:,2),leer_r
ad_60_ratio_06(:,1),leer_rad_60_ratio_06(:,3),leer_rad_60_rati
o_06(:,1),leer_rad_60_ratio_06(:,4));
plot(leer_rad_60_ratio_07(:,1),leer_rad_60_ratio_07(:,2),leer_r
ad_60_ratio_07(:,1),leer_rad_60_ratio_07(:,3),leer_rad_60_rati
o_07(:,1),leer_rad_60_ratio_07(:,4));
plot(leer_rad_60_ratio_08(:,1),leer_rad_60_ratio_08(:,2),leer_r
ad_60_ratio_08(:,1),leer_rad_60_ratio_08(:,3),leer_rad_60_rati
o_08(:,1),leer_rad_60_ratio_08(:,4));
plot(leer_rad_60_ratio_09(:,1),leer_rad_60_ratio_09(:,2),leer_r
ad_60_ratio_09(:,1),leer_rad_60_ratio_09(:,3),leer_rad_60_rati
o_09(:,1),leer_rad_60_ratio_09(:,4));
plot(leer_rad_60_ratio_10(:,1),leer_rad_60_ratio_10(:,2),leer_r
ad_60_ratio_10(:,1),leer_rad_60_ratio_10(:,3),leer_rad_60_rati
o_10(:,1),leer_rad_60_ratio_10(:,4));
plot(leer_rad_60_ratio_11(:,1),leer_rad_60_ratio_11(:,2),leer_r
ad_60_ratio_11(:,1),leer_rad_60_ratio_11(:,3),leer_rad_60_rati
o_11(:,1),leer_rad_60_ratio_11(:,4));
legend('First Axle','Second Axle','Third Axle',-1);
title('Bison Constant Radius Test, Radius 60 meters');
xlabel('Vehicle Speed [km/h]');
ylabel('Slip Angle [°]');
grid;
axis([30 60 0 15]);

```

```

figure;
hold;
plot(leer_rad_60_ratio_07(:,1),leer_rad_60_ratio_07(:,5),'r+-');
plot(leer_rad_60_ratio_07(:,1),leer_rad_60_ratio_07(:,6),'r+');
plot(leer_rad_60_ratio_05(:,1),leer_rad_60_ratio_05(:,5),'g+-');
plot(leer_rad_60_ratio_05(:,1),leer_rad_60_ratio_05(:,6),'g+');
plot(leer_rad_60_ratio_10(:,1),leer_rad_60_ratio_10(:,5),'b+-');
plot(leer_rad_60_ratio_10(:,1),leer_rad_60_ratio_10(:,6),'b+');
title('Constant Radius Test, Radius 60 meters');
xlabel('Speed [km/h]');
ylabel('Steering Angle [°]');
legend('R0.7, 1st Steering Axle','R0.7, 2nd Steering
Axle','R0.5, 1st Steering Axle','R0.5, 2nd Steering Axle','R1,
1st Steering Axle','R1, 2nd Steering Axle',-1);
%axis([30 60 0 18]);
grid;
figure;
hold;
plot(leer_rad_40_ratio_07(:,1),leer_rad_40_ratio_07(:,5),'r+-');
plot(leer_rad_40_ratio_07(:,1),leer_rad_40_ratio_07(:,6),'r+');
plot(leer_rad_40_ratio_05(:,1),leer_rad_40_ratio_05(:,5),'g+-');
plot(leer_rad_40_ratio_05(:,1),leer_rad_40_ratio_05(:,6),'g+');
plot(leer_rad_40_ratio_10(:,1),leer_rad_40_ratio_10(:,5),'b+-');
plot(leer_rad_40_ratio_10(:,1),leer_rad_40_ratio_10(:,6),'b+');
title('Constant Radius Test, Radius 40 meters');
xlabel('Speed [km/h]');

```



```

ylabel('Steering Angle [°]');
legend('R0.7, 1st Steering Axle','R0.7, 2nd Steering Axle','R0.5, 1st Steering Axle','R0.5, 2nd Steering Axle','R1, 1st Steering Axle','R1, 2nd Steering Axle',-1);
%axis([30 60 0 18]);
grid;
figure;
hold;
plot(leer_rad_20_ratio_07(:,1),leer_rad_20_ratio_07(:,5),'r+-');
plot(leer_rad_20_ratio_07(:,1),leer_rad_20_ratio_07(:,6),'r+-');
plot(leer_rad_20_ratio_05(:,1),leer_rad_20_ratio_05(:,5),'g+-');
plot(leer_rad_20_ratio_05(:,1),leer_rad_20_ratio_05(:,6),'g+-');
plot(leer_rad_20_ratio_10(:,1),leer_rad_20_ratio_10(:,5),'b+-');
plot(leer_rad_20_ratio_10(:,1),leer_rad_20_ratio_10(:,6),'b+-');
title('Constant Radius Test, Radius 20 meters');
xlabel('Speed [km/h]');
ylabel('Steering Angle [°]');
legend('R0.7, 1st Steering Axle','R0.7, 2nd Steering Axle','R0.5, 1st Steering Axle','R0.5, 2nd Steering Axle','R1, 1st Steering Axle','R1, 2nd Steering Axle',-1);
%axis([30 60 0 18]);
grid;
##### Plot Steering vs Lateral Acceleration

figure;
subplot(3,1,1);
hold;
v=30/3.6;
for q = 1:8
    %plot((v^2/600,leer_rad_60_ratio_07(q,5),'r+-');
    %plot((v^2/600,leer_rad_60_ratio_05(q,5),'g+-');
    %plot((v^2/600,leer_rad_60_ratio_10(q,5),'b+-');

plot((leer_rad_60_ratio_07(q,1)/3.6)^2/600,leer_rad_60_ratio_07(q,5),'r+-');

plot((leer_rad_60_ratio_05(q,1)/3.6)^2/600,leer_rad_60_ratio_05(q,5),'g+-');

plot((leer_rad_60_ratio_10(q,1)/3.6)^2/600,leer_rad_60_ratio_10(q,5),'b+-');
    v=v+(10/3.6);
end;
title('Constant Radius Test, Radius 60 meters');
xlabel('Lateral Acceleration [g]');
ylabel('1st Axle Steering Angle [°]');
legend('Ratio 0.7','Ratio 0.5','Ratio 1',-1);
grid;

subplot(3,1,2);
hold;
for q = 1:8

plot((leer_rad_40_ratio_07(q,1)/3.6)^2/400,leer_rad_40_ratio_07(q,5),'r+-');

plot((leer_rad_40_ratio_05(q,1)/3.6)^2/400,leer_rad_40_ratio_05(q,5),'g+-');

plot((leer_rad_40_ratio_10(q,1)/3.6)^2/400,leer_rad_40_ratio_10(q,5),'b+-');
end;
title('Constant Radius Test, Radius 40 meters');
xlabel('Lateral Acceleration [g]');
ylabel('1st Axle Steering Angle [°]');
legend('Ratio 0.7','Ratio 0.5','Ratio 1',-1);
grid;
subplot(3,1,3);
hold;
for q = 1:8

plot((leer_rad_20_ratio_07(q,1)/3.6)^2/200,leer_rad_20_ratio_07(q,5),'r+-');

plot((leer_rad_20_ratio_05(q,1)/3.6)^2/200,leer_rad_20_ratio_05(q,5),'g+-');

```

Appendix D

Lane change – Matlab M file

```
%*****  
%*** modified 29 Sept 2003*****  
%****29 Sept 2004*****  
%non-linear tire model  
% 90 km/h  
%voorzyk=26;%meter  
%stuurhoek=4;%grade  
%tydregs=20/V;
```



```
leer',num2str(runnr),'_',num2str(Vkm_h),'  
leerbaan',num2str(runnr),'_',num2str(Vkm_h),' -append']);  
    %load dataleer.mat  
  
end;%if  
clear X;  
clear Y;  
clear BAANX;
```

```
clear BAANX2;clear BAAN1;clear BAAN2;clear  
BAAN3;clear BAAN4;  
end;%for  
end %for  
bison_matriks_saam_opsomming
```

Appendix E

Lane change data manipulation – Matlab M file

```
% Program plot data vir BISON SINGLE LANE CHANGE  
% Run eers Bison_fiets, bison_fiets_sim.mdl, Bison_fiets_plot  
% Bison_fiets_plot roep automaties Bison_fiets_data op.
```

```
% Inset tot die program is n dataleer wat die matrikse bevat  
uitgeskryf deur bison_fiets_plot  
%19 Aug 2003
```

```

close all;
%clear;
%bison_fiets;
%load opsomming.mat;

datamatriks_30=[leer1_30
leer2_30
leer3_30
leer4_30
leer5_30
leer6_30
leer7_30
leer8_30];
datamatriks_40=[leer1_40
leer2_40
leer3_40
leer4_40
leer5_40
leer6_40
leer7_40
leer8_40];
datamatriks_50=[leer1_50
leer2_50
leer3_50
leer4_50
leer5_50
leer6_50
leer7_50
leer8_50];
datamatriks_60=[leer1_60
leer2_60
leer3_60
leer4_60
leer5_60
leer6_60
leer7_60
leer8_60];
datamatriks_70=[leer1_70
leer2_70
leer3_70
leer4_70
leer5_70
leer6_70
leer7_70
leer8_70];

%===== TIME
TO COMPLETE TE TRACK
=====
%t(plek),X(plek),Y(plek),V,ratio, lengte,max(AlfaF1)*57.3,max(
AlfaF2)*57.3,max(AlfaR1)*57.3,AlfaF1_AVG*57.3,AlfaF2_AVG
*57.3,AlfaR1_AVG*57.3]);
figure;
%plot(datamatriks_30(:,5),datamatriks_30(:,1),datamatriks_40(
(:,5),datamatriks_40(:,1),datamatriks_50(:,5),datamatriks_50(:,1
),datamatriks_60(:,5),datamatriks_60(:,1),datamatriks_70(:,5),d
atamatriks_70(:,1),datamatriks_80(:,5),datamatriks_80(:,1),dat
amatriks_90(:,5),datamatriks_90(:,1));
plot(datamatriks_30(:,5),datamatriks_30(:,1));hold on;
plot(datamatriks_40(:,5),datamatriks_40(:,1));
plot(datamatriks_50(:,5),datamatriks_50(:,1));
plot(datamatriks_60(:,5),datamatriks_60(:,1));
plot(datamatriks_70(:,5),datamatriks_70(:,1));

title('Bison Single Lane Change');
xlabel('Steering Ratio');
ylabel('time to complete the track [s]');
legend('30 km/h','40 km/h','50 km/h','60 km/h','70 km/h',-1);
hold off;

%===== MAX
SLIP ANGLE
=====
figure;
%plot(datamatriks_30(:,5),datamatriks_30(:,7),datamatriks_30(
(:,5),datamatriks_30(:,8),datamatriks_30(:,9),datamatriks_30(:,9
),datamatriks_40(:,5),datamatriks_40(:,7),datamatriks_40(:,5),d
atamatriks_40(:,8),datamatriks_40(:,9),datamatriks_40(:,9),dat
amatriks_50(:,5),datamatriks_50(:,7),datamatriks_50(:,5),datam
atriks_50(:,8),datamatriks_50(:,9),datamatriks_50(:,9),datam
atriks_60(:,5),datamatriks_60(:,7),datamatriks_60(:,5),datamatr
iks_60(:,8),datamatriks_60(:,9),datamatriks_60(:,9),datamatrik
s_70(:,5),datamatriks_70(:,7),datamatriks_70(:,5),datamatriks_
70(:,8),datamatriks_70(:,9),datamatriks_70(:,9),datamatriks_80
(:,5),datamatriks_80(:,7),datamatriks_80(:,5),datamatriks_80(
,8),datamatriks_80(:,9),datamatriks_80(:,9),datamatriks_90(:,5
),datamatriks_90(:,7),datamatriks_90(:,5),datamatriks_90(:,8),da
tamatriks_90(:,9),datamatriks_90(:,9));
subplot(3,2,1);
bar(datamatriks_30(:,5),datamatriks_30(:,7:9),'stacked');
axis([0.2 1.1 0 10]);grid;
title('Bison Single Lane Change 30 km/h');
legend('First Axle','Second Axle','Third Axle',-1);
xlabel('Steering Ratio');
ylabel('Max slip angle');
subplot(3,2,2);
bar(datamatriks_40(:,5),datamatriks_40(:,7:9),'stacked');
axis([0.2 1.2 0 10]);grid;
title('Bison Single Lane Change 40 km/h');
legend('First Axle','Second Axle','Third Axle',-1);
xlabel('Steering Ratio');
ylabel('Max slip angle');
subplot(3,2,3);
bar(datamatriks_50(:,5),datamatriks_50(:,7:9),'stacked');
axis([0.2 1.2 0 10]);grid;
title('Bison Single Lane Change 50 km/h');
legend('First Axle','Second Axle','Third Axle',-1);
xlabel('Steering Ratio');
ylabel('Max slip angle');
subplot(3,2,4);
bar(datamatriks_60(:,5),datamatriks_60(:,7:9),'stacked');
axis([0.2 1.2 0 10]);grid;
title('Bison Single Lane Change 60 km/h');
legend('First Axle','Second Axle','Third Axle',-1);
xlabel('Steering Ratio');
ylabel('Max slip angle');
subplot(3,2,5);
bar(datamatriks_70(:,5),datamatriks_70(:,7:9),'stacked');
axis([0.2 1.2 0 10]);grid;
title('Bison Single Lane Change70 km/h');
legend('First Axle','Second Axle','Third Axle',-1);
xlabel('Steering Ratio');
ylabel('Max slip angle');

%===== TIME
TO COMPLETE TE TRACK
=====
grid;
hold off;
%===== TIME
TO COMPLETE TE TRACK
=====

```



```

%===== LANE
CHANGE XY PLOT
=====
=====
hold off;figure;
hold on;
%=====PL
OT RATIO GRAPHS
=====
=====
V=[30 40 50 60 70];
for j=1:5
    for i=1:8
        eval(['q=size(leerbaan',num2str(i),'_',num2str(V(j)),')');
            if i == 1
                kleur='c';
                subplot(4,2,i);
                title('Bison Single Lane Change. Steering Ratio 0.4 ');
                xlabel('Distance [m]');
                ylabel('Distance [m]');

                lyn1=[15 1.8
                    157.230];
                lyn2=[45 -1.8
                    453.630];
                lyn3=[0.1 1.8
                    151.8];
                lyn4=[45 3.63
                    100 3.63];
                lyn5=[15 7.23
                    100 7.23];
                lyn6=[0.1 -1.8
                    45-1.8];
                lyn7=[0.01 0.01
                    300.01];
                lyn8=[30 0.01
                    305.430];
                lyn9=[30 5.43
                    100 5.43];
                lyn10=[100 3.63
                    100 7.23];

                plot(lyn9(:,1),lyn9(:,2),lyn8(:,1),lyn8(:,2),lyn7(:,1),lyn7(:,2),lyn6(:,1),lyn6(:,2),lyn5(:,1),lyn5(:,2),lyn4(:,1),lyn4(:,2),lyn3(:,1),lyn3(:,2),lyn2(:,1),lyn2(:,2),lyn1(:,1),lyn1(:,2),lyn10(:,1),lyn10(:,2));
                    axis([0 100 -2.5 8]);hold on;grid;

                eval(['plot(leerbaan',num2str(i),'_',num2str(V(j)),'(1,3;q(1,2)),leerbaan',num2str(i),'_',num2str(V(j)),'(2,3;q(1,2)),kleur)']);hold on;
            end;
            if i == 2
                kleur='y';
                subplot(4,2,i);
                title('Bison Single Lane Change. Steering Ratio 0.5 ');
                xlabel('Distance [m]');
                ylabel('Distance [m]');

                lyn1=[15 1.8
                    157.230];
                lyn2=[45 -1.8
                    453.630];
                lyn3=[0.1 1.8
                    151.8];
                lyn4=[45 3.63
                    100 3.63];
                lyn5=[15 7.23
                    100 7.23];
                lyn6=[0.1 -1.8
                    45-1.8];
                lyn7=[0.01 0.01
                    300.01];
                lyn8=[30 0.01
                    305.430];
            end;
            if i == 3
                kleur='m';
                subplot(4,2,i);
                title('Bison Single Lane Change. Steering Ratio 0.6 ');
                xlabel('Distance [m]');
                ylabel('Distance [m]');

                lyn1=[15 1.8
                    157.230];
                lyn2=[45 -1.8
                    453.630];
                lyn3=[0.1 1.8
                    151.8];
                lyn4=[45 3.63
                    100 3.63];
                lyn5=[15 7.23
                    100 7.23];
                lyn6=[0.1 -1.8
                    45-1.8];
                lyn7=[0.01 0.01
                    300.01];
                lyn8=[30 0.01
                    305.430];
                lyn9=[30 5.43
                    100 5.43];
                lyn10=[100 3.63
                    100 7.23];

                plot(lyn9(:,1),lyn9(:,2),lyn8(:,1),lyn8(:,2),lyn7(:,1),lyn7(:,2),lyn6(:,1),lyn6(:,2),lyn5(:,1),lyn5(:,2),lyn4(:,1),lyn4(:,2),lyn3(:,1),lyn3(:,2),lyn2(:,1),lyn2(:,2),lyn1(:,1),lyn1(:,2),lyn10(:,1),lyn10(:,2));
                    axis([0 100 -2.5 8]);hold on;grid;

                eval(['plot(leerbaan',num2str(i),'_',num2str(V(j)),'(1,3;q(1,2)),leerbaan',num2str(i),'_',num2str(V(j)),'(2,3;q(1,2)),kleur)']);hold on;
            end;
            if i == 4
                kleur='r';
                subplot(4,2,i);
                title('Bison Single Lane Change. Steering Ratio 0.7 ');
                xlabel('Distance [m]');
                ylabel('Distance [m]');

                lyn1=[15 1.8
                    157.230];
                lyn2=[45 -1.8
                    453.630];
                lyn3=[0.1 1.8
                    151.8];
                lyn4=[45 3.63
                    100 3.63];
                lyn5=[15 7.23
                    100 7.23];
                lyn6=[0.1 -1.8
                    45-1.8];
                lyn7=[0.01 0.01
                    300.01];
                lyn8=[30 0.01
                    305.430];
                lyn9=[30 5.43
                    100 5.43];
                lyn10=[100 3.63
                    100 7.23];
            end;
        end;
    end;
end;

```

```

lyn9=[30 5.43
100 5.43];
lyn10=[100 3.63
100 7.23];

```

```

plot(lyn9(:,1),lyn9(:,2),lyn8(:,1),lyn8(:,2),lyn7(:,1),lyn7(:,2),lyn6(:,1),lyn6(:,2),lyn5(:,1),lyn5(:,2),lyn4(:,1),lyn4(:,2),lyn3(:,1),lyn3(:,2),lyn2(:,1),lyn2(:,2),lyn1(:,1),lyn1(:,2),lyn10(:,1),lyn10(:,2));
axis([0 100 -2.5 8]);hold on;grid;

```

```

eval(['plot(leerbaan',num2str(i),'_',num2str(V(j)),'(1,3;q(1,2)),leerbaan',num2str(i),'_',num2str(V(j)),'(2,3;q(1,2)),kleur)']);hold on;
end;

```

```

if i == 3
    kleur='m';
    subplot(4,2,i);
    title('Bison Single Lane Change. Steering Ratio 0.6 ');
    xlabel('Distance [m]');
    ylabel('Distance [m]');

    lyn1=[15 1.8
        157.230];
    lyn2=[45 -1.8
        453.630];
    lyn3=[0.1 1.8
        151.8];
    lyn4=[45 3.63
        100 3.63];
    lyn5=[15 7.23
        100 7.23];
    lyn6=[0.1 -1.8
        45-1.8];
    lyn7=[0.01 0.01
        300.01];
    lyn8=[30 0.01
        305.430];
    lyn9=[30 5.43
        100 5.43];
    lyn10=[100 3.63
        100 7.23];

```

```

plot(lyn9(:,1),lyn9(:,2),lyn8(:,1),lyn8(:,2),lyn7(:,1),lyn7(:,2),lyn6(:,1),lyn6(:,2),lyn5(:,1),lyn5(:,2),lyn4(:,1),lyn4(:,2),lyn3(:,1),lyn3(:,2),lyn2(:,1),lyn2(:,2),lyn1(:,1),lyn1(:,2),lyn10(:,1),lyn10(:,2));
axis([0 100 -2.5 8]);hold on;grid;

```

```

eval(['plot(leerbaan',num2str(i),'_',num2str(V(j)),'(1,3;q(1,2)),leerbaan',num2str(i),'_',num2str(V(j)),'(2,3;q(1,2)),kleur)']);hold on;
end;

```

```

if i == 4
    kleur='r';
    subplot(4,2,i);
    title('Bison Single Lane Change. Steering Ratio 0.7 ');
    xlabel('Distance [m]');
    ylabel('Distance [m]');

    lyn1=[15 1.8
        157.230];
    lyn2=[45 -1.8
        453.630];
    lyn3=[0.1 1.8
        151.8];
    lyn4=[45 3.63
        100 3.63];
    lyn5=[15 7.23
        100 7.23];
    lyn6=[0.1 -1.8
        45-1.8];
    lyn7=[0.01 0.01
        300.01];
    lyn8=[30 0.01
        305.430];
    lyn9=[30 5.43
        100 5.43];
    lyn10=[100 3.63
        100 7.23];

```

```
plot(lyn9(:,1),lyn9(:,2),lyn8(:,1),lyn8(:,2),lyn7(:,1),lyn7(:,2),lyn6(:,1),lyn6(:,2),lyn5(:,1),lyn5(:,2),lyn4(:,1),lyn4(:,2),lyn3(:,1),lyn3(:,2),lyn2(:,1),lyn2(:,2),lyn1(:,1),lyn1(:,2),lyn10(:,1),lyn10(:,2));
axis([0 100 -2.5 8]);hold on;grid;
```

```
eval(['plot(leerbaan',num2str(i),'_',num2str(V(j)),'(1,3:q(1,2)),leerbaan',num2str(i),'_',num2str(V(j)),'(2,3:q(1,2)),kleur)']);hold on;
end;
if i == 5
subplot(4,2,i);
kleur='g';
title('Bison Single Lane Change. Steering Ratio 0.8 ');
xlabel('Distance [m]');
ylabel('Distance [m]');
lyn1=[15 1.8
157.230];
lyn2=[45 -1.8
453.630];
lyn3=[0.1 1.8
151.8];
lyn4=[45 3.63
100 3.63];
lyn5=[15 7.23
100 7.23];
lyn6=[0.1 -1.8
45-1.8];
lyn7=[0.01 0.01
300.01];
lyn8=[30 0.01
305.430];
lyn9=[30 5.43
100 5.43];
lyn10=[100 3.63
100 7.23];
```

```
plot(lyn9(:,1),lyn9(:,2),lyn8(:,1),lyn8(:,2),lyn7(:,1),lyn7(:,2),lyn6(:,1),lyn6(:,2),lyn5(:,1),lyn5(:,2),lyn4(:,1),lyn4(:,2),lyn3(:,1),lyn3(:,2),lyn2(:,1),lyn2(:,2),lyn1(:,1),lyn1(:,2),lyn10(:,1),lyn10(:,2));
axis([0 100 -2.5 8]);hold on;grid;
```

```
eval(['plot(leerbaan',num2str(i),'_',num2str(V(j)),'(1,3:q(1,2)),leerbaan',num2str(i),'_',num2str(V(j)),'(2,3:q(1,2)),kleur)']);hold on;
end;
if i == 6
kleur='b';
subplot(4,2,i);
title('Bison Single Lane Change. Steering Ratio 0.9 ');
xlabel('Distance [m]');
ylabel('Distance [m]');
lyn1=[15 1.8
157.230];
lyn2=[45 -1.8
453.630];
lyn3=[0.1 1.8
151.8];
lyn4=[45 3.63
100 3.63];
lyn5=[15 7.23
100 7.23];
lyn6=[0.1 -1.8
45-1.8];
lyn7=[0.01 0.01
300.01];
lyn8=[30 0.01
305.430];
lyn9=[30 5.43
100 5.43];
lyn10=[100 3.63
100 7.23];
```

```
plot(lyn9(:,1),lyn9(:,2),lyn8(:,1),lyn8(:,2),lyn7(:,1),lyn7(:,2),lyn6(:,1),lyn6(:,2),lyn5(:,1),lyn5(:,2),lyn4(:,1),lyn4(:,2),lyn3(:,1),lyn3(:,2),lyn2(:,1),lyn2(:,2),lyn1(:,1),lyn1(:,2),lyn10(:,1),lyn10(:,2));
axis([0 100 -2.5 8]);hold on;grid;
```

```
eval(['plot(leerbaan',num2str(i),'_',num2str(V(j)),'(1,3:q(1,2)),leerbaan',num2str(i),'_',num2str(V(j)),'(2,3:q(1,2)),kleur)']);hold on;
end;
if i == 7
kleur='c';
subplot(4,2,i);
title('Bison Single Lane Change. Steering Ratio 1 ');
xlabel('Distance [m]');
ylabel('Distance [m]');
lyn1=[15 1.8
157.230];
lyn2=[45 -1.8
453.630];
lyn3=[0.1 1.8
151.8];
lyn4=[45 3.63
100 3.63];
lyn5=[15 7.23
100 7.23];
lyn6=[0.1 -1.8
45-1.8];
lyn7=[0.01 0.01
300.01];
lyn8=[30 0.01
305.430];
lyn9=[30 5.43
100 5.43];
lyn10=[100 3.63
100 7.23];
```

```
plot(lyn9(:,1),lyn9(:,2),lyn8(:,1),lyn8(:,2),lyn7(:,1),lyn7(:,2),lyn6(:,1),lyn6(:,2),lyn5(:,1),lyn5(:,2),lyn4(:,1),lyn4(:,2),lyn3(:,1),lyn3(:,2),lyn2(:,1),lyn2(:,2),lyn1(:,1),lyn1(:,2),lyn10(:,1),lyn10(:,2));
axis([0 100 -2.5 8]);hold on;grid;
```

```
eval(['plot(leerbaan',num2str(i),'_',num2str(V(j)),'(1,3:q(1,2)),leerbaan',num2str(i),'_',num2str(V(j)),'(2,3:q(1,2)),kleur)']);hold on;
end;
if i == 8
kleur='m';
subplot(4,2,i);
title('Bison Single Lane Change. Steering Ratio 1.1 ');
xlabel('Distance [m]');
ylabel('Distance [m]');
lyn1=[15 1.8
157.230];
lyn2=[45 -1.8
453.630];
lyn3=[0.1 1.8
151.8];
lyn4=[45 3.63
100 3.63];
lyn5=[15 7.23
100 7.23];
lyn6=[0.1 -1.8
45-1.8];
lyn7=[0.01 0.01
300.01];
lyn8=[30 0.01
305.430];
lyn9=[30 5.43
100 5.43];
lyn10=[100 3.63
100 7.23];
```

```
plot(lyn9(:,1),lyn9(:,2),lyn8(:,1),lyn8(:,2),lyn7(:,1),lyn7(:,2),lyn6(:,1),lyn6(:,2),lyn5(:,1),lyn5(:,2),lyn4(:,1),lyn4(:,2),lyn3(:,1),lyn3(:,2),lyn2(:,1),lyn2(:,2),lyn1(:,1),lyn1(:,2),lyn10(:,1),lyn10(:,2));
axis([0 100 -2.5 8]);hold on;grid;
```

```
eval(['plot(leerbaan',num2str(i),'_',num2str(V(j)),'(1,3:q(1,2)),leerbaan',num2str(i),'_',num2str(V(j)),'(2,3:q(1,2)),kleur)']);hold on;
end;
end;%for
```

```

end;%for
hold off;
hold on;
%=====
=====
%=====
=====PLOT XY == 2
=====
=====
figure;
off30=910;
off40=910;
off50=910;
off60=905;
off70=910;
off80=910;
V=[30 40 50 60 70];
load rotate_dat;
for j=1:5
    for i=1:8
        eval(['q=size(leerbaan',num2str(i),'_',num2str(V(j)):',');]);
        if j == 1
            kleur='c';
            subplot(3,2,j);
            title('Bison Single Lane Change: 30 km/h ');
            xlabel('Distance [m]');
            ylabel('Distance [m]');
            lyn1=[15 1.8
                157.230];
            lyn2=[45 -1.8
                453.630];
            lyn3=[0.1 1.8
                151.8];
            lyn4=[45 3.63
                130 3.63];
            lyn5=[15 7.23
                130 7.23];
            lyn6=[0.1 -1.8
                45-1.8];
            lyn7=[0.01 0.01
                300.01];
            lyn8=[30 0.01
                305.430];
            lyn9=[30 5.43
                130 5.43];
            lyn10=[130 3.63
                130 7.23];
            plot(uitset_28_2(:,1)-off30,-1*uitset_28_2(:,2)-
                22.5,uitset_28_1(:,1)-off30,-1*uitset_28_1(:,2)-
                22.5,lyn9(:,1),lyn9(:,2),lyn8(:,1),lyn8(:,2),lyn7(:,1),lyn7(:,2),lyn6(
                :,1),lyn6(:,2),lyn5(:,1),lyn5(:,2),lyn4(:,1),lyn4(:,2),lyn3(:,1),lyn3(
                :,1),lyn2(:,1),lyn2(:,2),lyn1(:,1),lyn1(:,2),lyn10(:,1),lyn10(:,2));
            axis([0 130 -2.5 8]);hold on;grid on;

            eval(['plot(leerbaan',num2str(i),'_',num2str(V(j)):',(1,3:q(1,2)),lee
                rbaan',num2str(i),'_',num2str(V(j)):',(2,3:q(1,2)),kleur)']);hold on;
            end;
            if j == 2
                kleur='y';
                subplot(3,2,j);
                plot(uitset_43_2(:,1)-off40,-1*uitset_43_2(:,2)-
                    22.5,uitset_43_1(:,1)-off40,-1*uitset_43_1(:,2)-
                    22.5,lyn9(:,1),lyn9(:,2),lyn8(:,1),lyn8(:,2),lyn7(:,1),lyn7(:,2),lyn6(
                    :,1),lyn6(:,2),lyn5(:,1),lyn5(:,2),lyn4(:,1),lyn4(:,2),lyn3(:,1),lyn3(
                    :,1),lyn2(:,1),lyn2(:,2),lyn1(:,1),lyn1(:,2),lyn10(:,1),lyn10(:,2));
                axis([0 130 -2.5 8]);hold on;grid on;

                eval(['plot(leerbaan',num2str(i),'_',num2str(V(j)):',(1,3:q(1,2)),lee
                    rbaan',num2str(i),'_',num2str(V(j)):',(2,3:q(1,2)),kleur)']);hold on;

                title('Bison Single Lane Change 40 km/h ');
                xlabel('Distance [m]');
                ylabel('Distance [m]');
                lyn1=[15 1.8
                    157.230];
                lyn2=[45 -1.8
                    453.630];
                lyn3=[0.1 1.8
                    151.8];
                lyn4=[45 3.63
                    130 3.63];
                lyn5=[15 7.23
                    130 7.23];
                lyn6=[0.1 -1.8
                    45-1.8];
                lyn7=[0.01 0.01
                    300.01];
                lyn8=[30 0.01
                    305.430];
                lyn9=[30 5.43
                    130 5.43];
                lyn10=[130 3.63
                    130 7.23];

                end;
            if j == 3
                kleur='m';
                subplot(3,2,j);
                title('Bison Single Lane Change: 50 km/h ');
                xlabel('Distance [m]');
                ylabel('Distance [m]');
                lyn1=[15 1.8
                    157.230];
                lyn2=[45 -1.8
                    453.630];
                lyn3=[0.1 1.8
                    151.8];
                lyn4=[45 3.63
                    130 3.63];
                lyn5=[15 7.23
                    130 7.23];
                lyn6=[0.1 -1.8
                    45-1.8];
                lyn7=[0.01 0.01
                    300.01];
                lyn8=[30 0.01
                    305.430];
                lyn9=[30 5.43
                    130 5.43];
                lyn10=[130 3.63
                    130 7.23];

                plot(uitset_52_1(:,1)-off50,-1*uitset_52_1(:,2)-
                    22.5,uitset_52_2(:,1)-off50,-1*uitset_52_2(:,2)-
                    22.5,lyn9(:,1),lyn9(:,2),lyn8(:,1),lyn8(:,2),lyn7(:,1),lyn7(:,2),lyn6(
                    :,1),lyn6(:,2),lyn5(:,1),lyn5(:,2),lyn4(:,1),lyn4(:,2),lyn3(:,1),lyn3(
                    :,1),lyn2(:,1),lyn2(:,2),lyn1(:,1),lyn1(:,2),lyn10(:,1),lyn10(:,2));
                axis([0 130 -2.5 8]);
                hold on;grid on;

                eval(['plot(leerbaan',num2str(i),'_',num2str(V(j)):',(1,3:q(1,2)),lee
                    rbaan',num2str(i),'_',num2str(V(j)):',(2,3:q(1,2)),kleur)']);hold on;
            end;
            if j == 4
                kleur='r';
                subplot(3,2,j);
                title('Bison Single Lane Change: 60 km/h ');
                xlabel('Distance [m]');
                ylabel('Distance [m]');
                lyn1=[15 1.8
                    157.230];
                lyn2=[45 -1.8
                    453.630];
                lyn3=[0.1 1.8
                    151.8];
                lyn4=[45 3.63
                    130 3.63];
                lyn5=[15 7.23
                    130 7.23];
                lyn6=[0.1 -1.8
                    45-1.8];
                lyn7=[0.01 0.01
                    300.01];
                lyn8=[30 0.01
                    305.430];
                lyn9=[30 5.43
                    130 5.43];
                lyn10=[130 3.63
                    130 7.23];
            end;
        end;
    end;
end;

```



```

subplot(3,1,3);%F3

eval(['plot(gliphoek',num2str(i),'_',num2str(spoed),'(1,3:q(1,2)),
gliphoek',num2str(i),'_',num2str(spoed),'(4,3:q(1,2)),kleur)'];hold
on;
end;
if i == 5
    kleur='g';
    eval(['q=size(gliphoek',num2str(i),'_',num2str(spoed),'');]);
    subplot(3,1,1);%F1

eval(['plot(gliphoek',num2str(i),'_',num2str(spoed),'(1,3:q(1,2)),
gliphoek',num2str(i),'_',num2str(spoed),'(2,3:q(1,2)),kleur)'];hold
on;
    subplot(3,1,2);%F2

eval(['plot(gliphoek',num2str(i),'_',num2str(spoed),'(1,3:q(1,2)),
gliphoek',num2str(i),'_',num2str(spoed),'(3,3:q(1,2)),kleur)'];hold
on;
    subplot(3,1,3);%F3

eval(['plot(gliphoek',num2str(i),'_',num2str(spoed),'(1,3:q(1,2)),
gliphoek',num2str(i),'_',num2str(spoed),'(4,3:q(1,2)),kleur)'];hold
on;
end;
if i == 6
    kleur='b';
    eval(['q=size(gliphoek',num2str(i),'_',num2str(spoed),'');]);
    subplot(3,1,1);%F1

eval(['plot(gliphoek',num2str(i),'_',num2str(spoed),'(1,3:q(1,2)),
gliphoek',num2str(i),'_',num2str(spoed),'(2,3:q(1,2)),kleur)'];hold
on;
    subplot(3,1,2);%F2

eval(['plot(gliphoek',num2str(i),'_',num2str(spoed),'(1,3:q(1,2)),
gliphoek',num2str(i),'_',num2str(spoed),'(3,3:q(1,2)),kleur)'];hold
on;
    subplot(3,1,3);%F3

eval(['plot(gliphoek',num2str(i),'_',num2str(spoed),'(1,3:q(1,2)),
gliphoek',num2str(i),'_',num2str(spoed),'(4,3:q(1,2)),kleur)'];hold
on;
end;
if i == 7
    kleur='c';
    eval(['q=size(gliphoek',num2str(i),'_',num2str(spoed),'');]);
    subplot(3,1,1);%F1

eval(['plot(gliphoek',num2str(i),'_',num2str(spoed),'(1,3:q(1,2)),
gliphoek',num2str(i),'_',num2str(spoed),'(2,3:q(1,2)),kleur)'];hold
on;
    subplot(3,1,2);%F2

eval(['plot(gliphoek',num2str(i),'_',num2str(spoed),'(1,3:q(1,2)),
gliphoek',num2str(i),'_',num2str(spoed),'(3,3:q(1,2)),kleur)'];hold
on;
    subplot(3,1,3);%F3

eval(['plot(gliphoek',num2str(i),'_',num2str(spoed),'(1,3:q(1,2)),
gliphoek',num2str(i),'_',num2str(spoed),'(4,3:q(1,2)),kleur)'];hold
on;
end;
if i == 8
    kleur='k';
    eval(['q=size(gliphoek',num2str(i),'_',num2str(spoed),'');]);
    subplot(3,1,1);%F1

eval(['plot(gliphoek',num2str(i),'_',num2str(spoed),'(1,3:q(1,2)),
gliphoek',num2str(i),'_',num2str(spoed),'(2,3:q(1,2)),kleur)'];hold
on;
    subplot(3,1,2);%F2

eval(['plot(gliphoek',num2str(i),'_',num2str(spoed),'(1,3:q(1,2)),
gliphoek',num2str(i),'_',num2str(spoed),'(3,3:q(1,2)),kleur)'];hold
on;
    subplot(3,1,3);%F3

```

```

eval(['plot(gliphoek',num2str(i),'_',num2str(spoed),'(1,3:q(1,2)),
gliphoek',num2str(i),'_',num2str(spoed),'(4,3:q(1,2)),kleur)'];hold
on;
end;
if i == 9
    kleur='b';
    eval(['q=size(gliphoek',num2str(i),'_',num2str(spoed),'');]);
    subplot(3,1,1);%F1

eval(['plot(gliphoek',num2str(i),'_',num2str(spoed),'(1,3:q(1,2)),
gliphoek',num2str(i),'_',num2str(spoed),'(2,3:q(1,2)),kleur)'];hold
on;
    subplot(3,1,2);%F2

eval(['plot(gliphoek',num2str(i),'_',num2str(spoed),'(1,3:q(1,2)),
gliphoek',num2str(i),'_',num2str(spoed),'(3,3:q(1,2)),kleur)'];hold
on;
    subplot(3,1,3);%F3

eval(['plot(gliphoek',num2str(i),'_',num2str(spoed),'(1,3:q(1,2)),
gliphoek',num2str(i),'_',num2str(spoed),'(4,3:q(1,2)),kleur)'];hold
on;
end;

end;
legend('ratio 0.3','ratio 0.4','ratio 0.5','ratio 0.6','ratio 0.7','ratio
0.8','ratio 0.9','ratio 1','ratio 1.1');

end;

%===== PLOT
stuurhoeke
=====

spoed=20;
for s = 1:7
    spoed=spoed+10;
    figure;
    for i=1:8
        if i == 1
            eval(['q=size(gliphoek',num2str(i),'_',num2str(spoed),'');]);
            %kleur='c-<';
            kleur='c';

eval(['plot(gliphoek',num2str(i),'_',num2str(spoed),'(1,3:q(1,2)),
gliphoek',num2str(i),'_',num2str(spoed),'(7,3:q(1,2)),kleur)'];hold
on;
            eval(['title("Bison Single Lane Change ',num2str(spoed),'
km/h. First Steering Axle")']);
            xlabel('time [s]');
            ylabel('Steering Angle [°]');
            axis([0 15 -15 30]);grid;
        end;
        if i == 2
            kleur='y';
            eval(['q=size(gliphoek',num2str(i),'_',num2str(spoed),'');]);

eval(['plot(gliphoek',num2str(i),'_',num2str(spoed),'(1,3:q(1,2)),
gliphoek',num2str(i),'_',num2str(spoed),'(7,3:q(1,2)),kleur)'];hold
on;
            end;
            if i == 3
                kleur='m';
                eval(['q=size(gliphoek',num2str(i),'_',num2str(spoed),'');]);

eval(['plot(gliphoek',num2str(i),'_',num2str(spoed),'(1,3:q(1,2)),
gliphoek',num2str(i),'_',num2str(spoed),'(7,3:q(1,2)),kleur)'];hold
on;
            end;
            if i == 4
                kleur='r';
                eval(['q=size(gliphoek',num2str(i),'_',num2str(spoed),'');]);

eval(['plot(gliphoek',num2str(i),'_',num2str(spoed),'(1,3:q(1,2)),
gliphoek',num2str(i),'_',num2str(spoed),'(7,3:q(1,2)),kleur)'];hold
on;

```

```

end;
if i == 5
    kleur='g';
    eval(['q=size(gliphoeke',num2str(i),'_',num2str(spoed),');']);
eval(['plot(gliphoeke',num2str(i),'_',num2str(spoed),'(1,3:q(1,2)),
gliphoeke',num2str(i),'_',num2str(spoed),'(7,3:q(1,2)),kleur)'];hold
on;
end;
if i == 6
    kleur='b';
    eval(['q=size(gliphoeke',num2str(i),'_',num2str(spoed),');']);
eval(['plot(gliphoeke',num2str(i),'_',num2str(spoed),'(1,3:q(1,2)),
gliphoeke',num2str(i),'_',num2str(spoed),'(7,3:q(1,2)),kleur)'];hold
on;
end;
if i == 7
    kleur='c';
    eval(['q=size(gliphoeke',num2str(i),'_',num2str(spoed),');']);
eval(['plot(gliphoeke',num2str(i),'_',num2str(spoed),'(1,3:q(1,2)),
gliphoeke',num2str(i),'_',num2str(spoed),'(7,3:q(1,2)),kleur)'];hold
on;
end;
if i == 8
    kleur='k';
    eval(['q=size(gliphoeke',num2str(i),'_',num2str(spoed),');']);
eval(['plot(gliphoeke',num2str(i),'_',num2str(spoed),'(1,3:q(1,2)),
gliphoeke',num2str(i),'_',num2str(spoed),'(7,3:q(1,2)),kleur)'];hold
on;
end;
if i == 9
    kleur='b';
    eval(['q=size(gliphoeke',num2str(i),'_',num2str(spoed),');']);
eval(['plot(gliphoeke',num2str(i),'_',num2str(spoed),'(1,3:q(1,2)),
gliphoeke',num2str(i),'_',num2str(spoed),'(7,3:q(1,2)),kleur)'];hold
on;
end;

legend('ratio 0.3','ratio 0.4','ratio 0.5','ratio 0.6','ratio 0.7','ratio
0.8','ratio 0.9','ratio 1','ratio 1.1');

end;
%===== PLOT yaw
=====
spoed=20;
for s = 1:7
    spoed=spoed+10;
    figure;
    for i=1:8
        if i == 1
            eval(['q=size(gliphoeke',num2str(i),'_',num2str(spoed),');']);
            %kleur='c-';
            kleur='c';
eval(['plot(gliphoeke',num2str(i),'_',num2str(spoed),'(1,3:q(1,2)),
gliphoeke',num2str(i),'_',num2str(spoed),'(5,3:q(1,2)),kleur)'];hold
on;
            eval(['title("Bison Single Lane Change ',num2str(spoed),'
km/h. Yaw Angle")']);
            xlabel('time [s]');
            ylabel('Yaw Angle [°]');
            axis([0 15 -15 30]);grid;
        end;
        if i == 2
            kleur='y';
            eval(['q=size(gliphoeke',num2str(i),'_',num2str(spoed),');']);
eval(['plot(gliphoeke',num2str(i),'_',num2str(spoed),'(1,3:q(1,2)),
gliphoeke',num2str(i),'_',num2str(spoed),'(5,3:q(1,2)),kleur)'];hold
on;
        end;

```

```

if i == 3
    kleur='m';
    eval(['q=size(gliphoeke',num2str(i),'_',num2str(spoed),');']);
eval(['plot(gliphoeke',num2str(i),'_',num2str(spoed),'(1,3:q(1,2)),
gliphoeke',num2str(i),'_',num2str(spoed),'(5,3:q(1,2)),kleur)'];hold
on;
end;
if i == 4
    kleur='r';
    eval(['q=size(gliphoeke',num2str(i),'_',num2str(spoed),');']);
eval(['plot(gliphoeke',num2str(i),'_',num2str(spoed),'(1,3:q(1,2)),
gliphoeke',num2str(i),'_',num2str(spoed),'(5,3:q(1,2)),kleur)'];hold
on;
end;
if i == 5
    kleur='g';
    eval(['q=size(gliphoeke',num2str(i),'_',num2str(spoed),');']);
eval(['plot(gliphoeke',num2str(i),'_',num2str(spoed),'(1,3:q(1,2)),
gliphoeke',num2str(i),'_',num2str(spoed),'(5,3:q(1,2)),kleur)'];hold
on;
end;
if i == 6
    kleur='b';
    eval(['q=size(gliphoeke',num2str(i),'_',num2str(spoed),');']);
eval(['plot(gliphoeke',num2str(i),'_',num2str(spoed),'(1,3:q(1,2)),
gliphoeke',num2str(i),'_',num2str(spoed),'(5,3:q(1,2)),kleur)'];hold
on;
end;
if i == 7
    kleur='c';
    eval(['q=size(gliphoeke',num2str(i),'_',num2str(spoed),');']);
eval(['plot(gliphoeke',num2str(i),'_',num2str(spoed),'(1,3:q(1,2)),
gliphoeke',num2str(i),'_',num2str(spoed),'(5,3:q(1,2)),kleur)'];hold
on;
end;
if i == 8
    kleur='k';
    eval(['q=size(gliphoeke',num2str(i),'_',num2str(spoed),');']);
eval(['plot(gliphoeke',num2str(i),'_',num2str(spoed),'(1,3:q(1,2)),
gliphoeke',num2str(i),'_',num2str(spoed),'(5,3:q(1,2)),kleur)'];hold
on;
end;
if i == 9
    kleur='b';
    eval(['q=size(gliphoeke',num2str(i),'_',num2str(spoed),');']);
eval(['plot(gliphoeke',num2str(i),'_',num2str(spoed),'(1,3:q(1,2)),
gliphoeke',num2str(i),'_',num2str(spoed),'(7,3:q(1,2)),kleur)'];hold
on;
end;
legend('ratio 0.3','ratio 0.4','ratio 0.5','ratio 0.6','ratio 0.7','ratio
0.8','ratio 0.9','ratio 1','ratio 1.1');

end;

%===== DETAIL
SLIP ANGLES
=====
spoed=20;
for s = 1:7
    spoed=spoed+10;
    figure;
    for i=1:9
        if i == 1
            subplot(3,1,1);%F1
            eval(['q=size(gliphoeke',num2str(i),'_',num2str(spoed),');']);
            %kleur='c-';

```

```

    kleur='c';

eval(['plot(gliphoeek',num2str(i),'_',num2str(spoed),'(1,3:q(1,2)),
gliphoeek',num2str(i),'_',num2str(spoed),'(2,3:q(1,2)),kleur)'];hold
d on;
    eval(['title("Bison Single Lane Change ',num2str(spoed),'
km/h. First Steering Axle")']);
    xlabel('time [s]');
    ylabel('Slip Angle [°]');
    axis([0 3 -15 10]);grid;
    subplot(3,1,2);%F2

eval(['plot(gliphoeek',num2str(i),'_',num2str(spoed),'(1,3:q(1,2)),
gliphoeek',num2str(i),'_',num2str(spoed),'(3,3:q(1,2)),kleur)'];hold
d on;
    eval(['title("Bison Single Lane Change ',num2str(spoed),'
km/h. Second Steering Axle ")']);
    xlabel('time [s]');
    ylabel('Slip Angle [°]');
    axis([0 3 -15 10]);grid;
    subplot(3,1,3);%F3

eval(['plot(gliphoeek',num2str(i),'_',num2str(spoed),'(1,3:q(1,2)),
gliphoeek',num2str(i),'_',num2str(spoed),'(4,3:q(1,2)),kleur)'];hold
d on;
    eval(['title("Bison Single Lane Change ',num2str(spoed),'
km/h. Rear Axle ")']);
    xlabel('time [s]');
    ylabel('Slip Angle [°]');
    axis([0 3 -15 10]);grid;
end;
if i == 2
    kleur='y';
    eval(['q=size(gliphoeek',num2str(i),'_',num2str(spoed),'');]);
    subplot(3,1,1);%F1

eval(['plot(gliphoeek',num2str(i),'_',num2str(spoed),'(1,3:q(1,2)),
gliphoeek',num2str(i),'_',num2str(spoed),'(2,3:q(1,2)),kleur)'];hold
d on;
    subplot(3,1,2);%F2

eval(['plot(gliphoeek',num2str(i),'_',num2str(spoed),'(1,3:q(1,2)),
gliphoeek',num2str(i),'_',num2str(spoed),'(3,3:q(1,2)),kleur)'];hold
d on;
    subplot(3,1,3);%F3

eval(['plot(gliphoeek',num2str(i),'_',num2str(spoed),'(1,3:q(1,2)),
gliphoeek',num2str(i),'_',num2str(spoed),'(4,3:q(1,2)),kleur)'];hold
d on;
    end;
    if i == 3
        kleur='m';
        eval(['q=size(gliphoeek',num2str(i),'_',num2str(spoed),'');]);
        subplot(3,1,1);%F1

eval(['plot(gliphoeek',num2str(i),'_',num2str(spoed),'(1,3:q(1,2)),
gliphoeek',num2str(i),'_',num2str(spoed),'(2,3:q(1,2)),kleur)'];hold
d on;
        subplot(3,1,2);%F2

eval(['plot(gliphoeek',num2str(i),'_',num2str(spoed),'(1,3:q(1,2)),
gliphoeek',num2str(i),'_',num2str(spoed),'(3,3:q(1,2)),kleur)'];hold
d on;
        subplot(3,1,3);%F3

eval(['plot(gliphoeek',num2str(i),'_',num2str(spoed),'(1,3:q(1,2)),
gliphoeek',num2str(i),'_',num2str(spoed),'(4,3:q(1,2)),kleur)'];hold
d on;
    end;
    if i == 4
        kleur='r';
        eval(['q=size(gliphoeek',num2str(i),'_',num2str(spoed),'');]);
        subplot(3,1,1);%F1

eval(['plot(gliphoeek',num2str(i),'_',num2str(spoed),'(1,3:q(1,2)),
gliphoeek',num2str(i),'_',num2str(spoed),'(2,3:q(1,2)),kleur)'];hold
d on;
        subplot(3,1,2);%F2

eval(['plot(gliphoeek',num2str(i),'_',num2str(spoed),'(1,3:q(1,2)),
gliphoeek',num2str(i),'_',num2str(spoed),'(3,3:q(1,2)),kleur)'];hold
d on;
        subplot(3,1,3);%F3

eval(['plot(gliphoeek',num2str(i),'_',num2str(spoed),'(1,3:q(1,2)),
gliphoeek',num2str(i),'_',num2str(spoed),'(4,3:q(1,2)),kleur)'];hold
d on;
    end;
    if i == 5
        kleur='g';
        eval(['q=size(gliphoeek',num2str(i),'_',num2str(spoed),'');]);
        subplot(3,1,1);%F1

eval(['plot(gliphoeek',num2str(i),'_',num2str(spoed),'(1,3:q(1,2)),
gliphoeek',num2str(i),'_',num2str(spoed),'(2,3:q(1,2)),kleur)'];hold
d on;
        subplot(3,1,2);%F2

eval(['plot(gliphoeek',num2str(i),'_',num2str(spoed),'(1,3:q(1,2)),
gliphoeek',num2str(i),'_',num2str(spoed),'(3,3:q(1,2)),kleur)'];hold
d on;
        subplot(3,1,3);%F3

eval(['plot(gliphoeek',num2str(i),'_',num2str(spoed),'(1,3:q(1,2)),
gliphoeek',num2str(i),'_',num2str(spoed),'(4,3:q(1,2)),kleur)'];hold
d on;
    end;
    if i == 6
        kleur='b';
        eval(['q=size(gliphoeek',num2str(i),'_',num2str(spoed),'');]);
        subplot(3,1,1);%F1

eval(['plot(gliphoeek',num2str(i),'_',num2str(spoed),'(1,3:q(1,2)),
gliphoeek',num2str(i),'_',num2str(spoed),'(2,3:q(1,2)),kleur)'];hold
d on;
        subplot(3,1,2);%F2

eval(['plot(gliphoeek',num2str(i),'_',num2str(spoed),'(1,3:q(1,2)),
gliphoeek',num2str(i),'_',num2str(spoed),'(3,3:q(1,2)),kleur)'];hold
d on;
        subplot(3,1,3);%F3

eval(['plot(gliphoeek',num2str(i),'_',num2str(spoed),'(1,3:q(1,2)),
gliphoeek',num2str(i),'_',num2str(spoed),'(4,3:q(1,2)),kleur)'];hold
d on;
    end;
    if i == 7
        kleur='c';
        eval(['q=size(gliphoeek',num2str(i),'_',num2str(spoed),'');]);
        subplot(3,1,1);%F1

eval(['plot(gliphoeek',num2str(i),'_',num2str(spoed),'(1,3:q(1,2)),
gliphoeek',num2str(i),'_',num2str(spoed),'(2,3:q(1,2)),kleur)'];hold
d on;
        subplot(3,1,2);%F2

eval(['plot(gliphoeek',num2str(i),'_',num2str(spoed),'(1,3:q(1,2)),
gliphoeek',num2str(i),'_',num2str(spoed),'(3,3:q(1,2)),kleur)'];hold
d on;
        subplot(3,1,3);%F3

eval(['plot(gliphoeek',num2str(i),'_',num2str(spoed),'(1,3:q(1,2)),
gliphoeek',num2str(i),'_',num2str(spoed),'(4,3:q(1,2)),kleur)'];hold
d on;
    end;
    if i == 8
        kleur='k';
        eval(['q=size(gliphoeek',num2str(i),'_',num2str(spoed),'');]);
        subplot(3,1,1);%F1

eval(['plot(gliphoeek',num2str(i),'_',num2str(spoed),'(1,3:q(1,2)),
gliphoeek',num2str(i),'_',num2str(spoed),'(2,3:q(1,2)),kleur)'];hold
d on;
        subplot(3,1,2);%F2

```

```

eval(['plot(gliphhoek',num2str(i),'_',num2str(spoed),'(1,3:q(1,2)),
gliphhoek',num2str(i),'_',num2str(spoed),'(3,3:q(1,2)),kleur)'];hold
on;
    subplot(3,1,3);%F3

eval(['plot(gliphhoek',num2str(i),'_',num2str(spoed),'(1,3:q(1,2)),
gliphhoek',num2str(i),'_',num2str(spoed),'(4,3:q(1,2)),kleur)'];hold
on;
    end;
    if i == 9
        kleur='b';
        eval(['q=size(gliphhoek',num2str(i),'_',num2str(spoed),'');]);
        subplot(3,1,1);%F1

eval(['plot(gliphhoek',num2str(i),'_',num2str(spoed),'(1,3:q(1,2)),
gliphhoek',num2str(i),'_',num2str(spoed),'(2,3:q(1,2)),kleur)'];hold
on;
    subplot(3,1,2);%F2

eval(['plot(gliphhoek',num2str(i),'_',num2str(spoed),'(1,3:q(1,2)),
gliphhoek',num2str(i),'_',num2str(spoed),'(3,3:q(1,2)),kleur)'];hold
on;
    subplot(3,1,3);%F3

eval(['plot(gliphhoek',num2str(i),'_',num2str(spoed),'(1,3:q(1,2)),
gliphhoek',num2str(i),'_',num2str(spoed),'(4,3:q(1,2)),kleur)'];hold
on;
    end;

    end;
    legend('ratio 0.3','ratio 0.4','ratio 0.5','ratio 0.6','ratio 0.7','ratio
0.8','ratio 0.9','ratio 1','ratio 1.1');
end;

%=====PLOT
HEADING
ANGLE=====
=====

spoed=20;
for s = 1:7
    spoed=spoed+10;
    figure;
    for i=1:8
        eval(['q=size(gliphhoek',num2str(i),'_',num2str(spoed),'');]);
        if i == 1
            kleur='c';

eval(['plot(gliphhoek',num2str(i),'_',num2str(spoed),'(1,3:q(1,2)),
gliphhoek',num2str(i),'_',num2str(spoed),'(5,3:q(1,2)),kleur)'];hold
on;
        end;
        if i == 2
            kleur='y';

eval(['plot(gliphhoek',num2str(i),'_',num2str(spoed),'(1,3:q(1,2)),
gliphhoek',num2str(i),'_',num2str(spoed),'(5,3:q(1,2)),kleur)'];hold
on;
        end;
        if i == 3
            kleur='m';

eval(['plot(gliphhoek',num2str(i),'_',num2str(spoed),'(1,3:q(1,2)),
gliphhoek',num2str(i),'_',num2str(spoed),'(5,3:q(1,2)),kleur)'];hold
on;
        end;
        if i == 4
            kleur='r';

eval(['plot(gliphhoek',num2str(i),'_',num2str(spoed),'(1,3:q(1,2)),
gliphhoek',num2str(i),'_',num2str(spoed),'(5,3:q(1,2)),kleur)'];hold
on;
        end;
        if i == 5
            kleur='g';

```

```

eval(['plot(gliphhoek',num2str(i),'_',num2str(spoed),'(1,3:q(1,2)),
gliphhoek',num2str(i),'_',num2str(spoed),'(5,3:q(1,2)),kleur)'];hold
on;
    end;
    if i == 6
        kleur='b';

eval(['plot(gliphhoek',num2str(i),'_',num2str(spoed),'(1,3:q(1,2)),
gliphhoek',num2str(i),'_',num2str(spoed),'(5,3:q(1,2)),kleur)'];hold
on;
    end;
    if i == 7
        kleur='c';

eval(['plot(gliphhoek',num2str(i),'_',num2str(spoed),'(1,3:q(1,2)),
gliphhoek',num2str(i),'_',num2str(spoed),'(5,3:q(1,2)),kleur)'];hold
on;
    end;
    if i == 8
        kleur='k';

eval(['plot(gliphhoek',num2str(i),'_',num2str(spoed),'(1,3:q(1,2)),
gliphhoek',num2str(i),'_',num2str(spoed),'(5,3:q(1,2)),kleur)'];hold
on;
    end;
    if i == 9
        kleur='m';

eval(['plot(gliphhoek',num2str(i),'_',num2str(spoed),'(1,3:q(1,2)),
gliphhoek',num2str(i),'_',num2str(spoed),'(5,3:q(1,2)),kleur)'];hold
on;
    end;
    eval(['title("Bison Single Lane Change ',num2str(spoed),'
km/h")']);grid on;
    xlabel("Time [t]");
    ylabel("Yaw Angle [°]");
    legend('ratio 0.3','ratio 0.4','ratio 0.5','ratio 0.6','ratio
0.7','ratio 0.8','ratio 0.9','ratio 1','ratio 1.1');
    end;
end;

%=====
===== PLOT SUMMARY YAW ANGLE
=====

figure;
V=[30 40 50 60 70 80 90];
for j=1:7
    for i=1:8

        eval(['q=size(leerbaan',num2str(i),'_',num2str(V(j),'')]);
        if j == 1
            kleur='c';
            subplot(4,2,1);hold on;

eval(['plot(gliphhoek',num2str(i),'_',num2str(V(j)),'(1,3:q(1,2)),glip
hoek',num2str(i),'_',num2str(V(j)),'(5,3:q(1,2)),kleur)'];hold on;
            title("Bison Single Lane: Change: 30 km/h");
            xlabel("Time [t]");
            ylabel("Yaw Angle [°]");
            grid on;
            axis([-2 15 -20 30]);
        end;
        if j == 2
            subplot(4,2,2);hold on;
            kleur='y';

eval(['plot(gliphhoek',num2str(i),'_',num2str(V(j)),'(1,3:q(1,2)),glip
hoek',num2str(i),'_',num2str(V(j)),'(5,3:q(1,2)),kleur)'];hold on;
            title("Bison Single Lane Change: 40 km/h");
            xlabel("Time [t]");
            ylabel("Yaw Angle [°]");
            grid on;
            axis([-2 15 -20 30]);
        end;

```



```

if j == 3
    subplot(4,2,3);hold on;
    kleur='m';

eval(['plot(gliphoek',num2str(i),'_',num2str(V(j)),'(1,3:q(1,2)),glip
hoek',num2str(i),'_',num2str(V(j)),'(5,3:q(1,2)),kleur)']);hold on;
    title('Bison Single Lane Change: 50 km/h');
    xlabel('Time [t]');
    ylabel('Yaw Angle [°]');
    grid on;
    axis([-2 15 -20 30]);
end;
if j == 4
    subplot(4,2,4);hold on;
    kleur='r';

eval(['plot(gliphoek',num2str(i),'_',num2str(V(j)),'(1,3:q(1,2)),glip
hoek',num2str(i),'_',num2str(V(j)),'(5,3:q(1,2)),kleur)']);hold on;
    title('Bison Single Lane Change: 60 km/h');
    xlabel('Time [t]');
    ylabel('Yaw Angle [°]');
    grid on;
    axis([-2 15 -20 30]);
end;
if j == 5
    subplot(4,2,5);hold on;
    kleur='g';

eval(['plot(gliphoek',num2str(i),'_',num2str(V(j)),'(1,3:q(1,2)),glip
hoek',num2str(i),'_',num2str(V(j)),'(5,3:q(1,2)),kleur)']);hold on;
    title('Bison Single Lane Change: 70 km/h');
    xlabel('Time [t]');
    ylabel('Yaw Angle [°]');
    grid on;
    axis([-2 15 -20 30]);
end;
if j == 6
    subplot(4,2,6);hold on;
    kleur='b';

eval(['plot(gliphoek',num2str(i),'_',num2str(V(j)),'(1,3:q(1,2)),glip
hoek',num2str(i),'_',num2str(V(j)),'(5,3:q(1,2)),kleur)']);hold on;
    title('Bison Single Lane Change: 80 km/h');
    xlabel('Time [t]');
    ylabel('Yaw Angle [°]');
    grid on;
    axis([-2 15 -20 30]);
end;
if j == 7
    subplot(4,2,7);hold on;
    kleur='c';

eval(['plot(gliphoek',num2str(i),'_',num2str(V(j)),'(1,3:q(1,2)),glip
hoek',num2str(i),'_',num2str(V(j)),'(5,3:q(1,2)),kleur)']);hold on;
    title('Bison Single Lane Change: 90 km/h');
    xlabel('Time [t]');
    ylabel('Yaw Angle [°]');
    grid on;
    axis([-2 15 -20 30]);
end;
end;%for
end;%for
%=====PLOT YAW
ANGLE
VELOCITY=====
figure;
V=[30 40 50 60 70 80 90];
for j=1:7
    for i=1:8

eval(['q=size(gliphoek',num2str(i),'_',num2str(V(j)),')']);
if j == 1
    kleur='c';
    subplot(4,2,1);hold on;

eval(['plot(gliphoek',num2str(i),'_',num2str(V(j)),'(1,3:q(1,2)),glip
hoek',num2str(i),'_',num2str(V(j)),'(6,3:q(1,2)),kleur)']);hold on;
    title('Bison Single Lane Change: 30 km/h');
    xlabel('Time [t]');
    ylabel('Yaw Angle Velocity [°/s]');
    grid on;
    axis([-2 15 -20 30]);
end;
if j == 2
    subplot(4,2,2);hold on;
    kleur='y';

eval(['plot(gliphoek',num2str(i),'_',num2str(V(j)),'(1,3:q(1,2)),glip
hoek',num2str(i),'_',num2str(V(j)),'(6,3:q(1,2)),kleur)']);hold on;
    title('Bison Single Lane Change: 40 km/h');
    xlabel('Time [t]');
    ylabel('Yaw Angle Velocity [°/s]');
    grid on;
    axis([-2 15 -20 30]);
end;
if j == 3
    subplot(4,2,3);hold on;
    kleur='m';

eval(['plot(gliphoek',num2str(i),'_',num2str(V(j)),'(1,3:q(1,2)),glip
hoek',num2str(i),'_',num2str(V(j)),'(6,3:q(1,2)),kleur)']);hold on;
    title('Bison Single Lane Change: 50 km/h');
    xlabel('Time [t]');
    ylabel('Yaw Angle Velocity [°/s]');
    grid on;
    axis([-2 15 -20 30]);
end;
if j == 4
    subplot(4,2,4);hold on;
    kleur='r';

eval(['plot(gliphoek',num2str(i),'_',num2str(V(j)),'(1,3:q(1,2)),glip
hoek',num2str(i),'_',num2str(V(j)),'(6,3:q(1,2)),kleur)']);hold on;
    title('Bison Single Lane Change: 60 km/h');
    xlabel('Time [t]');
    ylabel('Yaw Angle Velocity [°/s]');
    grid on;
    axis([-2 15 -20 30]);
end;
if j == 5
    subplot(4,2,5);hold on;
    kleur='g';

eval(['plot(gliphoek',num2str(i),'_',num2str(V(j)),'(1,3:q(1,2)),glip
hoek',num2str(i),'_',num2str(V(j)),'(6,3:q(1,2)),kleur)']);hold on;
    title('Bison Single Lane Change: 70 km/h');
    xlabel('Time [t]');
    ylabel('Yaw Angle Velocity [°/s]');
    grid on;
    axis([-2 15 -20 30]);
end;
if j == 6
    subplot(4,2,6);hold on;
    kleur='b';

eval(['plot(gliphoek',num2str(i),'_',num2str(V(j)),'(1,3:q(1,2)),glip
hoek',num2str(i),'_',num2str(V(j)),'(6,3:q(1,2)),kleur)']);hold on;
    title('Bison Single Lane Change: 80 km/h');
    xlabel('Time [t]');
    ylabel('Yaw Angle Velocity [°/s]');
    grid on;
    axis([-2 15 -20 30]);
end;
if j == 7
    subplot(4,2,7);hold on;
    kleur='c';

eval(['plot(gliphoek',num2str(i),'_',num2str(V(j)),'(1,3:q(1,2)),glip
hoek',num2str(i),'_',num2str(V(j)),'(6,3:q(1,2)),kleur)']);hold on;
    title('Bison Single Lane Change: 90 km/h');
    xlabel('Time [t]');

```

```
ylabel('Yaw Angle Velocity [°/s]');  
grid on;  
axis([-2 15 -20 30]);
```

```
end;  
end;%for  
end;%for
```